UNIVERSITÀ DI SIENA 1240

USiena

Multitarget compounds bearing tacrine- and donepezil-like structural and functional motifs for the potential treatment of Alzheimer's disease

This is the peer reviewed version of the following article:

Original:

Ismaili, L., Refouvelet, B., Benchekroun, M., Brogi, S., Brindisi, M., Gemma, S., et al. (2017). Multitarget compounds bearing tacrine- and donepezil-like structural and functional motifs for the potential treatment of Alzheimer's disease. PROGRESS IN NEUROBIOLOGY, 151, 4-34 [10.1016/j.pneurobio.2015.12.003].

Availability:

This version is availablehttp://hdl.handle.net/11365/995484 since 2017-05-25T10:21:21Z

Published:

DOI:10.1016/j.pneurobio.2015.12.003

Terms of use:

Open Access

The terms and conditions for the reuse of this version of the manuscript are specified in the publishing policy. Works made available under a Creative Commons license can be used according to the terms and conditions of said license.
For all terms of use and more information see the publisher's website.

(Article begins on next page)

25 April 2024

Multitarget compounds bearing tacrine- and donepezil-like structural and functional motifs for the potential treatment of Alzheimer's disease

Lhassane Ismaili,*[,a] Bernard Refouvelet,[a] Mohamed Benchekroun,[a,♯] Simone Brogi,[b] Margherita Brindisi,[b] Sandra Gemma,[b] Giuseppe Campiani,[b] Slavica Filipic,[c] Danica Agbaba,[c] Gerard Esteban,[d] Mercedes Unzeta,[d] Katarina Nikolic,*[,c] Stefania Butini,*[,b] and José Marco-Contelles*[,e]

[a]Neurosciences Intégratives et Cliniques EA 481, Laboratoire de Chimie Organique et Thérapeutique, UFR SMP, 19 rue Ambroise Paré, Université de Franche-Comté, Université Bourgogne Franche-Comté, CHRU Besançon, F-25000 Besançon, France, [b]European Research Centre for Drug Discovery and Development (NatSynDrugs) and Department of Biotechnology, Chemistry and Pharmacy, Università di Siena, Via A. Moro, 53100 Siena, Italy; [c]Institute of Pharmaceutical Chemistry, Faculty of Pharmacy, University of Belgrade, Vojvode Stepe 450, 11000 Belgrade, Serbia; [d]Departament de Bioquímica i Biologia Molecular, Facultat de Medicina, Institut de Neurociències, Universitat Autònoma de Barcelona, 08193 Bellaterra, Barcelona, Spain [e]Laboratory of Medicinal Chemistry (IQOG, CSIC), C/ Juan de la Cierva 3, 28006-Madrid, Spain
[♯]Current Address: Centre de recherche de Gif-sur-Yvette, Institut de Chimie des Substances Naturelles, UPR 2301, CNRS, Avenue de la Terrasse, 91198-Gif-sur-Yvette, France

Corresponding authors:

Lhassane Ismaili
Neurosciences Intégratives et Cliniques EA 481, Laboratoire de Chimie Organique et Thérapeutique, UFR SMP, 19 rue Ambroise Paré, Université de Franche-Comté, Université Bourgogne Franche-Comté, CHRU Besançon, F-25000 Besançon, France
Tel 0033 381665543; Fax 0033 363082319
Email: lhassane.ismaili@univ-fcomte.fr

Katarina Nikolic
Institute of Pharmaceutical Chemistry, Faculty of Pharmacy, University of Belgrade, Vojvode Stepe 450, 11000 Belgrade, Serbia
Tel: 0038 1 113951259; Fax 00381 113974349
Email: knikolic@pharmacy.bg.ac.rs

Stefania Butini
European Research Centre for Drug Discovery and Development (NatSynDrugs) and Department of Biotechnology, Chemistry and Pharmacy, Università di Siena, Via A. Moro, 53100 Siena, Italy
Tel 0039 05770234161; Fax 0039 0577234254
Email: butini3@unisi.it

José Marco-Contelles
Laboratory of Medicinal Chemistry (IQOG, CSIC), C/ Juan de la Cierva 3, 28006-Madrid, Spain
Tel 0034 915622900; Fax: 003491 5644853
Email: iqoc21@iqog.csic.es

ABSTRACT

Alzheimer's disease is a multifactorial and fatal neurodegenerative disorder characterized by decline of cholinergic function, deregulation of other neurotransmitter systems, beta-amyloid fibril deposition, and beta-amyloid oligomers formation. Based on the involvement of a relevant number of biological systems in Alzheimer's disease progression, multitarget compounds may enable therapeutic efficacy. Accordingly, compounds possessing, besides anticholinergic activity and beta-amyloid aggregation inhibition properties, metal chelating and/or nitric oxide releasing properties with additional antioxidant capacity were developed. Other targets relevant to Alzheimer's disease have also been considered in the last years for producing multitarget compounds such as beta-secretase, monoamino oxidases, serotonin receptors and sigma 1 receptors. The purpose of this review will be to highlight recent reports on the development of multitarget compounds for Alzheimer's disease published within the last years focusing on multifunctional ligands characterized by tacrine-like and donepezil-like structures.

Keywords: Cholinesterases, Acetylcholinesterase, Butyrylcholinesterase, Alzheimer's disease, β-Amyloid, Multi-Target-Directed Ligand, Beta secretase, Monoamine oxidases, Reactive Oxygen Species, Nitric oxide, Histamine receptor, Serotonin receptors

Contents

Abbreviations:

ACh, acetylcholine; Cholinesterases, ChEs; AChE, acetylcholinesterase; *Ee*AChE, AChE from *Electrophorus electricus; h*AChE, human acetylcholinesterase; BuChE, butyrylcholinesterase; *eq*BuChE, BChE from equine serum; ChEI, ChE inhibitor; AChEI, AChE inhibitor; AD, Alzheimer's disease; DMAAD, disease modifying anti Alzheimer's drug; CNS, central nervous system; Aβ, β-amyloid peptide; CAS, catalytic active site; PAS, peripheral anionic site; MTDL, multi-target-directed ligand; APP, amyloid precursor protein; β-secretase, BACE-1, beta-site APP cleaving enzyme 1; MAO-A/B, monoamine oxidase A/B; *h*MAO-A/B, human monoamine oxidase A/B; ROS, reactive oxygen species; BBB, blood brain barrier; NO, nitric oxide; H_3R, histamine H_3 receptor; NMDA, *N*-methyl-*D*-aspartate.

1. Introduction

Alzheimer disease (AD), the leading cause of dementia among elderly people, is a multifactorial and fatal neurodegenerative disorder characterized by a decline of cholinergic function. AD is hallmarked by the neuropathological accumulation of amyloid beta (Aβ) plaques in the extracellular compartment and by the intracellular accumulation of hyperphosphorylated tau protein in the form of neurofibrillary tangles.

Although the molecular mechanisms of AD pathogenesis have not yet been clearly understood, so far the use of acetylcholinesterase (AChE) and butyrylcholinesterase (BuChE) inhibitors represents the only therapeutic approach to the disease. Cholinesterase inhibitors (ChEIs), able to improve cognitive functions, only treat disease symptoms and lack disease-modifying effects (Sadowski and Wisniewski, 2007), though, as better explained later, AChE also accelerates the assembly of Aβ into amyloid fibrils (Alvarez *et al.*, 1997). Nevertheless, all the currently registered drugs for the treatment of AD are ChEIs (donepezil, rivastigmine, and galantamine, Fig. 1) with the exception of the *N*-methyl-*D*-aspartate (NMDA) antagonist memantine (licensed in several countries for treatment of moderate to severe AD) (Cummings, 2004; Standridge, 2004). The ChEI tacrine, the first drug approved for the treatment of AD, was withdrawn (Qizilbash *et al.*, 2007) due to its hepatotoxicity (Lagadic-Gossmann *et al.*, 1998). The narrowness of the therapeutic options makes treatment of AD the current biggest unmet medical need in neurology. Further, as the human population continues to age, AD prevalence is expected to reach epidemic levels unless a disease-modifying anti-Alzheimer's drug (DMAAD) can be found (Mount and Downton, 2006). Although incomplete, the current understanding of the disease process is sufficient to facilitate the development of rational therapeutic strategies. AChE and BuChE are the catabolic enzymes responsible for acetylcholine (ACh) hydrolysis, and it is known that in brains with degenerative changes which suffer a loss of AChE, BuChE has a compensatory role in the hydrolysis of ACh thus making it an additional target for increasing the cholinergic tone in AD patients affected by severe symptoms (Greig *et al.*, 2005). Indeed, in those patients, the levels of AChE decrease while those of BuChE increase, particularly in brain areas associated with learning and memory (Reid *et al.*, 2013). In fact, BuChE influences cognition, awareness, and behavior by modulating ACh levels in the central nervous system (CNS) (Podoly *et*

al., 2009). Thus, dual inhibition of AChE and BuChE could improve the symptomatic treatment of AD.

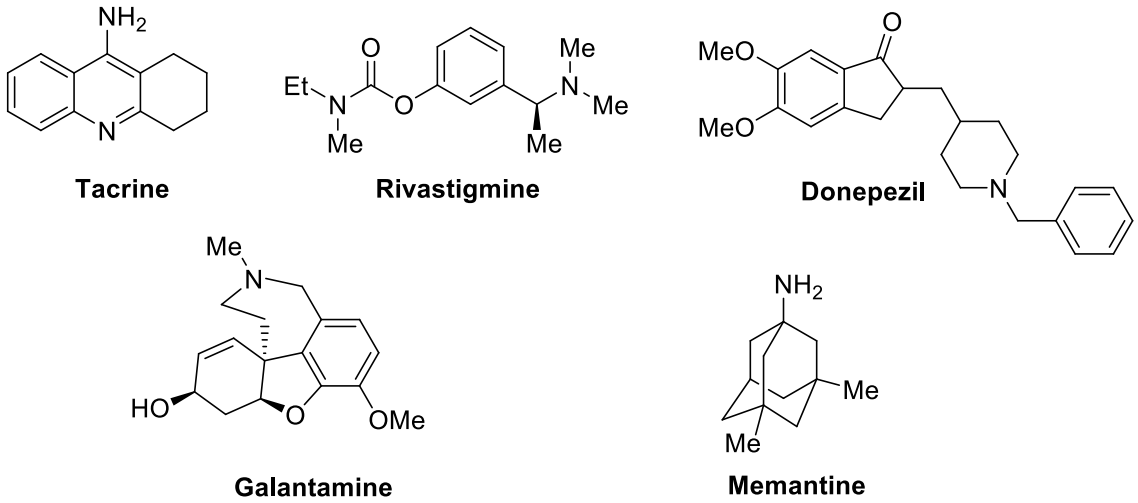

Fig. 1 Drugs approved by the U.S. Food and Drug Administration (FDA) for the treatment of AD (note that tacrine, approved in 1993, was discontinued in the U.S. in May 2012 as better specified in the text in introduction paragraph).

Dysfunction of the cholinergic system has been established as the most prominent neurotransmitter abnormality of AD patients (cholinergic hypothesis of AD); however cognitive, behavioural and neuropsychiatric symptoms have been linked to deregulation of other neurotransmitter systems such as glutamatergic, serotonergic, adrenergic and peptidergic (Thathiah and De Strooper, 2011). Increasing evidence supports the role of the serotonergic system in learning and memory processes and serotonergic system signaling impairment has been well documented in AD patients (Thathiah and De Strooper, 2011).

The amyloid cascade hypothesis of AD postulates that aberration in the proteolytic processing of amyloid precursor protein (APP) leads to increased levels of

soluble Aβ peptides which unbalance the amyloid deposits and correlates with cognitive decline and synaptic dysfunction in AD (Benilova *et al.*, 2012; Hamley, 2012; Walsh and Selkoe, 2007). Sequential APP proteolysis by α-, β-, and γ-secretases produces $A\beta_{1-40}$ and $A\beta_{1-42}$, the two major isoforms of Aβ found in AD brains (Butini *et al.*, 2013b). Since β-secretase (beta-site APP-cleaving enzyme 1, BACE-1) catalyzes the key step in the production of Aβ, (Hong *et al.*, 2000) it has been proposed as an attractive target for AD therapy (Venugopal *et al.*, 2008). As a consequence, a series of inhibitors of this enzyme have been developed in the last decade (Butini *et al.*, 2013b; Butini *et al.*, 2013c). It is known that ChEs also play a key role in the progress of AD since AChE co-localizes with Aβ in the senile plaques and enhances the formation of Aβ fibrils rate, forming stable complexes with them (Bartolini *et al.*, 2003). It has also been proved that this process takes place in the proximity of the peripheral anionic binding site (PAS) of AChE (Ferrari *et al.*, 2001). Consequently, AChEIs able to bind the PAS of the enzyme are potential inhibitors of Aβ-accelerated aggregation, and can be considered multitarget compounds (Bartolini *et al.*, 2003).

The formation of Aβ deposits in the brain is a seminal step and it was associated with the development and progression of AD. Recent advances have demonstrated that the pathological assembly of Aβ closely correlates with the level of soluble Aβ oligomers. It is indeed now widely accepted that Aβ toxicity is mainly related to Aβ prefibrillar and brain permeable species since Aβ oligomers have been shown to accelerate neuronal cell death and to adversely affect synaptic function (Hamley, 2012). Moreover, the interaction of Aβ oligomers was recently reported with several proteins such as glutamatergic receptors (NMDA) and proteins responsible for maintaining glutamate homeostasis (Danysz and Parsons, 2012; Lauren *et al.*, 2009). Since the

NMDA receptors are involved in neuronal plasticity (including learning and memory) their interaction with Aβ makes evident the central role of Aβ also in neuronal plasticity.

Other significant factors have been undoubtedly related to AD, which might be relevant for the development of DMAADs. Aging people display a dysfunctional antioxidant protection system which lacks efficacy in abolishing the effects of oxidative species. This leads to an increase of oxidative stress (OS) that represents a risk factor for the beginning and progression of AD (Rosini *et al.*, 2014). This hypothesis is supported by evidence linking OS to the onset of the classical signs of AD (senile plaques and neurofibrillary tangles) (Zhu *et al.*, 2004).

Overwhelming evidence points iron, copper, and zinc as relevant metals in the pathogenesis of AD, either by direct interaction with Aβ, thus increasing its aggregation, or by enhancing the production of reactive oxygen species (ROS) and hydrogen peroxide induced by Aβ (Nasica-Labouze *et al.*, 2015; Smith *et al.*, 2007). Consequently, the modulation of the homeostasis of these biometals is a potential therapeutic strategy for AD therapy (Storr *et al.*, 2006). In non-AD individuals, APP and Aβ interact with the mentioned metal species in a subtle equilibrium. Disruption of this balance drives to an anomalous Aβ metabolism as well as to a change in copper and zinc uptake, leading to the formation of fibrillar Aβ. The formation of fibrils can induce an inflammatory reaction with consequent decrease of pH, also modifying the zinc homeostasis (Cuajungco and Faget, 2003). Zinc is thus released into the cellular environment and this triggers the events that lead to OS-induced cell death. Copper ions are then free to compete for zinc binding site on extracellular Aβ deposits, which can catalyse hydrogen peroxide production by Aβ. The reaction of copper (II) ions with Aβ produces Aβ radicals and copper (I) ions. These latter ions can react with molecular oxygen thus producing hydrogen peroxide. As a consequence of the inflammatory response, a highly

reactive free radical, nitric oxide (NO) is released to regulate the process (Thomas et al., 2008).

The therapeutic potential of monoamine oxidase inhibitors (MAOIs) for the treatment of AD and other neurodegenerative diseases has been proposed based on their neuroprotective properties (Finberg, 2014). It is well known their ability to reduce the formation of neurotoxic products, such as hydrogen peroxide and aldehydes, which can promote the generation of ROS (Song *et al.*, 2013).

Based on the multiple evidence that supports the involvement of a relevant number of biological systems in AD progression, multitarget compounds may enable therapeutic efficacy. This has led to the innovative approach based on multi-target directed ligands (MTDLs) for the development of DMAADs possessing, besides anticholinergic activity and Aβ aggregation inhibition properties, metal chelating and/or NO releasing properties with additional antioxidant capacity (Bolognesi *et al.*, 2007).

The increasing number of reviews published during the last few years (Bajda *et al.*, 2011; Carreiras *et al.*, 2013; Leon *et al.*, 2013) on multifunctional agents as potential drug candidates for AD, testifies the attractiveness of this topic and the continuously growing research activity in the field. Accordingly, the purpose of this review has been to update and highlight recent reports on multitarget compounds for AD published within the last years. We have paid particular attention to multifunctional ligands designed from tacrine and donepezil as reference drugs, and in each section we have discussed the chemical hits and their modifications providing lead compounds for possible pre-clinical studies.

1.1 Mechanism of action of the AChE Inhibitors.

Based on the mode of inhibition, the therapeutically-used ChEIs outlined in Fig. 1 behave as reversible inhibitors. In the last decades a large number of crystallographic analyses have been made available allowing a better understanding of the recognition pattern between the AChE enzyme and its inhibitors at the molecular level. These data have greatly helped the scientists in the rational design of novel chemical entities able to maximize the interactions within the enzyme gorge by specifically targeting key enzyme hot-spots (Butini *et al.*, 2008a) and particularly relevant recognition sites. The same studies have clearly highlighted the different regions that can be targeted by a ligand to potently inhibit AChE. As depicted in Fig. 2, AChE features two distinct binding sites, which are respectively placed at the entrance of the gorge and at the bottom of the same, namely the PAS and the Catalytic Site (CAS), respectively. While CAS represents the binding site for both substrates and inhibitors, the PAS is targeted by enzyme inhibitors. The PAS is mainly composed of aromatic residues such as Y124, W286, F295, R296 and F297 (human AChE numbering), where the presence of W286 confers to this region an anionic character. The CAS is formed by W86 (which is known to stabilize the cationic head of ACh) and the catalytic triad (H447, E334 and S203). Between CAS and PAS, a mid-gorge recognition site (Y72, D74, S125 F338 and Y341) was also identified where the D74 lateral chain represents a key enzyme moiety which plays a role in improving inhibition potency (Butini *et al.*, 2008a; Savini *et al.*, 2003).

Based on the mode of interaction with the gorge, the AChE inhibitors (AChEIs) can be further grouped in catalytic site inhibitors (e.g. tacrine), which only bind the CAS of the enzyme, and dual site inhibitors (e.g. donepezil) able to bind both CAS and PAS.

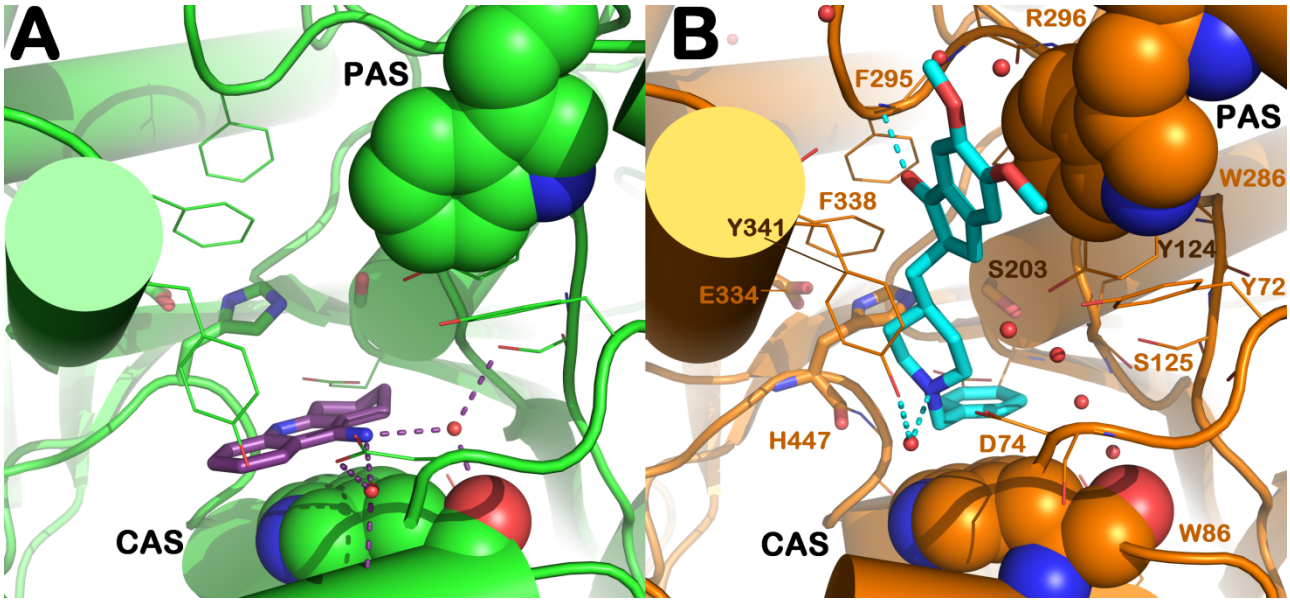

Fig 2. Crystal structures of tacrine (violet purple sticks) in complex with *Torpedo californica* AChE (*Tc*AChE) (panel A; PDB ID: 1ACJ in green cartoon) (Harel *et al.*, 1993), and of donepezil (cyan sticks) in complex with *h*AChE (panel B; PDB ID: 4EY7 in orange cartoon) (Cheung *et al.*, 2012). H-bonds are represented by dotted lines, while the catalytic triad (*h*AChE H447, E334 and S203) is represented by sticks and the red spheres represent the water molecules. CAS and PAS tryptophan residues (W) are highlighted as spheres. The pictures were generated by PyMOL (The PyMOL Molecular Graphics System, v1.6-alpha; Schrodinger LLC, New York, NY, 2013).

Notably, the interaction with AChE of the potent (IC_{50} < 10 nM) inhibitors tacrine and donepezil was studied at the molecular level by means of X-ray diffraction analysis. Since the complex *h*AChE/tacrine is not available, given the sequence identity of the binding site of *human* and *Tc*AChE the interactions of tacrine into *Tc*AChE are expected to be superimposable to those with *h*AChE. Particularly, tacrine is able to interact only with the residues located at CAS and mid-gorge recognition sites (Fig. 2A). In fact, it establishes a π- π stacking with W86 (corresponding to W84 in *Tc*AChE) and a series of

hydrophobic contacts with Y341 (Y334 in *Tc*AChE) and H447 (H440 in *Tc*AChE) at the CAS. Furthermore through two bridged H-bonds formed by its NH_2 group, tacrine interacts with the backbone of W86 (W84 in *Tc*AChE), with S125 (S122 in *Tc*AChE) and with D74 (D72 in *Tc*AChE) thus targeting the mid-gorge recognition site. Notably, the dual site inhibitor donepezil is able to interact with CAS and PAS establishing H-bonds with F295 and a π-π stacking with W286 coupled with a series of hydrophobic interactions with residues Y124 and F295 belonging to the PAS region. The mid-gorge recognition site is partly targeted by the piperidine moiety which interacts, by hydrophobic contacts, with Y72, F338 and with Y341 trough a water molecule bridged H-bond. The benzyl terminal portion of the molecule interacts with the CAS by a π-π stacking with W86 and by hydrophobic contacts with the catalytic residue H447 (Fig. 2B).

2. Tacrine derivatives as multitarget compounds for Alzheimer's disease

2.1. Cholinesterase inhibitors with anti β-amyloid aggregation properties

As mentioned in the introduction, the ChEs are relevant targets for the development of potential compounds for the treatment of AD. Accordingly, the structure of tacrine (Fig. 1) has been widely used in the development of new MTDLs showing inhibitory activity against ChEs and Aβ aggregation (Romero *et al.*, 2013).

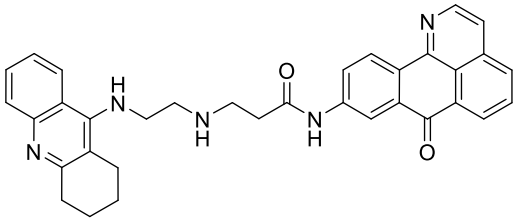

1 [*N*-(7-Oxo-7*H*-dibenzo[*de*,*h*]quinolin-9-yl)-3-((2-((1,2,3,4-tetrahydroacridin-9-yl)amino)ethy)lamino)propanamide]

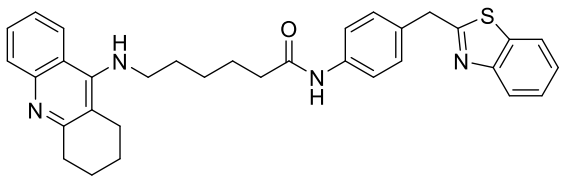

2 [*N*-(4-(Benzo[*d*]thiazol-2-ylmethyl)phenyl)-6-((1,2,3,4-tetrahydroacridin-9-yl)amino)hexanamide]

Fig. 3 Tacrine heterodimers as ChE and Aβ-aggregation inhibitors.

Oxoisoaporphine-tacrine heterodimers were designed based on the CAS/PAS dual binding-site approach (Tang *et al.*, 2011). It was known that oxoisoaporphine alkaloids were potent and selective AChEIs, the 1-azabenzanthrone structural and functional motif of these compounds being able to bind the PAS (Tang *et al.*, 2007). Thus, new ChEIs were synthesized by connecting differently substituted tacrines with the oxoisoaporphine moiety, through an aminoalkyl spacer of diverse length and fixed functionality (Fig. 3). The synthesized tacrine-oxoisoaporphine heterodimers showed higher inhibitory effect on AChE, compared with their carbocyclic-contracted or ring-expanded congeners. The linker composed of six atoms, including secondary amine and carbonyl group, between the 9-aminoacridine and 9-amino-1-azabenzanthrone moieties in tacrine-oxoisoaporphine hybrids provided optimal binding in the CAS, PAS and mid-gorge region sites and the strongest AChE inhibition (Tang *et al.*, 2011).

Pharmacological evaluation (IC_{50} values) confirmed that these hybrids were nanomolar inhibitors of AChE from *Electrophorus electricus* (*Ee*AChEI), but non-selective inhibitors of BuChE from equine serum (*eq*BChEI). In addition, all these hybrids inhibited the self-induced $A\beta_{1-42}$ aggregation in the 36-86% range, as well as the AChE-induced $A\beta_{1-40}$ aggregation. To sum up, the most interesting tacrine-oxoisoaporphine was compound **1** (*Ee*AChE IC_{50} = 3.4 nM; *eq*BChE IC_{50} = 110 nM; self-induced $A\beta_{1-42}$ aggregation inhibition = 80% (10 μM); AChE-induced $A\beta_{1-40}$ aggregation inhibition = 83% (at 100 μM)) (Fig. 3).

Other MTDLs, such as the tacrine-benzothiazole hybrids, have also been developed (Fig. 3) (Keri *et al.*, 2013), showing moderate *Ee*AChE inhibition, in the low micromolar range, and from low to moderate inhibition of self-induced $A\beta_{1-42}$ aggregation, the most active being hybrid **2** (Fig. 3) (*Ee*AChE IC_{50} = 0.57 μM; self-

induced $A\beta_{1-42}$ aggregation inhibition = 61%). Based on the results of the molecular docking studies the tacrine moiety of the tacrine-benzothiazole hybrids is always bounded to the CAS by π-π stacking, while the spacer is accommodated along the hydrophobic mid-gorge cavity and forms additional favorable H-bond interaction with amide NH group of the linker. Conversely, the benzothiazole moiety was always placed at the entrance of the gorge able to bind to PAS forming aromatic interaction. Linker composed of six atoms, including carbonyl group, between benzothiazole and tacrine moieties, and aromatic properties of the spacer nearby the benzothiazole were defined as determinant for strong AChE inhibiting activity.

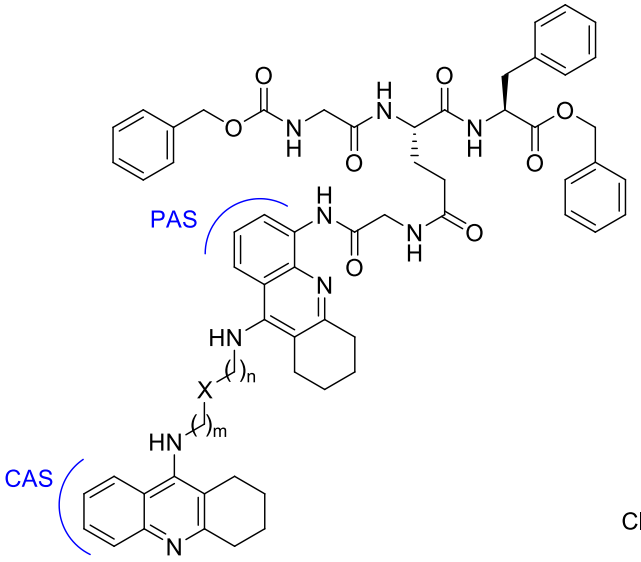

3, X = CH_2, n = 3, m = 4
4a, X = NMe, n = 3, m = 4
4b, X = NMe, n = 4, m = 3

5 [N^1-((6-((10-((6-Chloro-1,2,3,4-tetrahydroacridin-9-yl)amino)decyl)amino)pyridin-2-yl)methyl)-N^4,N^4-dimethylbenzene-1,4-diamine]

Fig. 4 Bis-tacrine heterodimers as *h*ChEIs, inhibitors of Aβ aggregation and oligomerization, and able to disgregate preformed fibrils.

Recently, Butini et al, in an effort to facilitate the identification of potential DMAADs, developed MTDLs (compounds **3** and **4a,b** Fig. 4) (Butini *et al.*, 2013a) where the bis-tacrine scaffold, needed for achieving *h*ChEs inhibition, was connected to a hydrophobic peptide-like sequence. The two tacrine moieties, based on the experience of the research group in the development of bis-tacrine *h*ChEIs (Campiani *et al.*, 2005)

(Butini *et al.*, 2008a; Butini *et al.*, 2008b), were connected by appropriate spacers bearing or not a basic nitrogen. The hydrophobic peptide-like sequence was conceived for interfering with: i) the surface binding region of Aβ around the PAS of the enzyme, thus interfering with *h*AChE- induced Aβ aggregation, and ii) Aβ self-association. Compounds **3** and **4a,b** displayed inhibition properties of both *h*AChE and *h*BuChE in the nanomolar range and also affected *h*AChE non-catalytic functions, by binding the PAS of the enzyme thus interfering with AChE-induced Aβ aggregation with micromolar potency. The replacement of a methylene (compound **3**) with an N-Me group in the linker between the tacrine moieties (compounds **4a** and **4b**) allows the formation of an additional polar interaction with the key mid-gorge region of AChE. Specifically, this interaction relies on the polar contact with the Ω loop residue D74 (*h*AChE numbering) as reported in Fig. 2. Introduction, between the two tacrines, of a moiety (**4a** and **4b**) for targeting the mid-gorge recognition site pushes their peptide portion to occupy the surface of AChE critical for Aβ binding. All these features were demonstrated by the help of the molecular docking studies.

The interference of **3** with the toxic Aβ oligomeric species and with the post-aggregation states of Aβ was assessed by capillary electrophoresis analysis and transmission electron microscopy. Later, the same authors (Brogi *et al.*, 2014) reported the efficacy of compounds **3** and **4a** in reducing Aβ oligomers-mediated toxicity in SH-SY5Y human neuroblastoma cells, while the key interactions of **3** with the Aβ-preformed fibrils were computationally analyzed at the molecular level. Molecular modeling studies such as molecular docking and molecular dynamics (MD) allowed the authors to propose the molecular mechanism that governs the inhibitory activity of **3** in the Aβ self-aggregation process. It was observed that interaction of Aβ monomers with compound **3** does not allow the peptide to assume the conformation that triggers the oligomerization

process. Moreover, the *in silico* MD investigation also evidenced the possible molecular basis governing the observed Aβ pre-formed fibrils disruption process operated by compound **3**. These studies clearly evidenced that compound **3** is able to intercalate within the ordered fibril ensemble and can gradually destroy it. Notably, this report is the only one which describes MD to analyze the interaction of effective tacrine-based MTDLs with both the Aβ monomer and the Aβ pre-formed fibrils (a detailed discussion is reported in the paragraph 4.2). Assessment of the toxicity profile of compounds **3** and **4a,b** on human hepatocytes (WRL-68) and mouse fibroblasts (NIH3T3) revealed that **3** was more toxic than tacrine while **4a** and **4b** displayed comparable or lower toxicity with respect to tacrine (being however more potent ChEIs than tacrine). Cytotoxicity data for the NIH3T3 cells were more encouraging since **4a** and **4b** did not show relevant toxicity on these cells up to 100 μM while **3** was slightly more toxic than the reference tacrine that displayed some toxicity from 1 μM.

In a recent publication, the synthesis and biochemical evaluation of a novel hybrid **5** (Fig. 4) has been reported (Grant *et al.*, 1995; Kochi *et al.*, 2013). 6-Chlorotacrine **5** combines an AChEI and an Aβ-targeted metal chelator into a single molecule. This hybrid shows potent inhibition of AChE (*Ee* IC_{50} = 2.37 nM) under various conditions, interaction with biometals (Cu^{2+} and Zn^{2+}), control of metal-free and metal-induced Aβ aggregation, and disaggregation of Aβ aggregates. Consequently, hybrid **5** was proposed as a promising, new multitarget compound for further studies.

2.2. Hybrids with AChE/BuChE and beta secretase inhibitory properties

Numerous BACE-1 inhibitors have been investigated, and among them, some compounds have been tested in pre-clinical trials (Luo and Yan, 2010). Accordingly, multifunctional ChEIs and BACE-1 inhibitors have been developed.

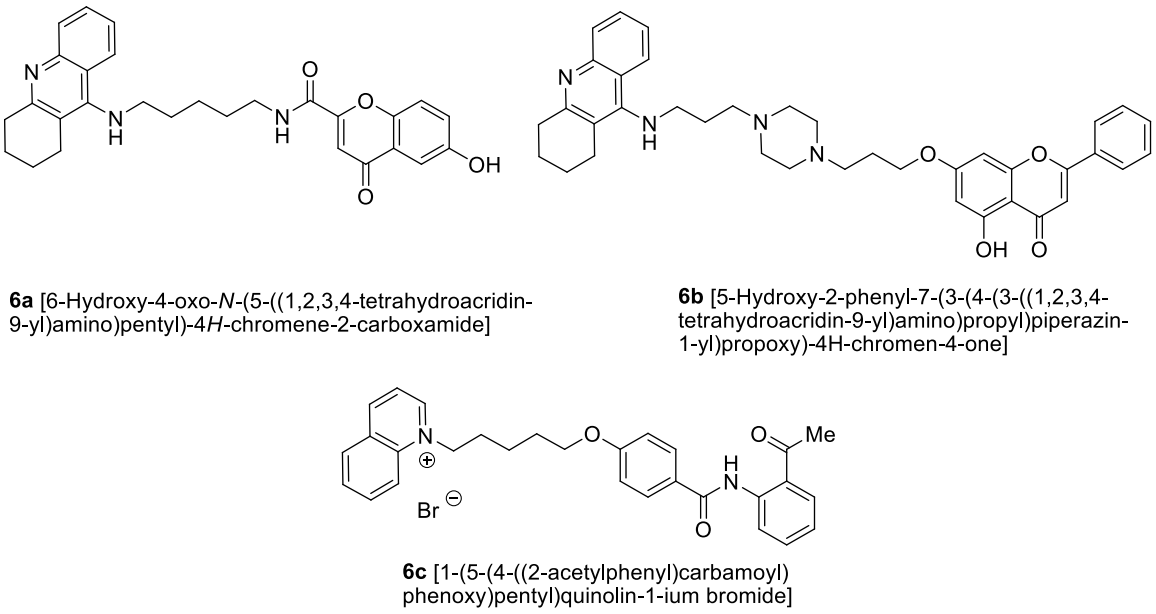

Fig. 5 Tacrine-4-oxo-4*H*-chromene hybrids and quinolinium-benzamide hybrid **6c** as AChE, BuChE and BACE-1 inhibitors.

Tacrine-4-oxo-4*H*-chromene hybrids have been described, and a large family of heterodimers have been synthesized by modifying the structure and the substitution pattern of reference compounds, as well as the length in the spacer (Fernandez-Bachiller *et al.*, 2012).

The tacrine moiety of the tacrine-4-oxo-4*H*-chromene hybrids was selected for its inhibition of cholinesterases while the 4-oxo-4*H*-chromene scaffold was chosen for radical capture and BACE-1 inhibitory activities. A linker composed of five carbon atoms between the tacrine and 4-oxo-4*H*-chromene-2-carboxamide scaffold was optimal for both ChE and BACE-1 inhibition. Among the described hybrids, compound **6a** (Fig. 5) shows a very attractive and multipotent pharmacological profile being a potent *h*AChEI, *h*BChEI, and *h*BACE-1 inhibitor (IC_{50} = 2.80 μM), and the best antioxidant analogue in the reported series, being 1.3-fold more potent than trolox (Davalos *et al.*, 2004) and CNS permeable in the performed assay (Di *et al.*, 2003).

Related tacrine-flavonoid hybrids were designed by linking these functional motifs by a substituted di-*N*,*N*'-alkyl piperazine spacer. Molecule **6b** (Fig. 5) shows an attractive multitarget biological profile (*Ee*AChE IC_{50} = 0.133 μM; *eq*BuChE IC_{50} = 0.558 μM; $A\beta_{1-42}$: IC_{50} = 6.5 μM) in addition to its strong metal-chelating effect (Li *et al.*, 2013a). Hepatotoxicity analysis carried out with hybrid **6b** showed this compound to be safer and slightly less hepatotoxic than the reference tacrine.

In the search of potent dual-biding site AChE inhibitors having innovative scaffolds and devoid of the known toxicity issues displayed by tacrine and its congeners, new MTDLs have been developed (Peng *et al,* 2012). These new compounds designed by molecular modeling and characterized by a central benzamide moiety connected head-to-tail to a quinoline or an isoquinoline and acetophenone, presented an interesting polypharmacological profile. Although the quinoline and isoquinoline motifs are structurally different from tacrine, one can consider them as tacrine substructures since they both share at least a fused pyridine ring. The authors have identified compound **6c** as very promising lead for the potential treatment of AD with a Ki value against *h*AChE of 6.47 nM, 4-fold more potent than tacrine but 6-fold less active against *h*BuChE. The benzamide **6c** also displayed an interesting inhibitory effect against Aβ self-aggregation (IC_{50} = 79 μM) and β-secretase (IC_{50} = 85 μM) compared to reference compound curcumine (IC_{50} = 10 μM and IC_{50}= 5.7 μM respectively for the inhibitions of Aβ self-aggregation and β-secretase).

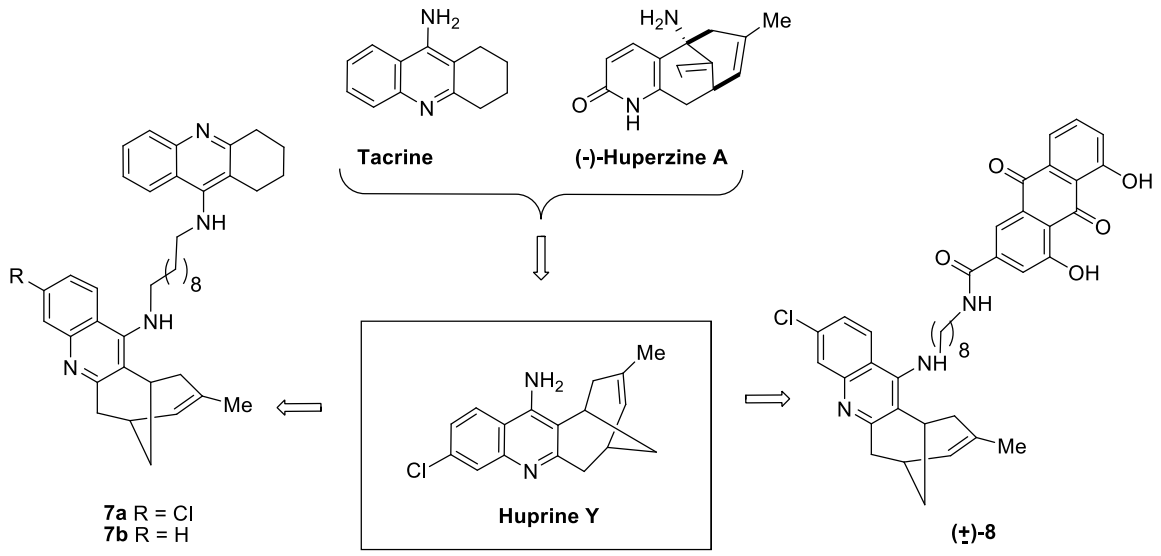

Fig. 6 Tacrine-Huprine Y hybrids.

In 2000 Camps' group designed huprines (e.g. huprine Y, Fig. 6) as tacrine and huperzine A hybrids (Camps *et al.*, 2000). Soon after the huprine derivatives such as **7a,b** and (±)-**8** (Fig. 6) were developed, connecting huprine by an alkyl or alkylamine linker to tacrine or other moieties, which behaved as ChEI, and BACE-1 inhibitors for the potential treatment of AD (Galdeano *et al.*, 2012). All the tested compounds were brain permeable, potent *h*AChEIs, with IC_{50} values in the nanomolar range, and moderately potent *h*BuChEIs showing a good inhibitory potency against BACE-1 (**7a**: *h*BACE-1 IC_{50} = 4.9 μM (Fig. 6)), toward *h*AChE-induced $A\beta_{1\text{-}40}$ aggregation (**7b**: IC_{50} = 61.3 μM (Fig. 6)), and against self-induced $A\beta_{1\text{-}42}$ aggregation. More recently, the same group reported heterodimers of huprine Y and rhein (Viayna *et al.*, 2014), connected by an alkyl or arylalkyl chain of different length, showing inhibition of *h*AChE and *h*BChE in the nanomolar and in the micromolar range, respectively, being also brain permeable. Racemic compound **8** (Fig. 6) resulted the most balanced hybrid for the tested biological targets (*h*AChE: IC_{50} = 3.60 nM; BACE-1: IC_{50} = 120 nM). Therefore, this novel

huprine-rhein compound was identified as an interesting starting point for further development.

2.3. Chlorotacrines and tacrine dimers as acetylcholinesterase inhibitors

Tacrine dimers and heterodimers played a key role in the development of new anti-AD agents (Carlier *et al.*, 1999a; Carlier *et al.*, 1999b). Two recently published papers on this topic (Eckroat *et al.*, 2013; Qian *et al.*, 2014) have particularly attracted our attention. In the first work, (Eckroat *et al.*, 2013) the authors synthesized and evaluated as AChEIs a number of 6-chlorotacrine (**9a**, Fig. 7) derivatives with linkers functionalized with amine, methyl or hydroxyl groups in their terminal positions, putting the focus in elucidating the role of the linker portion of the tacrine hybrid molecules and the potential benefit of linking together AChEIs and other small molecules. From the IC_{50} values, it was concluded that chlorotacrines **9** bearing an amine terminal group were the most potent, non-competitive *Ee*AChEIs. Regarding the length of the linker, compounds **9** with n = 8, 9, and 11 were the most potent compounds among these derivatives, exhibiting IC_{50} values lower than 1 nM thus being over 50-fold more active than tacrine. Of note chlorotacrine **9b** (Fig. 7) was a subnanomolar inhibitor of *Ee*AChE (IC_{50} (*Ee*AChE) = 0.604 nM). In the second paper (Qian *et al.*, 2014) the authors designed four new tacrine dimers (**9c-f**, Fig. 7) based on the heptylene-linked tacrine dimer **9g** (Fig. 7) (Carlier *et al.*, 1999a) which is 150-fold more potent than tacrine. As for other bis-tacrine AChEIs one tacrine moiety binds the CAS and the other is positioned in the PAS of the enzyme (molecular docking studies). From the new bis-tacrines, only **9c** showed a ChE inhibition profile similar to that tested for reference tacrine **9g** (Fig. 7).

2.4. Inhibitors of cholinesterase and monoamine oxidases

Among the number of multitarget ligands described for treating AD and endowed with MAO inhibition properties, tacrine-selegiline hybrids, connected by a suitable

linker, have been designed (Lu *et al.*, 2013). Inhibition studies showed that the new hybrids were effective dual inhibitors of both MAO enzymes, in the micromolar range, and ChEs with nanomolar potency. Molecule **10** (Fig. 7), bearing a nine carbon atom spacer, was indeed a potent AChEI and BuChEI, (*Ee*AChE: IC_{50} = 22.6 nM; *eq*BuChE: IC_{50} = 9.37 nM), and a moderate MAOI (*h*MAO-A: IC_{50} = 0.372 μM; *h*MAO-B IC_{50} = 0.181 μM).

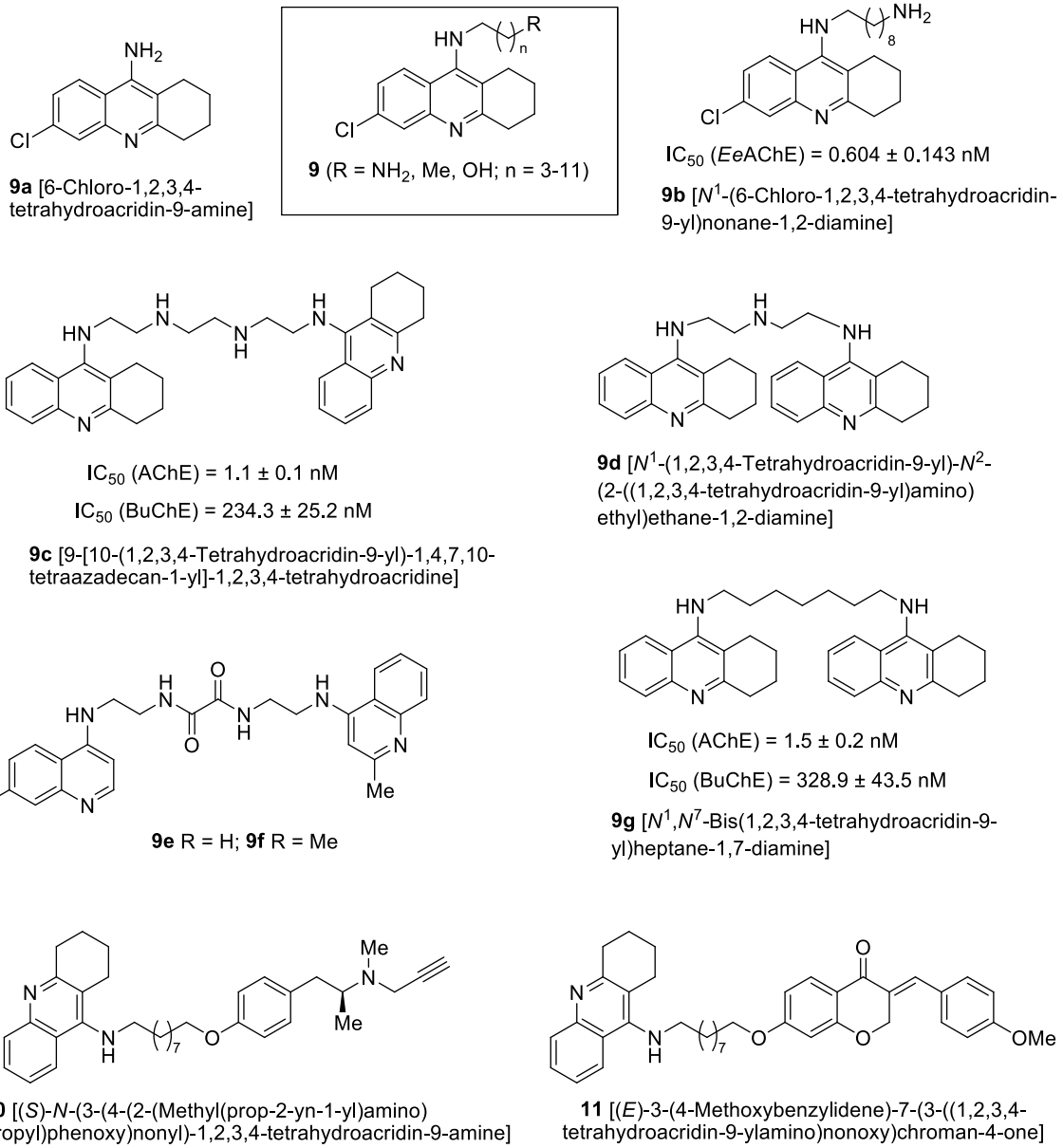

Fig. 7 Tacrine hybrids showing ChEs inhibitory activity.

Based on the well-known pharmacological profile of homoisoflavonoids as MAO-BIs (Desideri *et al.*, 2011), tacrine-homoisoflavonoid hybrids (Sun *et al.*, 2013) have been designed, synthesized and evaluated, showing nanomolar ChE inhibition potency, and MAO-B selectivity over MAO-A. Based on the observed AChE inhibiting activities it was concluded that the length of the alkyl chain between tacrine and homoisoflavonoid moieties did not significantly affect activity. The tacrine-homoisoflavonoid hybrids with a fluorine atom at the para-position of homoisoflavonoid moiety provided better AChE inhibiting activity than hybrid with a methoxy group at the para-position of homoisoflavonoid moiety (compound **11** (Fig. 7)), while compound **11** seems to be a better dual AChE and MAO-B inhibitor. Therefore, the CNS permeable product **11** (Fig. 7) was identified as the most balanced and multipotent ligand (*Ee*AChE: IC_{50} = 67.9 nM; *eq*BChE IC_{50} = 33.0 nM; *h*MAO-B inhibition: IC_{50} = 0.401 μM).

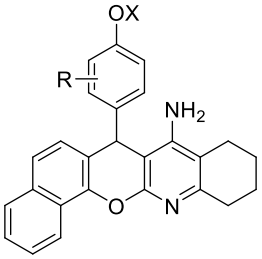

12a (R = 3-OMe, X = H) [4-(8-Amino-9,10,11,12-tetrahydro-7*H*-benzo[7,8]chromeno[2,3-*b*]quinolin-7-yl)-2-methoxyphenol]

12b (R = 2-OMe, X = Me) [7-(3,4-Dimethoxyphenyl)-9,10,11,12-tetrahydro-7*H*-benzo[7,8]chromeno[2,3-*b*]quinolin-8-amine]

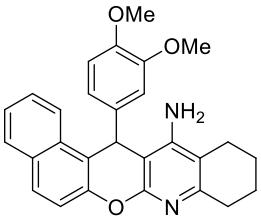

13i [14-(3,4-Dimethoxyphenyl)-9,11,12,14-tetrahydro-10*H*-benzo[5,6]chromeno[2,3-*b*]quinolin-13-amine]

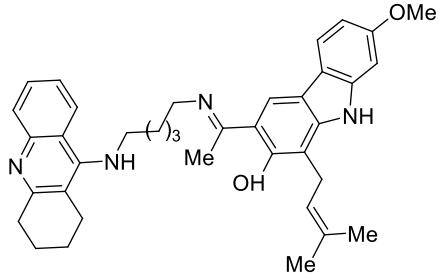

14 [(*E*)-7-Methoxy-1-(3-methylbut-2-en-1-yl)-3-(1-((5-((1,2,3,4-tetrahydroacridin-9-yl)amino)pentyl)imino)ethyl)-9*H*-carbazol-2-ol]

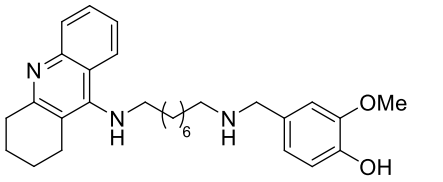

15 [2-Methoxy-4-((8-((1,2,3,4-tetrahydroacridin-9-yl)amino)octyl)amino)phenol]

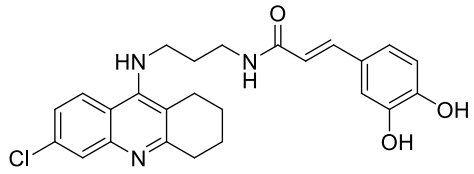

16a [(*E*)-*N*-(3-((6-Chloro-1,2,3,4-tetrahydroacridin-9-yl)amino)propyl)-3-(3,4-dihydroxyphenyl)acrylamide]

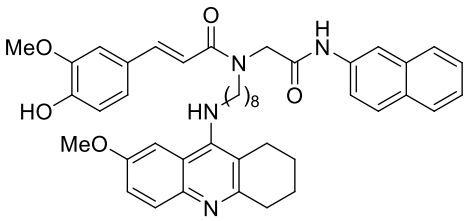

16b [(*E*)-3-(4-Hydroxy-3-methoxyphenyl)-*N*-(8-((7-methoxy-1,2,3,4-tetrahydroacridin-9-yl)amino)octyl)-*N*-(2-(naphthalen-2-ylamino)-2-oxoethyl)acrylamide]

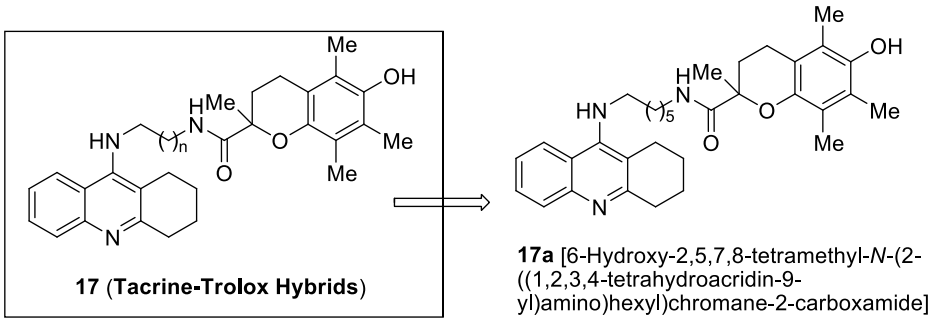

17 (**Tacrine-Trolox Hybrids**)

17a [6-Hydroxy-2,5,7,8-tetramethyl-*N*-(2-((1,2,3,4-tetrahydroacridin-9-yl)amino)hexyl)chromane-2-carboxamide]

Fig. 8 Novel tacrine-based ChEIs with antioxidant properties.

2.5. Inhibitors of cholinesterases with neuroprotective and antioxidant properties

Given the relevance of ROS in the progress and development of AD (Rosini *et al.*, 2014) the search for multipotent ligands showing a profile of ChEIs flanked by antioxidant capacity has been object of intense research in the last years.

Marco-Contelles and Chabchoub have prepared and analyzed a series of racemic benzochromenquinolinamines differently substituted at the benzene ring at C-7 exemplified by **12a** and **12b** (Fig. 8) (Maalej *et al.*, 2012), as new tacrine analogues.

The most potent *h*AChE inhibitor was the parent compound without any substituent in the benzene ring (IC_{50} = 0.30 μM), followed by products bearing two electron-donating groups, such as -OH and -OMe (**12a** and **12b**), showing IC_{50} values of 0.33 and 0.37 μM respectively.

All these compounds were selective *h*AChEI in the micromolar range (with IC_{50} values in the range of 0.30-5.74 μM), with the blood-brain barrier (BBB) permeable compound **12a** (Fig. 8) showing good antioxidant activity (1.5-fold more potent than Trolox) in ORAC (Oxygen Radical Antioxidant Capacity) assay. The BBB permeable analogue **12b** (Fig. 8) was found not endowed with antioxidant potential, but acted as neuroprotective agent against mitochondrial chain blocker-induced cell death (90.18% at 50 μM) by oligomycin-A/rotenone. Remarkably, compound **12b** showed lower hepatotoxicity than tacrine in a cell-based assay (HepG2 and MTT for the viability test).

Continuing with this collaboration, they reported the design, synthesis, and biological evaluation of new isomeric racemic angular pentacyclic pyranotacrines (Esquivias-Perez *et al.*, 2013; Maalej *et al.*, 2011). Compared to previous pyranotacrines **12**, an unsubstituted 2,1-naphthalene motif was installed at C2/C3 in the pyran ring, leading to the new racemic pyranotacrines **13a**-**m** (Table 1) bearing diverse electron-donor or electron-withdrawing substituents on the aromatic ring at C14. In the early communication (Maalej *et al.*, 2011) it was reported that pyranotacrine **13c** (Table 1), bearing a hydroxyl group in the aromatic ring at C14 behaved as the most potent (in the nanomolar range) mixed-type, totally selective *Ee*AChEI. In a subsequent paper (Esquivias-Perez *et al.*, 2013), new compounds **13a**, **13l** and **13m** (Table 1) were

developed. The pyranotacrine **13d**, bearing a methoxy group in the aromatic ring at C14 was the most potent (in the high nanomolar range) mixed-type at high concentrations, totally selective *h*AChEI, 4-fold more potent than tacrine. Of note, regardless the origin of the enzyme, pyranotacrines bearing electron-withdrawing substituents, such as NO_2 in **13k**, or two chlorine atoms in **13l** and **13m**, were the poorest AChEIs in this group of pyranotacrines.

Table 1. IC_{50} (nM) values for the inhibition of AChE by (±)-pyranotacrines **13a-m**.

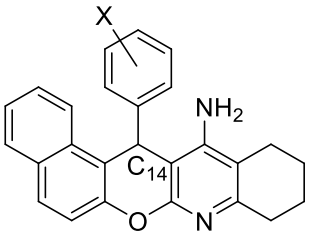

(±)-13a-m

Pyranotacrine	*Ee*AChE (nM) (Maalej *et al.*, 2011)	*h*AChE (nM) (Esquivias-Perez *et al.*, 2013))
Tacrine	27 ± 2	190 ± 50
13a (X = H)	-	240 ± 70
13b (X = 4'-Me)	43 ± 2	4480 ± 1560
13c (X = 4'-OH)	7 ± 2	980 ± 80
13d (X = 4'-OMe)	18 ± 1	48 ± 16
13e (X = 3'-OMe)	16 ± 3	470 ± 230
13f (X = 2'-OMe)	20 ± 1	1460 ± 210
13g (X = 4'-OH,3'-OMe)	28 ± 1	1540± 220
13h (X = 2',4'-di-OMe)	-	2940 ± 110
13i (X = 3',4'-di-OMe)	26 ± 2	83 ± 24
13j (X = 3',4',5'-tri-OMe)	26 ± 2	3140 ± 1620
13k (X = 4'-NO_2)	170 ± 30	11870 ± 530
13l (X = 2',6'-di-Cl)	-	59410 ± 2180

13m (X = 3',4'-di-Cl)	-	33540 ± 1230

It is also interesting to highlight that pyranotacrine **13j**, bearing a 3',4',5'-trimethoxyphenyl motif at C14, is now a very poor *h*AChEI, and that compound **13i** (Fig. 8) with only two methoxy groups at C3', and C4', is however a 2-fold less potent inhibitor than compound **13d**. Very interestingly, pyranotacrine **13i** was one of the less toxic tacrines investigated in the HepG2 cell viability test at different concentrations, showing a 84.1% at 300 mM, while tacrine, at the same concentration, shows a value of 40%. A good neuroprotective effect was observed for pyranotacrine **13i** in a neuronal cortical culture exposed to a combination of oligomycin A/rotenone. Finally, with respect to the virtual ADME analysis to evaluate the drug likeness, all the pyranotacrines **13** fulfill the molecular weight, and the number of H-bonds donors/acceptors requirements. The solubility (logS) of organic molecules in water has a significant impact on many ADME-related properties like uptake, distribution, transport, and eventually bioavailability. Only pyranotacrine **13c** (logS = -6.3) shows predicted solubility values within the limits (-6.5 – 0.5 as reported in QikProp user manuals (QikProp, Schrodinger, LLC, New York, NY)), while the rest of the compounds show values between -6.5 and -7.3, indicating poor aqueous solubility. The most used parameter for BBB penetration is logBB. The logBB of many prescribed CNS drugs is > -0.5 and compounds with logBB < -1.0 poorly penetrate into the brain. Pyranotacrines **13** present acceptable logBB values, not being smaller than -1.0, in particular compound **13c** presents a logBB value of -0.53. To sum up, pyranotacrine **13i** (Fig. 8) is a mixed-type selective *h*AChEI (IC_{50}= 0.083 μM) less toxic than tacrine, neuroprotectant, and non-neurotoxic (Esquivias-Perez *et al.*, 2013).

Based on the well-known antioxidant properties of carbazole (Songsiang *et al.*, 2011), carbazole-tacrine hybrids were designed and prepared connecting these two moieties by carbon atom chains of different length (Thiratmatrakul *et al.*, 2014). These products, represented by compound **14** (Fig. 8), were moderate *Ee*AChEIs with potency in the micromolar range, exhibited very potent antioxidant activity in the ABTS (2,2'-azino-bis(3-ethylbenzthiazoline-6-sulfonic acid) radical test, higher radical scavenging activity than Trolox, and neuroprotective effect against the oxidative stress induced by either hydrogen peroxide or $A\beta_{1-42}$. The most interesting analogue of the series (**14**) was selected for *in vivo* studies performed in the rodent model of scopolamine-induced cognitive deficits in male "Imprinting Control Region" (ICR) mice. These studies indicated that both short- and long-term memory deficits were improved by enhancing the cholinergic signaling, thus highlighting **14** as a promising candidate for AD therapy.

Tacrine hybrids linked by an alkyl linker to a substituted benzylamine (one or two hydroxyl or methoxy groups) have been described (Luo *et al.*, 2011). These products are potent antioxidants in the ORAC assay, and nanomolar ChEIs. The most interesting is compound **15** (Fig. 8) (*Ee*AChE IC_{50} = 4.55 nM and *eq*BuChE IC_{50} = 3.41 nM), showing also self-promoted $A\beta_{1-42}$ aggregation inhibition properties (71% at 20 μM).

Caffeic acid antioxidant and neuroprotective properties have prompted the design of tacrine-caffeic acid hybrids in the search for MTDLs able to inhibit ChEs while displaying antioxidant properties (Chao *et al.*, 2012). Among them, compound **16a** resulted to be the most active (Fig. 8) (AChE: IC_{50} = 0.3 μM against; BuChE: IC_{50} = 5 μM; self-promoted $A\beta_{1-42}$ aggregation inhibition (36.2% at 20 μM) and AChE-induced Aβ aggregation inhibition (67.7% at 100 μM)).

Tacrine-ferulic acid hybrids have been described and afforded good antioxidant multipotent anti-AD agents (Fang *et al.*, 2008c; Pi *et al.*, 2012; Sun *et al.*, 2014b). Based

on these previous works, Ismaili and Marco-Contelles designed new tacrine ferulic acid hybrids (TFAHs), synthesized by an efficient one-pot Ugi four-component reaction, and submitted them to extensive biological evaluation including *Ee* and *human* AChE inhibition, *eq* and *human* BuChE inhibition, evaluation of hepatotoxicity on HepG2 cells, neuroprotection, ORAC test for antioxidant capacity, inhibition of $A\beta_{1-42}$ self-aggregation, *in vitro* BBB permeation assays and *in silico* ADMET analysis (Benchekroun *et al.*, 2015a). From this complex work, it was difficult to select one best-performing hybrid out of all the conducted experiments. However, hybrid **16b** (Fig. 8) was identified as a potential agent for the treatment of AD, due to its overall interesting multipotent profile that shows moderate and completely selective inhibition of *h*BuChE (IC_{50} = 68.2 nM), strong antioxidant activity (4.29 equiv trolox in the ORAC-FL assay), good anti Aβ aggregation properties (65.6% at 1:1 ratio), and ability to permeate CNS, as determined by PAMPA-BBB assay. Notably, even when tested at very high concentrations, TFAH **16b** easily surpasses the other TFAHs in hepatotoxicity profiling (59.4% cell viability at 1000 μM), affording good neuroprotection against toxic insults such as $A\beta_{1-40}$, $A\beta_{1-42}$, hydrogen peroxide, and oligomycin A/rotenone on SHSY5Y cells, at 1 μM.

Trolox is a potent antioxidant agent (Cordes *et al.*, 2009), that protects liver from diverse insult damages and shows neuroprotective effect through scavenging ROS and attenuating the neurotoxicity mediated by Aβ (Thiratmatrakul *et al.*, 2014). Consequently, and not surprisingly, trolox has been used to build tacrine-based multitarget compounds for AD. Thus, in a very recent paper (Xie *et al.*, 2015), by combining tacrine with trolox in a single molecule, novel hybrids of type **17** (Fig. 8) were designed, synthesized and submitted to biological evaluation. Among them, compound **17a** was of particular interest, as the most potent *Ee*AChEI (IC_{50} = 9.8 nM) and *h*AChEI

(IC_{50} = 23.5 nM), showing also a strong inhibition for *eq*BuChE (IC_{50} = 22.2 nM and *h*BuChE (IC_{50} = 20.5 nM), behaving as a mixed-type inhibitor and binding simultaneously to CAS and PAS of AChE. *In vivo* hepatotoxicity assays indicated that hybrid **17a** was much less toxic than tacrine, showed neuroprotective effect and good BBB penetration, thus suggesting that this molecule is a promising multitarget agent for the potential treatment of AD.

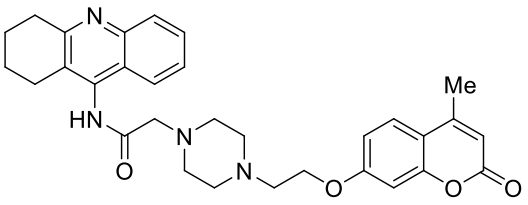

18a [2-(4-(2-((4-Methyl-2-oxo-2*H*-chromen-7-yl)oxy)ethyl)piperazin-1-yl)-*N*-(1,2,3,4-tetrahydroacridin-9-yl)acetamide]

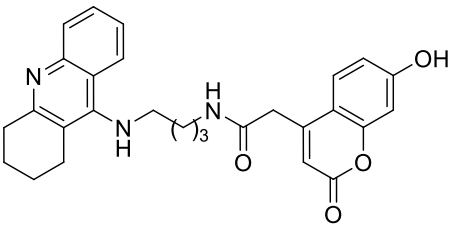

18b [2-(7-Hydroxy-2-oxo-2*H*-chromen-4-yl)-*N*-(2-((1,2,3,4-tetrahydroacridin-9-yl) amino)butyl)acetamide]

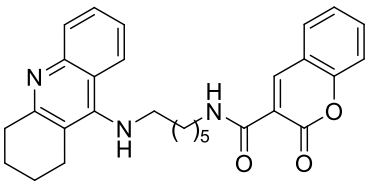

18c [2-Oxo-*N*-(2-((1,2,3,4-tetrahydroacridin-9-yl)amino)hexyl)-2*H*-chromene-3-carboxamide]

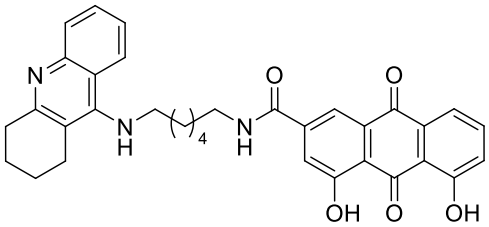

19a [4,5-Dihydroxy-9,10-dioxo-*N*-(3-((1,2,3,4-tetrahydroacridin-9-yl)amino)hexyl)-9,10-dihydroanthracene-2-carboxamide]

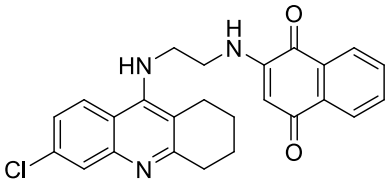

19b [2-((2-((6-Chloro-1,2,3,4-tetrahydroacridin-9-yl) amino)ethyl)amino)naphthalene-1,4-dione]

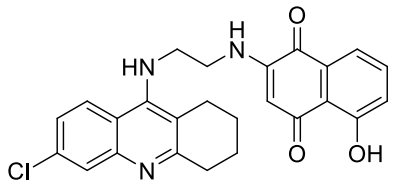

19c [2-((2-((6-Chloro-1,2,3,4-tetrahydroacridin-9-yl)amino)ethyl)amino)-5-hydroxynaphthalene-1,4-dione]

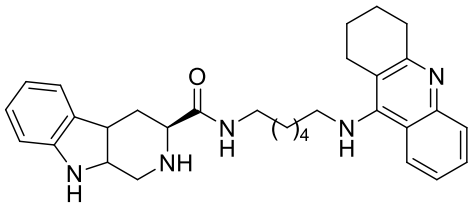

19d [(3*S*)-*N*-(6-((1,2,3,4-Tetrahydroacridin-9-yl)amino)hexyl)-2,3,4,4a,9,9a-hexahydro-1*H*-pyrido[3,4-*b*]indole-3-carboxamide]

Fig. 9 Tacrine hybrids with metal chelating properties.

2.6. Multifunctional compounds with metal-chelating properties

Overwhelming evidence points to iron, copper, and zinc as relevant metals in the pathogenesis of AD, either by direct interaction with Aβ by increasing its aggregation, or by enhancing the production of ROS induced by Aβ. Consequently, the homeostasis of these biometals is a potential therapeutic strategy for AD therapy (Storr *et al.*, 2006), and the identification of multitarget metal-chelating compounds represents one of the most developed alternatives.

Coumarins are privileged scaffolds in medicinal chemistry, and particularly in drug discovery for neurodegenerative diseases (Anand *et al.*, 2012), due to their anti Aβ aggregation properties. Several tacrine-coumarin hybrids have been reported and **18a** (Fig. 9) was described as a multifunctional compound being a potent *Ee*AChEI (IC_{50} = 0.092 μM), a moderate *eq*BuChEI (IC_{50} = 0.234 μM), a potent Aβ-aggregation inhibitor (67.8% inhibition at 20 μM), and an efficient copper and iron chelating agent (Xie *et al.*, 2013). New tacrine-coumarin heterodimers, such as **18b** (Fig. 9), were found to be potent *h*AChE/*h*BuChE inhibitors, with **18b** showing IC_{50} values of 0.0154 μM and 0.328 μM, respectively (Hamulakova *et al.*, 2014). Finally, and very recently, related tacrine-coumarin hybrids have been reported (Sun *et al.*, 2014a). In this new family of compounds, 2-oxo-2*H*-chromene-3-carboxylic acid was used as the coumarin motif, the tacrine and the linker coupled to the carboxylic acid yielding the corresponding target amides. Particularly interesting was hybrid **18c** (Fig. 9) as a 2-fold more potent (K_i = 16.7 nM) *h*AChEI and 2-fold less potent (K_i = 16.1 nM) BuChEI than tacrine (Sun *et al.*, 2014a).

Several QuinoTacrines (QTs) have been recently developed by the hybridization of either a benzoquinone or an anthraquinone core with a tacrine motif through a suitable

tether. First of all tacrine-rhein hybrids, spaced by alkylene linkers of different lengths, have been described, and molecule **19a** (Fig. 9) was found as a potent AChEI (IC_{50} = 27.3 nM), a potent inhibitor of AChE-induced $A\beta_{1\text{-}40}$ aggregation (70.2% at 100 μM), and a good metal chelating agent (Li *et al.*, 2014). The hepatotoxicity analysis has been carried out on hybrid **19a**. After being treated with **19a** or with tacrine, the heparinized serum of adult mice was obtained after different times, and the levels of aspartate aminotransferase (ALT) and alanine aminotransferases (ASAT) were measured. In comparison to the control, tacrine showed to induce hepatotoxicity as indicated by the high ALT and ASAT activities, while product **19a** was less hepatotoxic and safer than tacrine. In addition, the liver tissue was stained with hematoxylin and eosin. Total pericentral necrosis and distinct fatty degeneration of the hepatocytes of the surrounding intermediate and periportal zones were observed 30 hours after administration of tacrine, but only minor morphological changes were observed after identical treatment with compound **19a**.

In a very elegant, complete and dense recent study, 15 new multifunctional anti-AD agents have been designed by combining a naphthoquinone portion and a tacrine motif (Nepovimova *et al.*, 2014). *In vitro* analysis showed that QTs **19b** (*h*AChE: IC_{50} = 1.93 nM; *h*BuChE: IC_{50} = 256 nM), and **19c** (*h*AChE: IC_{50} = 0.72 nM; *h*BuChE: IC_{50} = 542 nM) (Fig. 9) displayed very good AChE inhibitory potency, coupled to the ability to moderately block $A\beta_{1\text{–}42}$ self-aggregation (**19b** (22.6%); **19c** (37.5%)). The authors successfully achieved the X-ray analysis of the complex of QT **19c** with *Tc*AChE. These two hybrids were non neurotoxic in immortalized mouse cortical neurons Neuro2A (N2A cell line) (mean percentage of viable N2A cells: **19b**, 105.16 ; **19c**, 85.63) and primary rat cerebellar granule neurons (CGN cell line) (mean percentage of viable CGN cells: **19b**, 75.04; **19c**, 73.5). Regarding the neuroprotective effect, both compounds showed antioxidant activity, following NQO1 induction, and in N2A cells, they were able to

completely revert the decrease in viability induced by Aβ. However, only QT **19b** was less hepatotoxic than tacrine in a HepG2 cells viability test. Finally, both molecules crossed the BBB, as demonstrated in *ex vivo* experiments with rats.

β-Carboline analogues are known to show a wide range of pharmacological properties, including their ability to inhibit the phosphorylation of tau protein (Adayev *et al.*, 2011; Frost *et al.*, 2011), AChE inhibitory activity with IC_{50} values in the nanomolar range (Rook *et al.*, 2010; Schott *et al.*, 2006), as well as ability to scavenge a variety of ROS (Matsutomo *et al.*, 2013). Based on these pharmacological properties related to neurological disorders and the interest of tacrine scaffold, Kong and Wang designed and prepared new tacrine/β-carboline hybrids tethered with the appropriate alkylidene linker (Lan *et al.*, 2014). Thus, several hybrids were proved as AChE/BuChE inhibitors, self-induced Aβ-aggregation and Cu^{2+}-induced $Aβ_{1-42}$ aggregation inhibitors, metallic ions chelators and antioxidants. Among them, hybrid **19d** (Fig. 9) showed a good overall balanced profile with nanomolar inhibition of ChEs (*Ee*AChE: IC_{50} = 21.6 nM, *h*AChE IC_{50} = 63.2 nM; *eq*BuChE IC_{50} = 39.8 nM), a Aβ self-aggregation inhibition of 65.8% at 20 μM, and fair antioxidant activity in the ABTS antioxidant assay (1.57 trolox equivalents). To complete this profile, compound **19d** is also able to bind Cu^{2+} ions, to hamper the PC12 cells death induced by oxidative stress as well as to penetrate the BBB.

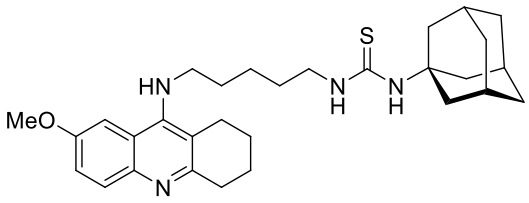

20 [1-((3*S*,5*S*,7*S*)-Adamantan-1-yl)-3-(5-((7-methoxy-1,2,3,4-tetrahydroacridin-9-yl)amino)pentyl)thiourea]

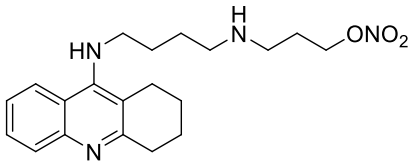

21 [3-((4-((1,2,3,4-Tetrahydroacridin-9-yl) amino)butyl)amino)propyl nitrate]

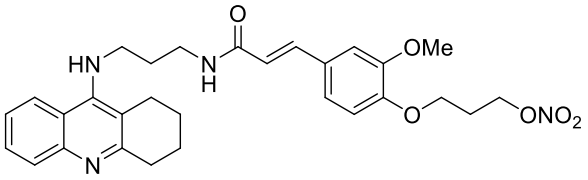

22 [(*E*)-3-(2-Methoxy-4-(3-oxo-3-((3-(1,2,3,4-tetrahydroacridin-9-yl)amino)propy)lamino)prop-1-en-1-yl)phenoxy)propyl nitrate]

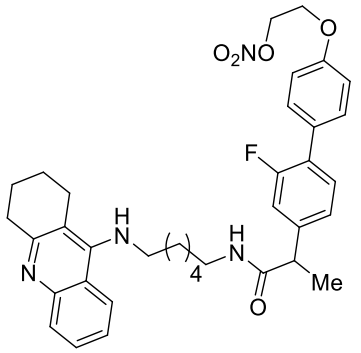

23 [2-((2'-Fluoro-4'-(1-oxo-1-(3-((1,2,3,4-tetrahydroacridin-9-yl)amino)propyl)amino)hexan-2-yl)-[1,1'-biphenyl]-4-yl)oxy)ethyl nitrate]

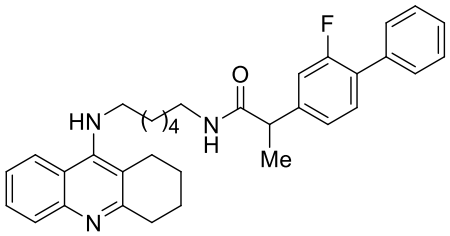

24 2-(2-Fluoro-[1,1'-biphenyl]-4-yl)-*N*-(3-((1,2,3,4-tetrahydroacridin-9-yl) amino)hexyl)propanamide]

Fig. 10 Tacrine-adamantylamine hybrids (**20**), and tacrine-hybrids with nitric oxide-releasing properties (**21-24**).

2.7. 7-Methoxytacrine-adamantylamine heterodimers

In a very attractive and interesting communication, Kuca and colleagues (Spilovska *et al.*, 2013) designed new anti-AD agents by combining in on molecule 7-methoxytacrine (7-MEOTA) motif with adamantine (1-adamantylamine hydrochloride), a well-known NMDA antagonist. As a result, a series of multitarget-directed 7-MEOTA-adamantylamine thioureas were obtained and submitted to biological evaluation as *h*AChEIs and *h*BChEIs. Note that memantine (Fig. 1), a derivative of adamantane and uncompetitive NMDA receptor antagonist, is currently used in AD treatment (Chen *et al.*, 1992), and on the other hand, 7-MEOTA was found to be an active ChEI with

significantly lower side effects compared to tacrine (Patocka *et al.*, 2008). The most potent ChEI was thiourea analogue **20** (Fig. 10) (*h*AChE: IC_{50} = 0.47 μM; *h*BChE: IC_{50} = 0.11 μM). The authors conclude that hybrid **20** is a suitable novel lead compound for further evaluation for the development of novel AD drugs.

2.8. Multifunctional compounds with nitric oxide-releasing properties

NO (Kerwin *et al.*, 1995) is an important and ubiquitous signaling molecule that plays a significant role in the regulation of a diverse set of mammalian physiological processes, such as cerebral circulation and inflammatory reactions (Thomas *et al.*, 2008).

Starting from the tacrine-ferulic acid hybrids (Fang *et al.*, 2008c), displaying excellent AChE/BuChE inhibitory profile, and good antioxidant activity, a new series of tacrine-derivatives with a NO-donating nitrate were designed (Fang *et al.*, 2008a). Among them, compound **21** (Fig. 10) showed ChE inhibitory potency in the nanomolar range, moderate blood vessel relaxant activity, and very interestingly, no hepatotoxicity (Fang *et al.*, 2008b). Soon after, tacrine-ferulic acid/NO donor trihybrids (Fig. 10) (Chen *et al.*, 2012b) were developed the most active being compound **22**, that displayed good ChE inhibitory activity, NO-releasing capacity, vasorelaxant effects, and lower hepatotoxicity than tacrine.

In a similar approach, tacrine-flurbiprofen-NO donor trihybrids were described as potent *Ee*AChEIs and *eq*BuChEIs, able to release NO in amounts comparable to isosorbide mononitrate. Particularly, when tested in an *ex vivo* isolated organ (coronary arteries from rats) study, hybrid **23** (Fig. 10) improved memory impairment and showed lower hepatotoxicity than tacrine and compound **24** thus indicating the hepatoprotective role of NO (Chen *et al.*, 2013).

Lehmann and co-workers designed and synthesized five tacrine-flurbiprofen hybrids (Chen *et al.*, 2013) in which the tacrine was connected to racemic flurbiprofen *via*

alkylenediamine linkers in order to achieve potential multipotent anti-AD drugs. The compounds were evaluated as ChEI, and IC_{50} values proved that the length of the diamine linker may influence the ability to inhibit ChE. Among them, compound **24** (Fig. 10), with six-atom spacer length, showed higher activity towards AChE (IC_{50} = 19.3nM) and BuChE (IC_{50} = 2.1 nM) than tacrine (AChE: IC_{50} = 61.7 nM; BuChE : IC_{50} = 9.0 nM). Kinetic studies on hybrid **24** displayed a competitive inhibition for BuChE, and a mixed-type inhibition for AChE. This result demonstrates that compound **24** behaves as an AChE dual site inhibitor binding both CAS and PAS. In fact the tacrine fragment interacts by a π–π with W86 at the CAS while the benzene ring of flurbiprofen showed a hydrophobic interaction with the key PAS residue W286. This PAS interaction well fits with the significant potency at inhibiting the formation of $A\beta_{1-40}$ by hybrid **24** (31% reduction of $A\beta_{1-40}$ formation at the concentration of 0.25 μM) (Chen *et al.*, 2013).

2.9. Multifunctional compounds with anti-inflammatory properties

Based on the well-known anti-inflammatory properties of aminothiazoles (Zhang *et al.*, 2009), tacrine-aminothiazole hybrids, connected by various linkers, were developed. The most potent *Ee*AChEI was hybrid **25a** (Fig. 11) (pIC_{50} = 7.14) displaying the most significant Ca^{2+} antagonism effect, but product **25b** (Fig. 11) stood out as quite interesting due its potency to inhibit *Ee*AChE (pIC_{50} = 6.98) and *eq*BuChE (pIC_{50} = 10.35) (Wang *et al.*, 2012).

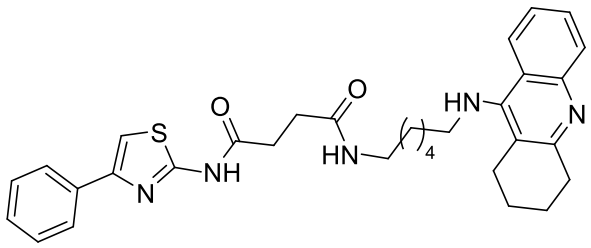

25a [N^1-(4-Phenylthiazol-2-yl)-N^4-(3-((1,2,3,4-tetrahydroacridin-9-yl)amino)propyl)succinamide]

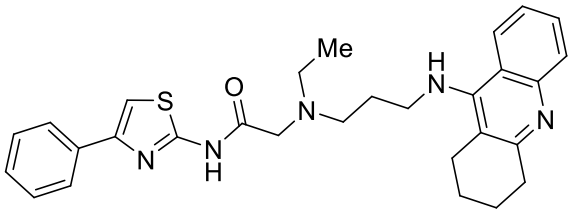

25b [2-(Ethyl(3-((1,2,3,4-tetrahydroacridin-9-yl) amino)propyl)amino)-*N*-(4-phenylthiazol-2-yl) acetamide]

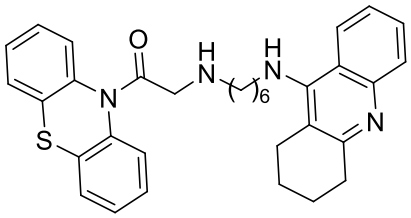

26 [(10*H*-Phenothiazin-10-yl)-3-((6-((1,2,3,4-tetrahydroacridin-9-yl)amino) hexyl)amino)propan-1-one]

Fig. 11 Tacrine-aminothiazole hybrids showing ChE and Aβ-aggregation inhibition, Ca^{2+} antagonism, and anti-inflammatory properties.

2.10. Multifunctional compounds with tau protein hyperphosphorylation inhibition properties

The phenothiazine core present in the methylene blue dye, and known to prevent tau fibrillization (Taniguchi *et al.*, 2005), can reduce soluble tau and regenerate cognition (O'Leary *et al.*, 2010). Thus, it was judiciously associated to tacrine (Hui *et al.*, 2014) to design 26 new MTDLs by varying the length of alkylenediamine-type spacer. Based on ADME properties and molecular docking of all these ligands on AChE and GSK-3β, the

authors have identified 3 representative compounds for further synthesis and biological evaluation as AChEIs, tau protein inhibition and ability to bind with Aβ fibrils. Interestingly, the ligand **26** (Fig. 11) displayed a good rat brain AChE inhibition (IC_{50}= 89 nM), being 3-fold more potent than tacrine, and no tau protein hyperphosphorylation induced by okadaic acid in N2α cells. Moreover, hybrid **26** proved tightly binding to Aβ fibrils with a K_D of 5.51 9 10^{-8} M as revealed by surface plasmon resonance analysis. It is worth noting that those hybrids constitute, according to our knowledge, the only tacrine heterodimers targeting tau protein hyperphosphorylation.

To conclude this section on tacrine-based derivatives as potential AD therapeutics, it must be noted that despite the well documented hepatotoxicity of tacrine (Watkins *et al.*, 1994) and in front of a notable number of recent reports describing tacrine-based derivatives, very few of them reported the hepatotoxicity profile of the described compounds. This lack of information seriously compromises the interest of the newly identified tacrine-based leads for further development. Hoverer it must be noted that the reports herein described highlight that tacrine hepatotoxicity may be limited by introducing appropriate functions on the molecule such as trolox (e.g. compound **17**) or functions able to release NO (e.g. compounds **21-23**). Further the functionalization of the tricyclic system of tacrine, as in compound **19b**, may also provide tacrine analogues characterized by lower hepatotoxicity.

3. Donepezil-related derivatives as multitarget compounds for Alzheimer's disease

The AChEI donepezil (Fig. 1) (marketed in the U.S. and in some European and Asian countries under the trade name of Aricept®) was the second drug approved by the U.S. Food and Drug Administration for the treatment of mild to moderate AD. Donepezil

has *N*-benzylpiperidine and indanone moieties and exhibits selectivity for the inhibition of AChE over BuChE. It was developed as a racemic mixture since the enantiomers showed the same inhibitory profiles (Kawakami *et al.*, 1996).

From the earlier report on the synthesis of donepezil, (Sugimoto *et al.*, 1992) we learn that the initial leads were compounds **27** and **28** (Fig. 12) both containing an amide group and a benzylpiperidine moiety.

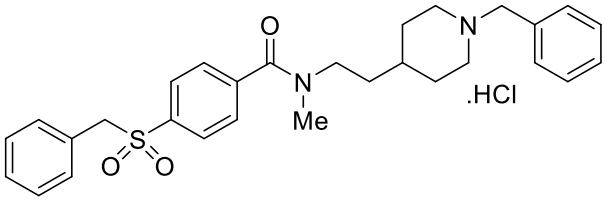

27 [*N*-(2-(1-Benzylpiperidin-4-yl)ethyl)-4-(benzylsulfonyl)-*N*-methylbenzamide hydrochloride]

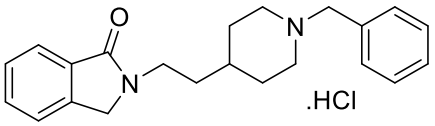

28 [2-(2-(1-Benzylpiperidin-4-yl)ethyl) isoindolin-1-one hydrochloride]

Fig. 12 Initial leads for the design of donepezil.

Compound **27** displayed a strong inhibition of AChE (IC_{50} = 0.56 nM), and at a dose of 3 mg/kg it produced a marked and significant increase in ACh content in the cerebral cortex and hippocampus of rats, but a poor bioavailability and a short duration of action were described (Sugimoto *et al.*, 1990). The structural modification transforming the amide group into a lactam yielded compound **28** showing a lower but still interesting inhibition potency of AChE (IC_{50} = 98 nM) (Sugimoto, 2008; Sugimoto *et al.*, 2002). After a number of transformations, including the replacement of the phtalamide by an indanone moiety, donepezil was generated as a potent AChEI (IC_{50} = 5.7 nM) with large selectivity versus BuChE (IC_{50} = 7138 nM) (Sugimoto, 2008).

3.1. Inhibitors targeting one enzyme (cholinesterase)

3.1.1. Inhibitors of cholinesterases

With donepezil (Fig. 1) being on clinical study, many groups started to undertake the design and synthesis of donepezil-1ike compounds (for a recent, complementary review, see: (Rodrigues Simoes *et al.*, 2014)) incorporating bioisosteric replacements of the indanone system. Very few studies described the replacement of benzylpiperidine, for example a series of 2-phenoxy-indan-1-one derivatives were designed and synthesized (Sheng *et al.*, 2005) in order to create a new class of AChEIs. In this approach the phenoxy group was introduced in place of the benzylpiperidine group. The inhibition studies showed that the new analogues were AChEIs of micromolar potency, while molecule **29** (Fig. 13) was a potent inhibitor (AChE: IC_{50} = 50 nM).

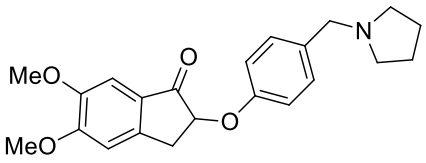

29 [5,6-Dimethoxy-2-(4-(pyrrolidin-1-ylmethyl) phenoxy)-2,3-dihydro-1*H*-inden-1-one]

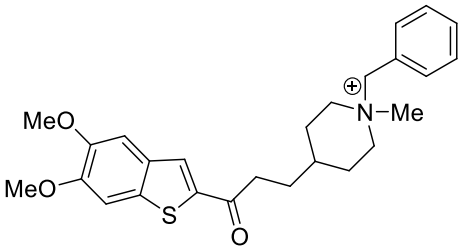

30 [(4-(3-(5,6-Dimethoxybenzo[*b*]thiophen-2-yl)-3-oxopropyl)-1-methyl-1λ^4-piperidin-1-yl)(phenyl)methylium]

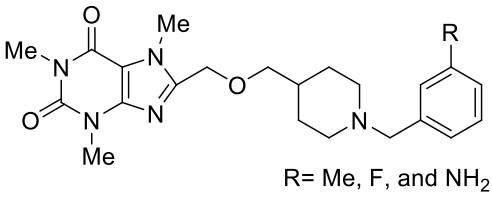

31 [8-(((1-Benzylpiperidin-4-yl)methoxy)methyl) -1,3,7-trimethyl-3,7-dihydro-1*H*-purine-2,6-dione]

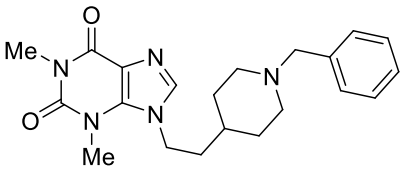

32 [9-(2-(1-Benzylpiperidin-4-yl)ethyl)-1,3-dimethyl-3,9-dihydro-1*H*-purine-2,6-dione]

Fig. 13 Inhibitors of cholinesterases.

One of the first studies concerning a bioisosteric replacement of the indanone system reported the synthesis of a series of benzylpiperidinium and benzylpyridinium quaternary salts and their evaluation on AChE inhibition and on reversal of

neuromuscular block induced by vecuronium (Clark *et al.*, 2002). In this study, the authors aimed at developing water-soluble reversal agents with reduced cardiovascular side effects, based on charged quaternary amino compounds that are more water soluble and less likely to penetrate into the CNS. The authors obtained diverse series of benzylpiperidinium quaternary salts with AChE nanomolar inhibition potencies, ranging from 131 nM to 8 nM, and with the property to potently reverse vecuronium-induced neuromuscular block (*in vitro* GP, *in vivo* anaesthetised GP, and *in vivo* anaesthetized cat). Particularly, compound **30** (Fig. 13) is a potent AChEI (IC_{50} = 8 nM) and a potent antagonist of vecuronium-induced neuromuscular block (*in vitro Guinea pig*) (IC_{50} = 19 nM). Very interestingly, the quaternary salt of donepezil showed slight variations in the inhibition of AChE when compared to donepezil (IC_{50} = 26 nM and IC_{50} = 18 nM, respectively).

N-Benzylpiperidine purines were developed (Rodriguez-Franco *et al.*, 2005) and they displayed moderate ChE inhibition and no remarkable selectivity towards the two enzymes. In fact, compounds **31** and **32** (Fig. 13) showed an inhibitory potency against of Bovine erythrocyte AChE with IC_{50} values of 0.75 μM and 2 μM, respectively, and compound **31** showed an IC_{50} value of 2.50 μM for *eq*BuChE inhibition. The substitution of R by phenyl group, Me, F and NH_2 did not significantly affect potency. With the aim of obtaining some information about the interactions of **32** with the enzyme, the authors performed a molecular modeling study comparing **32** with donepezil by employing a semi-empirical method (Dewar *et al.*, 1985).

Based on the interest for the coumarin scaffold in the drug discovery for neurodegenerative diseases, due to its properties of ChE inhibition (Anand *et al.*, 2012), a number of donepezil/coumarin hybrids have recently been designed (Catto *et al.*, 2013) by connecting a methoxy-substituted coumarin portion to the benzylpiperidine moiety

present in donepezil. The developed products **33** and **34** (Fig. 14) are potent Bovine erythrocyte AChEIs (IC_{50} = 0.028 μM and 0.014 μM respectively) and efficient *eq*BuChEIs (IC_{50} = 19 μM and 12 μM respectively). Transformation of the amide group of **33** into an ester (**34**) resulted in a higher potency on Bovine erythrocyte AChE, while a further elongation of the linker in aminoester led to a less active AChEI.

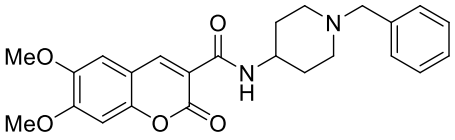

33 [*N*-(1-Benzylpiperidin-4-yl)-6,7-dimethoxy-2-oxo-2*H*-chromene-3-carboxamide]

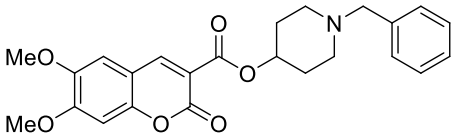

34 [1-Benzylpiperidin-4-yl 6,7-dimethoxy-2-oxo-2*H*-chromene-3-carboxylate]

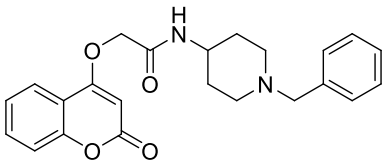

35 [*N*-(1-Benzylpiperidin-4-yl)-2-((2-oxo-2*H*-chromen-4-yl)oxy)acetamide]

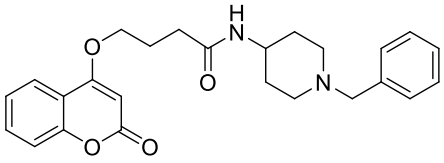

36 [*N*-(1-Benzylpiperidin-4-yl)-4-((2-oxo-2*H*-chromen-4-yl)oxy)butanamide]

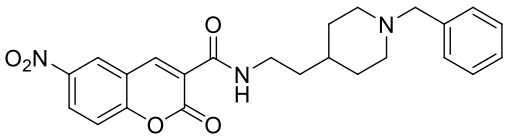

37 [*N*-(2-(1-Benzylpiperidin-4-yl)ethyl)-6-nitro-2-oxo-2*H*-chromene-3-carboxamide]

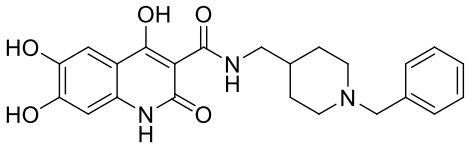

38 [*N*-((1-Benzylpiperidin-4-yl)methyl)-4,6,7-trihydroxy-2-oxo-1,2-dihydroquinoline-3-carboxamide]

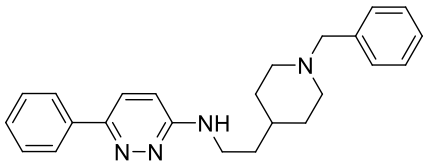

39 [*N*-(2-(1-Benzylpiperidin-4-yl)ethyl)-6-phenylpyridazin-3-amine]

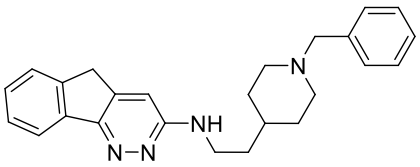

40 [*N*-(2-(1-Benzylpiperidin-4-yl)ethyl)-5*H*-indeno[1,2-*c*]pyridazin-3-amine]

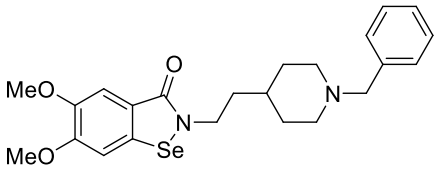

41a [2-(2-(1-Benzylpiperidin-4-yl)ethyl)-5,6-dimethoxybenzo[*d*][1,2]selenazol-3(2*H*)-one]

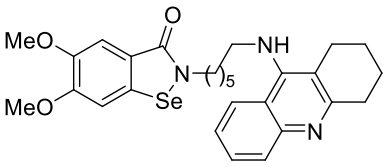

41b [5,6-Dimethoxy-2-(2-((1,2,3,4-tetrahydroacridin-9-yl)amino)hexyl)benzo[*d*][1,2]selenazol-3(2*H*)-one]

Fig. 14 Donepezil hybrids as novel cholinesterase inhibitors.

Another study by Foroumadi and Shafiee described the synthesis of series of 4-hydroxycoumarin derivatives (Razavi *et al.*, 2013), showing a moderate inhibition towards *Ee*AChE and *eq*BuChE. Among them, compounds **35** and **36** (Fig. 14) showed AChE IC_{50} values of 1.2 and 2.7 μM, respectively, and a lower inhibition potency against BuChE (**35**, IC_{50} = 45 μM; **36** IC_{50} = 41 μM). Generally, in both 2-oxoethoxy and 4-oxobutoxy series (n = 1 or 3), *N*-(1-benzylpiperidin-4-yl) derivatives **35** and **36** exhibited the strongest inhibitory activity toward AChE. Notably, when tested in a ferric reducing/antioxidant power (FRAP) assay (Benzie and Strain, 1999), these compounds revealed lower antioxidant properties than ascorbic acid.

In an additional study reported by the same group a series of coumarin-3-carboxamide derivatives connected to the *N*-benzylpiperidine moiety was described. This new set of compounds showed potent AChE inhibitory activity in the nanomolar range (Asadipour *et al.*, 2013). Particularly, compound **37** (Fig. 14) bearing an *N*-ethylcarboxamide linker and a 6-nitro substituent on the coumarin scaffold showed the highest activity of the series against *eq*AChE (IC_{50} = 0.3 nM) and the highest selectivity versus BuChE (selectivity ratio 26,300). Kinetic studies, in line with molecular modeling prediction, highlighted that this compound behaved as a dual inhibitor being able to strongly interact with the PAS and CAS of AChE. In addition, it exhibited protective properties against oxidative stress-induced cell death in differentiated PC12 cells.

In the same context, and in order to take advantage of ROS scavenging ability of the quinoline derivatives (Naito *et al.*, 1995), this scaffold was attached to a benzylpiperidine motif. Some compounds were designed and evaluated as new AChEIs and antioxidant agents (Pudlo *et al.*, 2014). They exhibited a moderate and much lower activity against *Ee*AChE than that displayed by the coumarin analogue **37** (Fig. 14). This may be ascribed to the longer side chain that separates the quinoline carboxamide from

the benzylpiperidine. The IC_{50} values obtained with the above-mentioned compounds against *Ee*AChE ranged from 3.89 to 0.11 μM. The most balanced *Ee*AChE inhibition and antioxidant activity was found for compound **38** (Fig. 14). It displayed an IC_{50} = 0.48 μM against *Ee*AChE, and over 20-fold selectivity against *eq*BuChE. Regarding its antioxidant activity, it showed a strong capacity of scavenging superoxide anion and DPPH radical with EC_{50} = 140 μM (2.8-fold more active than quercetin) and 12 μM (1.2-fold more active than quercetin), respectively.

The synthesis and the biochemical evaluation of a series of 3-aminoalkyl-6-arylpyridazine derivatives based on the structure of minaprine (Wermuth and Exinger, 1972), an original lead compound with antidepressant properties, were reported (Contreras *et al.*, 1999). Among them, compound **39** (Fig. 14), which corresponds to a bioisosteric replacement of indanone of donepezil by a pyridazine system, showed an interesting *Ee*AChE inhibitory activity (IC_{50} = 120 nM). Several structural modifications operating on this lead were reported (Contreras *et al.*, 2001). The introduction of a lipophilic group in the C-5 position of the pyridazine system was favorable for the AChE-inhibitory activity and the AChE/BuChE selectivity. Functionalization and/or replacement of the phenyl placed at C-6 position of the pyridazine system were compatible with activity, while a variation of the side chain between the pyridazine and the benzylpiperidine was not favorable for activity. Pyridazine derivative **40** (Fig. 14) was found to be the more potent *Ee*AChE inhibitor with an IC_{50} value of 10 nM.

A new series of selenpezil derivatives have been described by Huang and Li (Luo *et al.*, 2013) in which the ebselen (2-phenyl-1,2-benzisoselenazol-3(2*H*)-one) moiety was linked to an *N*-benzylpiperidine group. The authors adopted ebselen scaffold for its antioxidant and anti-inflammatory properties. Indeed, ebselen is a mimic of glutathione peroxidase (GPx) (Wilson *et al.*, 1989) and protects cells by catalysing the reduction of

peroxides with glutathione. Furthermore, another recent study indicates (Xie *et al.*, 2012) that ebselen could be used as a potential anti-AD agent on the basis of its ability to inhibit iron-induced tau phosphorylation. Next, some compounds were prepared by changing the length of the alkylene chain (from zero to four carbon atoms) and by functionalizing once or twice the benzene group of ebselen by chloro, fluoro or methoxy groups. These Selenpezils were evaluated for their capacity to inhibit ChE, as antioxidant agents against hydrogen peroxide and peroxynitrite, and as GPx mimics. The authors concluded that **41a** (Fig. 14) is a potential lead compound for the treatment of AD. It showed the highest AChE inhibitory activity of the series (IC_{50} values of 0.042 μM for *Ee*AChE, 0.097 μM for *h*AChE) and was found to be also a moderate BuChEI (IC_{50} = 1.586 μM). **41a** showed a GPx-like activity of 123.5 μM/min. Finally, the authors demonstrated the ability of compound **41a** to penetrate into the CNS as well as its safety since it presented no acute toxicity at doses up to 2000 mg/kg. It must also be highlighted that related tacrine-ebselen hybrids have been recently described (Mao *et al.*, 2013). Among them, compound **41b** (Fig. 14) which is tacrine-linked by a six-carbon spacer to 5,6-dimethoxybenzo[*d*][1,2]selenazol-3(2*H*)-one, was the most potent *Ee*AChEI (IC_{50} = 2.55 nM) and *eq*BuChEI (IC_{50} = 2.80 nM), showing also similar hydrogen peroxyde and peroxynitrite scavenging activity as ebselen, indorsing this compound as a multipotent agent candidate for the treatment of AD.

In order to develop tacrine/donepezil hybrids (Shao *et al.*, 2004) a series of compounds were obtained by replacing the indanone with different scaffolds **42-46** (Fig. 15). Interestingly, derivatives containing tacrine and benzylpiperidine moieties were the most potent among the synthesized compounds. In particular, the compound obtained by introducing scaffold **42** showed an IC_{50} value of 6.0 nM against AChE resulting more potent and selective against AChE over BuChE than tacrine (37-fold and 31-fold

respectively). Compound obtained by introducing the scaffold **43**, with a shorter spacer than **42**, resulted in potent but not selective AChE inhibition. Compound **45** had similar AChE inhibition potency as tacrine, while compounds **44** and **46** were weaker AChEIs.

The binding mode analyses of **42**-hybrids into AChE revealed that this class of compounds interacts with AChE by establishing strong interactions along the active-site gorge of the enzyme: the benzyl ring displayed a π–π stacking with W84, while the charged nitrogen of the piperidine ring makes a cation–π interaction with the phenyl ring of F330. The amide establishes a H-bond with the oxygen of Y121, finally, at the top of the gorge in the PAS of the enzyme, the acridine ring stacks with W279 by a classical π–π stacking.

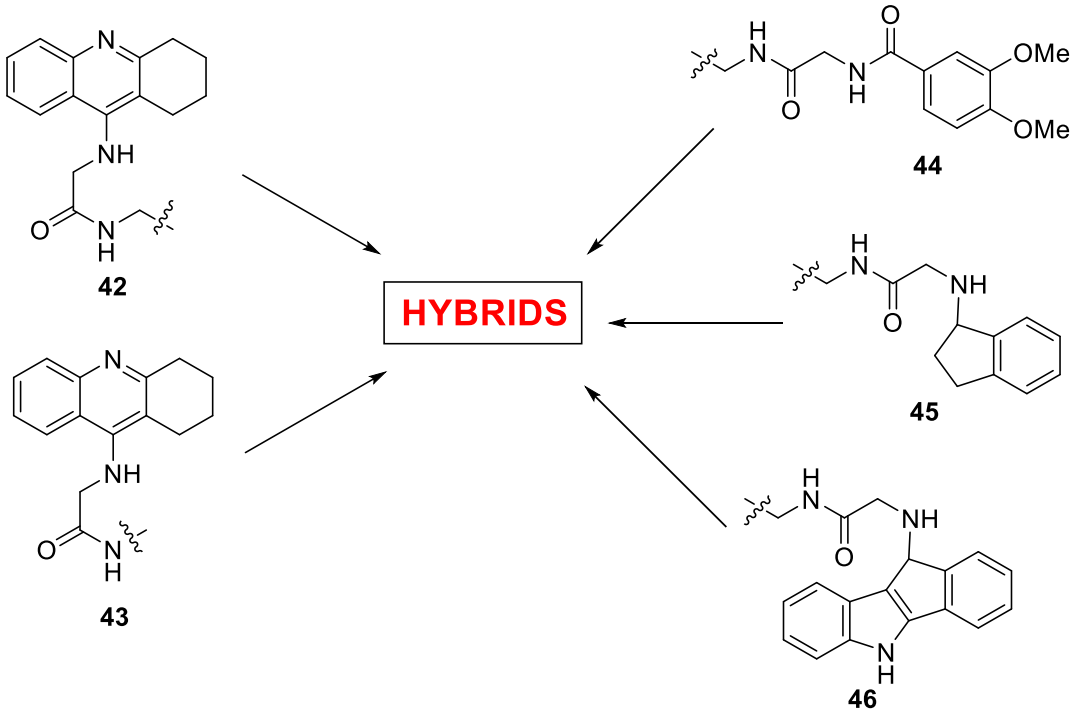

Fig. 15 Bioisosteric replacement for the indanone.

New chloropyridonepezils (Samadi et al., 2013) were designed by combining an *N*-benzylpiperidine moiety tethered by an appropriate polymethylene linker to a 2-chloropyridine-3,5-dicarbonitrile, an heterocyclic ring system identified in earlier work (Samadi *et al.*, 2010) as an interesting scaffold for inhibition of ChEs. All the obtained

compounds were tested against *h*AChE and *h*BuChE and showed submicromolar activity. In particular compound **47** (Fig. 16) was found to be a good *h*BuChEI (IC_{50} = 0.47 μM), while compound **48** (Fig. 16) was 625-fold more selective for *h*AChE over *h*BuChE and its activity against *h*AChE was comparable to that found for donepezil (IC_{50} = 0.013 μM). In addition, the calculated ADME+T properties revealed that **48** satisfied all the characteristics for a CNS-acting drug. Molecular modeling studies indicated that these compounds interact with both the PAS and CAS of the enzyme.

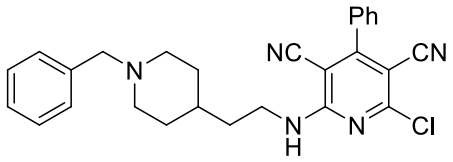

47 [2-((2-(1-Benzylpiperidin-4-yl)ethyl)amino)-6-chloro-4-phenylpyridine-3,5-dicarbonitrile]

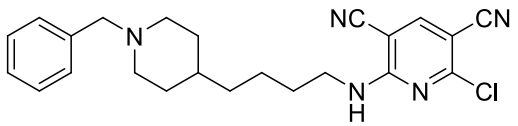

48 [2-((4-(1-Benzylpiperidin-4-yl)butyl)amino)-6-chloropyridine-3,5-dicarbonitrile]

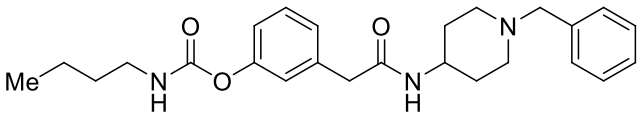

49 [3-(2-((1-Benzylpiperidin-4-yl)amino)-2-oxoethyl)phenyl butylcarbamate]

Fig. 16 Donepezil hybrids as ChEIs.

A series of novel alkyl and arylcarbamate derivatives with *N*-benzylpiperidine moieties (Wieckowska *et al.*, 2010) were designed as ChEIs. The developed compounds showed moderate activity, and some of them exhibited a higher selectivity for BuChE. The most potent and non-selective inhibitor of the series (**49**) (Fig. 16) showed a pIC_{50} = 5.24 as BuChEI and an inhibition ranging from 40% to 90% against AChE and BuChE, respectively (when tested at 100 μM). The authors carried out a preliminary kinetic study indicating the dimethylcarbamate analogue of **49** as a non-competitive AChEI and a mixed-type BuChEI, which is in agreement with the reported molecular modeling studies, displaying that this compound can bind to the PAS of the enzyme.

3.1.2. Inhibitors of cholinesterases with 5-hydroxytryptamine receptors agonist properties

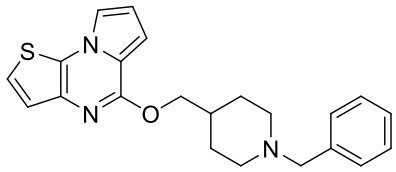

Ki 5-HT_4R = 59.9 nM; IC_{50} AChE = 551 nM

50a (**MR22493**)
[5-((1-Benzylpiperidin-4-yl)methoxy)pyrrolo[1,2-*a*]thieno[3,2-*e*]pyrazine]

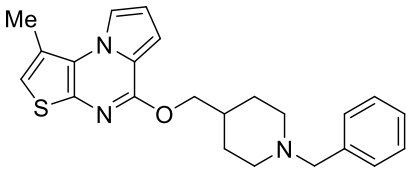

Ki 5-HT_4R = 22.0 nM; IC_{50} AChE = 165 nM

50b (**MR22322**)
[5-((1-Benzylpiperidin-4-yl)methoxy)-1-methylpyrrolo[1,2-*a*]thieno[2,3-*e*] pyrazine]

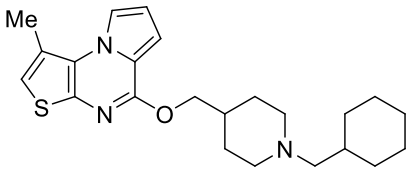

Ki 5-HT_4R = 4.2 nM; IC_{50} AChE = 95.8 nM

50c [5-((1-(Cyclohexylmethyl)piperidin-4-yl)methoxy)-1-methylpyrrolo[1,2-*a*]thieno[2,3-*e*]pyrazine]

Fig. 17 Pyrrolothienopyrazines donepezil hybrids as ChEIs and 5-HT receptors ligands.

In the context of a drug-discovery program based on the MTDL strategy for AD, Dallemagne and colleagues have reported the novel multipotent pyrrolothienopyrazines **50a** and **50b** (Fig. 17), able to inhibit *Ee*AChE activity showing additional *Guinea pig* 5-HT_4R agonist activity intended to favour the non-amyloidogenic cleavage of APP. It is noteworthy to remark that both compounds presented the *N*-benzylpiperidine at C-4 motif (Lecoutey *et al.*, 2012). Moreover, the authors also developed compound **50c** (Fig. 17), as the *N*-cyclohexyl analogue of **49**. Concerning AChE, the docking results showed that compound **50c** has very similar binding mode as donepezil in the AChE active site. Compound **50c** showed an interesting pharmacological profile deserving attention for further development.

3.1.3. Inhibitors of cholinesterase with neuroprotective effect and/or anti β-amyloid aggregation properties

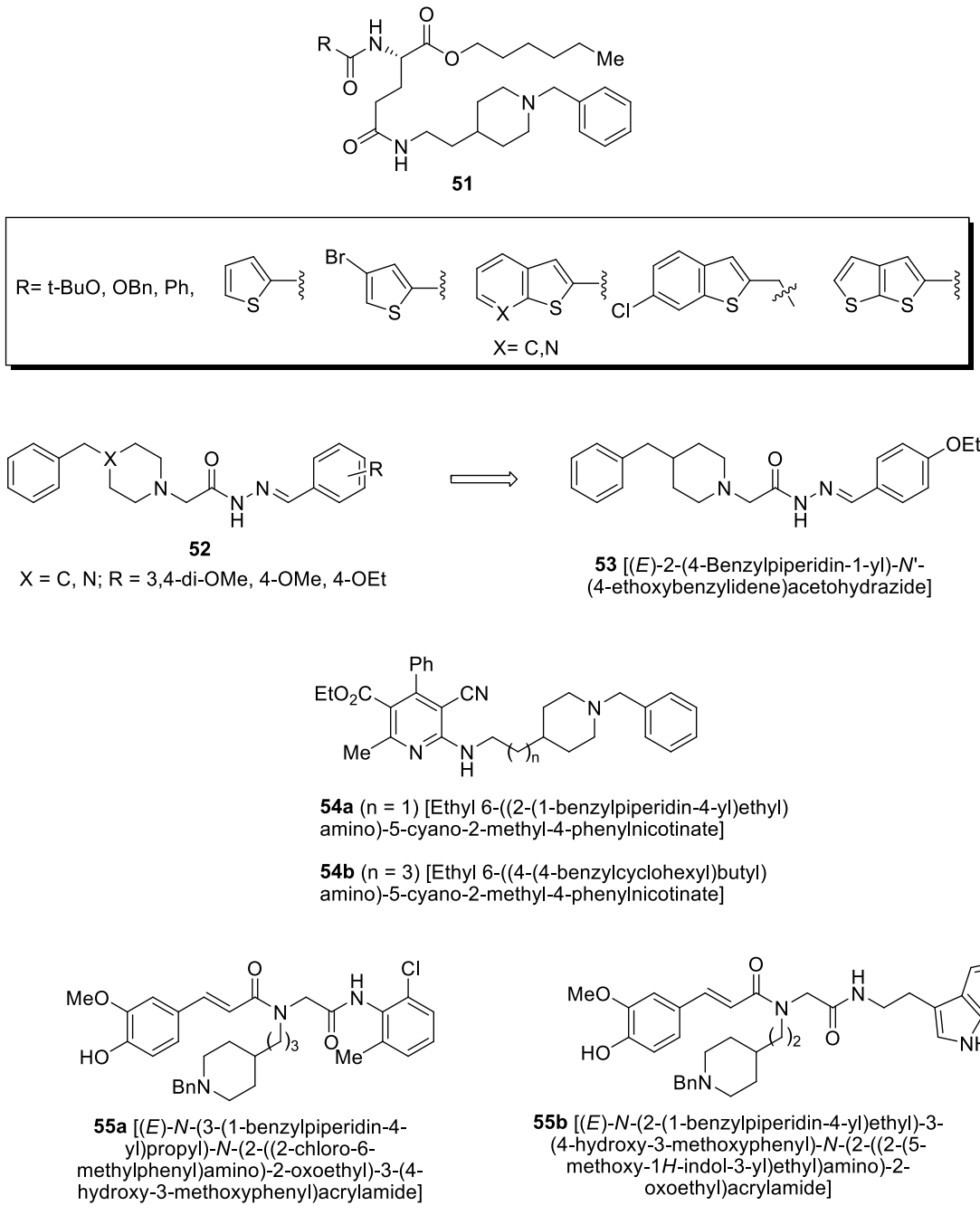

Fig. 18 Multitarget ligands as ChEIs with neuroprotective effect, antioxidant, and/or anti β-amyloid aggregation properties.

Novel multitarget compounds (Arce *et al.*, 2009) of type I represented by scaffold **51** (Fig. 18) have been investigated as potential drugs for the treatment of AD, based on L-glutamic moiety as a suitable biocompatible linker, incorporating three key pharmacophore features: (1) an *N*-benzylpiperidine fragment selected to inhibit AChE by interacting with the CAS; (2) an *N*-protecting group of the amino acid, capable of interacting with the PAS and protecting neurons against oxidative stress, and (3) a lipophilic alkyl ester that would facilitate brain penetration. All derivatives inhibited *h*AChE, showing IC_{50} values in the submicromolar range (0.10 – 0.53 μM), while they inhibited *h*BuChE in the micromolar range. These compounds also displayed neuroprotective properties against mitochondrial free radicals, showed low toxicity, and were able to penetrate into the CNS (Arce *et al.*, 2009).

Based on the evidence that the presence of the *N*-benzyl piperidine motif in ChEIs improves the inhibitory activity of a ligand against AChE by interacting with the CAS of the enzyme, and that interactions with aromatic residues located in the PAS of the AChE resulted in potent dual-binding site AChEIs, Ozadali and colleagues (Ozturan Ozer *et al.*, 2013) have reported six new *N*'-2-(4-benzylpiperidin-/piperazin-1-yl)acylhydrazone derivatives of type II (general structure **52**) (Fig. 18), which were expected to inhibit both AChE and BuChE, and to prevent Aβ aggregation by combining 4-benzylpiperidine/piperazine and methoxybenzyl scaffolds linked with *N*-acylhydrazone moiety. The analyses showed that these compounds possessed very weak and non-selective inhibitory activity against both enzymes: the most potent uncompetitive inhibitor of the series was **53** (Fig. 18). However, they all showed surprisingly high and similar effects ranging from 69% to 90% on Aβ aggregation inhibitory activity at 100 μM.

Silva and co-workers reported synthesis, molecular modeling, and pharmacological analysis of a series of new pyridonepezils and quinolinodonepezils. These compounds were designed as hybrids resulting from the juxtaposition between donepezil and selected poly-functionalized heterocyclic ring systems, such as pyridines and quinolones (Silva *et al.*, 2013). The authors observed that, while pyridonepezils behaved as selective and moderately potent *h*AChEIs, quinolinodonepezils were found to be poor *h*AChEIs. The most potent and selective *h*AChEI was represented by the ethyl analogue **54a** (Fig. 18) with an IC_{50} value against *Ee*AChE of 0.0167 μM. In addition, pyridonepezils and quinolinodonepezils proved to be more potent inhibitors of *Ee*AChE than *h*AChE, with the most potent *Ee*AChEI being ethyl **54b** (IC_{50} (*h*AChE) = 0.25 μM) (Fig. 18), which exhibited the same inhibitory potency of donepezil against *h*AChE. In the pyridonepezil series, the inhibition of *h*AChE increased as the length of the linker enlarged, with compound **54b** being the most potent and selective for *h*AChE. Furthermore, most of the new molecules significantly prevented the decrease in cell viability caused by $A\beta_{1-42}$, and were effective in preventing the enhancement of $A\beta_{1-42}$ production induced by AChE, and may act as antagonists of voltage sensitive calcium channels, since they significantly prevented the Ca^{2+} influx evoked by KCl depolarization. The data indicated that these donepezil-like compounds are attractive multipotent molecules for the potential treatment of AD (Silva *et al.*, 2013).

3.1.4. Inhibitors of cholinesterases with antioxidant capacity

New donepezil-ferulic acid hybrids (Benchekroun *et al.*, 2015b) were designed and prepared by combining the potent antioxidant ferulic acid, isonitriles, and benzylpiperidines substituted with alkylene-linkers of different length, in a “one-pot” Ugi four-component reaction. Not surprisingly, all the hybrids showed strong antioxidant activity based on the ORAC-FL assay. However, their ChE inhibition relied on structure.

For *Ee*AChE inhibition, it was observed that the longer the linker, the more potent the inhibitors resulted. For the inhibition of *eq*BuChE, the two best compounds bearing an ethylene and propylene linker were substituted with a melatonin motif, a potent and well-known antioxidant agent. The most potent compounds identified were hybrids **55a** and **55b** (Fig. 18). Compound **55a** showed non-selective inhibition against AChE (IC_{50} = 29.3 nM), only 1.4-fold less potent than donepezil, and BuChE (IC_{50} = 52.3 nM). Product **55b** was characterized by ORAC assay as a strong antioxidant agent, more potent than ferulic acid or melatonin, (8.71 trolox equivalents), and also behaved as a potent and selective *eq*BuChEI (IC_{50} = 10.39 nM).

3.2. Inhibitors targeting cholinesterases and other enzymes

3.2.1. Inhibitors of cholinesterases and beta secretase and other pharmacological targets

Zhu and co-workers have explored and reported novel multipotent effective drugs for the treatment of AD, characterized by dual AChE and BACE-1 inhibition properties. Compounds belonging to the scaffold **56** (Zhu *et al.*, 2009) (Fig 19) are hybrids resulting from the juxtaposition of pharmacophore of donepezil with isophthalamide, a widely used pharmacophore in BACE-1 inhibitors (Hom *et al.*, 2004).

Among them, the enantiomerically pure inhibitor **57** (Zhu *et al.*, 2009) (Fig. 19) showed good dual potency in an enzyme inhibitory activity test (*h*BACE-1: IC_{50} = 0.567 μM; rat cortex AChE: IC_{50} = 1.83 μM). It also displayed excellent inhibitory activity on Aβ production in APP-transfected HEK293 cells (IC_{50} = 98.7 nM) and a mild protective effect against hydrogen peroxide-induced injury in PC12 cells. Furthermore, intracerebroventricular injection of **57** into APP transgenic mice caused a 29% reduction of $A\beta_{1–40}$ production. To summarize, compound **57** was identified as a good lead compound for further studies and it may represent a good example of successful MTDL

approach to treat AD by simultaneously inhibiting AChE and BACE-1 enzymes and reducing endogenous $A\beta_{1\text{-}40}$ production in APP transgenic mice. Compound **57** was also used to prepare new pyrazoles as C-terminus of selective BACE-1 inhibitors (Zou *et al.*, 2013).

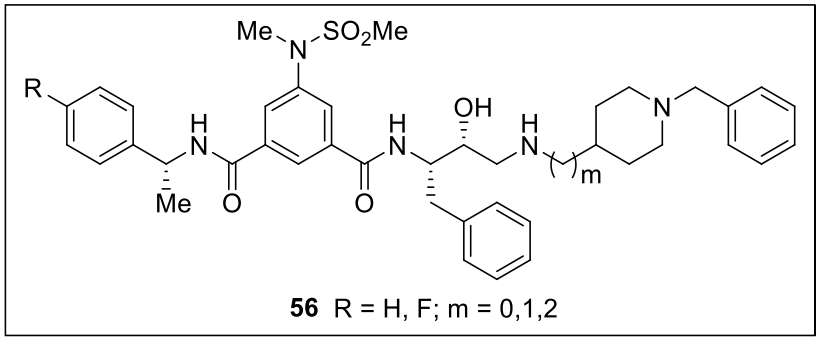

56 R = H, F; m = 0,1,2

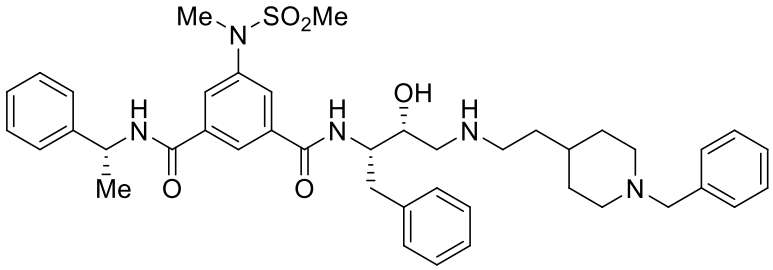

57 [N^1-((2*S*,3*R*)-4-((2-(1-Benzylpiperidin-4-yl)ethyl)amino)-3-hydroxy-1-phenylbutan-2-yl)-5-(*N*-methylmethylsulfonamido)-N^3-((*R*)-1-phenylethyl) isophthalamide]

Fig. 19 New multipotent AChE and BACE-1 inhibitors.

A novel series of quinoxaline-based MTDLs for AD treatment have been designed bearing core structural elements required for H_3R antagonists, BACE-1 and AChE inhibitors, by using compound **58** and **59** (Fig. 20) as reference structures (Huang *et al.*, 2011a). Among the synthesized quinoxalines compound **60** (Fig. 20) was the most effective MTDL, showing a potent activity against H_3R/AChE/BACE-1 (H_3R antagonism, IC_{50} = 280 nM; H_3R inverse agonism, IC_{50} = 189.3 nM; AChE, IC_{50} = 483 nM; BACE-1, 46.64 % inhibition at 20 μM) and high selectivity over $H_1R/H_2R/H_4R$.

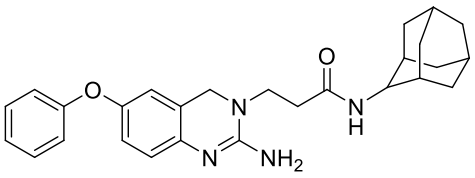

58 [*N*-((1*r*,3*r*,5*r*,7*r*)-Adamantan-2-yl)-3-(2-amino-6-phenoxyquinazolin-3(4*H*)-yl)propanamide]

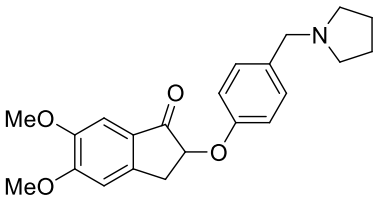

59 (BYYT-25) [5,6-Dimethoxy-2-(4-(pyrrolidin-1-ylmethyl)phenoxy)-2,3-dihydro-1*H*-inden-1-one]

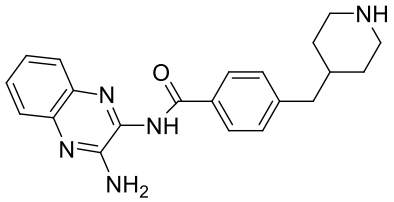

60 [4-((1λ^2-Piperidin-4-yl)methyl)-*N*-(3-aminoquinoxalin-2-yl)benzamide]

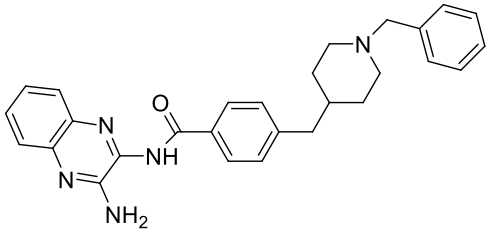

61 [*N*-(3-Aminoquinoxalin-2-yl)-4-((1-benzylpiperidin-4-yl)methyl)benzamide]

Fig. 20 Quinoxaline-based ChE and BACE-1 inhibitors and histamine receptor antagonist.

Very interestingly, compound **61**, (Fig. 20) bearing the *N*-benzylpiperidine, compared to product **60**, showed no H_3R inverse agonist action and AChE inhibition, while either the BACE-1 (8.96 % inhibition at 20 μM), and the H_3R antagonism activities were very poor (Huang *et al.*, 2011a).

Mohamed *et al.* have synthesized a series of *N*-benzylpyrimidin-4-amines bearing the benzylpiperidine pharmacophoric group at C-2 position as multitarget AD therapeutics (Mohamed *et al.*, 2012). Their ChEs inhibition, anti-Aβ-aggregation (AChE- and self-induced), and BACE-1 inhibition properties were evaluated in an effort to identify new multifunctional lead candidates to treat AD. As a result, N^2-(1-benzylpiperidin-4-yl)-N^4-(3,4-dimethoxybenzyl)pyrimidine-2,4-diamine **62** (Fig. 21) was proposed as a new lead compound with a dual ChE (AChE IC_{50} = 9.9 μM; BuChE IC_{50} = 11.4 μM), Aβ-aggregation (AChE-induced = 59.3%; self-induced = 17.4% at 100 μM),

and BACE-1 (34% inhibition at 10 μM) inhibitory profile along with good cell viability (81% neuroblastoma cell viability at 40 μM).

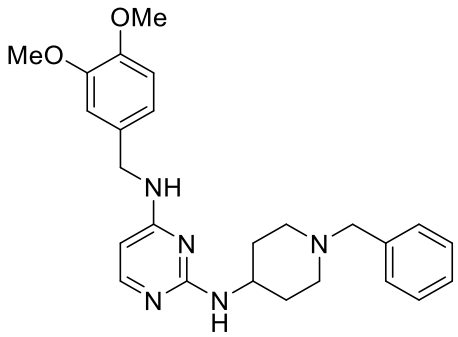

62 [N^2-(1-Benzylpiperidin-4-yl)-N^4-(3,4-dimethoxybenzyl)pyrimidine-2,4-diamine]

Fig. 21 Pyrimidine donepezil hybrid as MTDL.

3.2.2. Inhibitors of cholinesterases and monoamine oxidases

An elegant approach by Marco-Contelles and co-workers reported original, innovative and promising data. They designed new hybrids by combining the benzylpiperidine motif present in donepezil with PF9601N, a potent and selective MAO-B inhibitor, developed in Fernández-Álvarez group at the IQOG (CSIC, Madrid, Spain) (Perez *et al.*, 1999). Both reference molecules' cores were linked by chains of different lengths, whose nature had a significant effect on the MAO, AChE, and BuChE inhibition (Bolea *et al.*, 2011). Hybrid **63** (Fig. 22) was found to be the most balanced and multipotent molecule against the four targeted enzymes (*r*MAO-A IC_{50} = 5.2 nM, *r*MAO-B IC_{50} = 43 nM; *Ee*AChE IC_{50} = 0.35 μM, *eq*BChE IC_{50} = 0.46 μM) while being able to inhibit the $A\beta_{1\text{-}42}$ self-aggregation (32.4% at 100 μM), and the AChE-induced $A\beta_{1\text{-}40}$ aggregation (47.8% at 10 μM). Based on these preliminary and encouraging results, compound **63** was further investigated, showing *inter alia* anti-apoptotic, and antioxidant properties (Bolea *et al.*, 2013; del Pino *et al.*, 2014; Esteban *et al.*, 2014), as well as favorable BBB permeability (Stasiak *et al.*, 2014). Overall, these results indicate that **63**

is a potential MTDL hit for further development for the treatment of AD. Compound **63** has been used as a valuable scaffold for the novel multifunctional compounds endowed with MAO and ChE inhibition properties (Bautista-Aguilera *et al.*, 2014c; Samadi *et al.*, 2012).

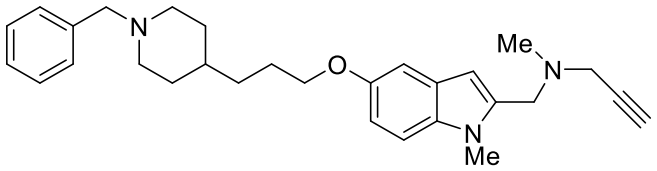

63 (ASS234) [*N*-((5-(3-(1-Benzylpiperidin-4-yl)propoxy)-1-methyl-1*H*-indol-2-yl)methyl)-*N*-methylprop-2-yn-1-amine]

Fig. 22 Donepezil-PF9601N hybrid as ChEI and MAOI.

After these promising results, Marco-Contelles and colleagues (Wang *et al.*, 2014; Wu *et al.*, 2015) designed various **ASS234** derivatives (**64a** and **64b**) resulting by connecting *N*-benzylpiperidine to M30 (**65**) (Avramovich-Tirosh *et al.*, 2007) and HLA20A (**66**) (Zheng *et al.*, 2009) (Fig. 23). M30 is a potent brain selective MAO-A/B inhibitor and a neuroprotective biometal-chelator while HLA20A is a novel pro-chelator with improved cytotoxicity profile exhibiting poor affinity for metal ions while not being activated to an effective chelating agent by binding and inhibiting AChE. In addition, HLA20A is able to modulate APP and to reduce Aβ aggregation.

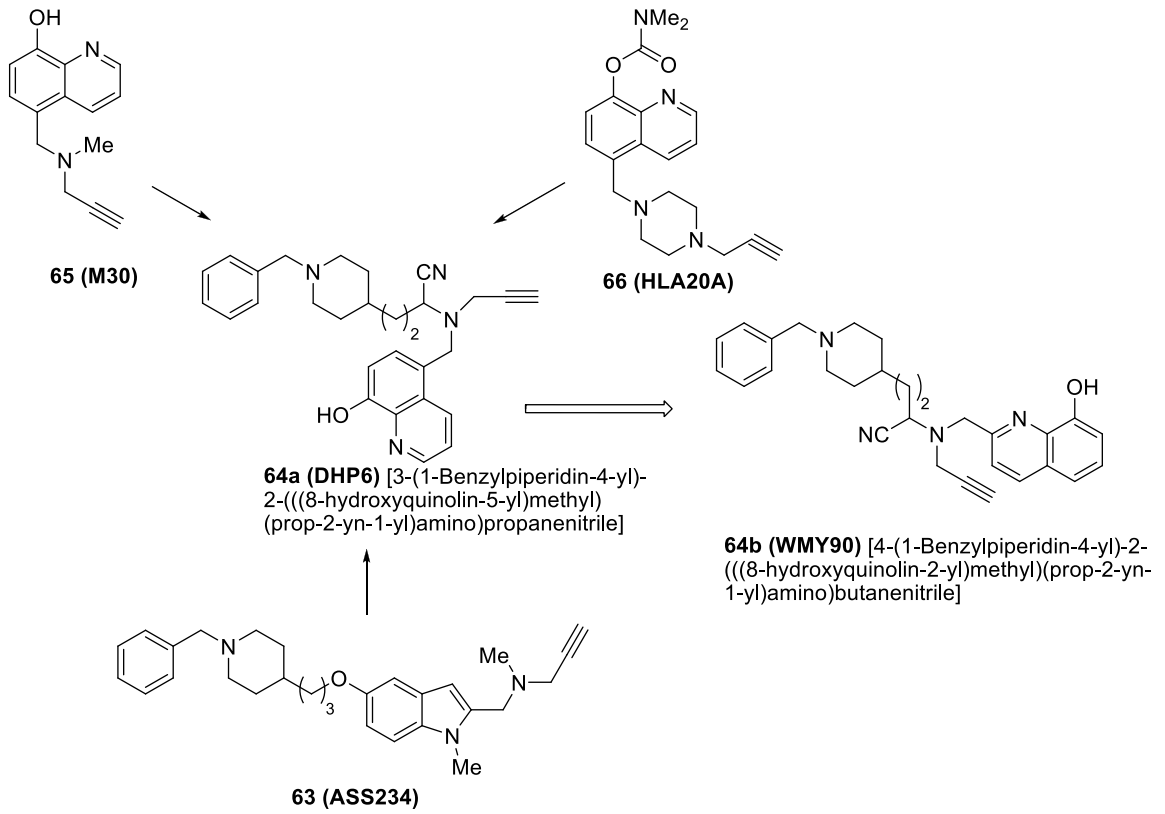

Fig. 23 ASS234 derivative (**64a** and **64b**) as multipotent compound in AD drug discovery.

Seven compounds were prepared and evaluated on several targets, particularly derivative **64a** (Fig. 23), identified as a multi-functional chelator for biometals able to interact with two key enzymatic systems involved in AD, represents a new lead compound for the potential treatment of this disease. Indeed, **64a** showed an irreversible and moderate inhibition of MAO-A and B compared to M30, with IC_{50} values of 6.2 μM and 10.2 μM, respectively. Moreover, this compound was found as an *Ee*AChEI able to complex biometals such as Cu(II) and Zn(II) and Fe(III). In a theoretical ADMET analysis, **64a** showed proper drug-like properties and brain penetration capacity for CNS activity. In addition, **64a** presented less toxicity than donepezil at high concentrations in an *in vitro* model of toxicity using HepG2 cells. Furthermore, compound **64a** was also able to enhance cognitive functions in scopolamine-induced learning deficits in healthy

adult mice. Very recently, the same authors (Wu *et al.*, 2015) have developed **64b** as a novel analogue of **64a** characterized by a similar multifunctional profile which was improved in terms of activity against ChEs (*h*AChE IC_{50} = 29 nM; Ki = 15 nM; *h*BuChE IC_{50} = 39 nM; Ki = 52 nM) and with MAO enzymes selectivity (MAO-A IC_{50} = 10.1 μM; MAO-B IC_{50} > 100 μM). **64b** was found to be a strong complexing agent for Cu(II) and Zn(II), while the effect on iron resulted less evident, showing also moderate antioxidant properties.

3.3. Ligands of sigma-1 receptors

The *N*-benzylpiperidine moiety and its derivatives have been largely studied to design compounds binding sigma 1 (σ_1) receptors. The σ binding sites were originally defined and classified as opioid receptor subtypes (Martin *et al.*, 1976). Two different subtypes, designated σ_1 and σ_2, were identified (Hellewell *et al.*, 1994). The σ_1 receptors may be involved in regulating a variety of neurotransmitters in the CNS, including cholinergic (Senda *et al.*, 1998; Senda *et al.*, 1996) dopaminergic (Kamei *et al.*, 1997), and glutamatergic systems (Bergeron *et al.*, 1996; Maurice and Privat, 1997). They are involved in many cellular functions and biological processes (Maurice and Su, 2009), including neuroprotection (DeCoster *et al.*, 1995; Nakazawa *et al.*, 1998; Tchedre and Yorio, 2008). Many investigations have documented the involvement of σ receptors in some important pathways implicated in different neurodegenerative illnesses such as AD (Huang *et al.*, 2011b) and Parkinson's disease (Mishina *et al.*, 2005).

In order to develop selective σ_1 ligands with antioxidant properties, some compounds were prepared by connecting a natural antioxidant moiety lipoic acid to piperidine or piperazine derivatives (Prezzavento *et al.*, 2013). In this work, the authors found that the most promising compounds were those bearing the *N*-benzylpiperidine moiety. In particular, among the synthesized analogues, compound **67** (Fig. 24) displayed

the highest affinity and selectivity for the σ_1 receptors (Ki σ_1 = 5.5 nM; Ki σ_2/σ_1 = 414). In addition, **67** showed *in vivo* anti-opioid effects on kappa opioid (KOP) receptor-mediated analgesia and reduced the swelling and the oxidation of thiol groups induced by calcium ions in rat liver and brain mitochondria.

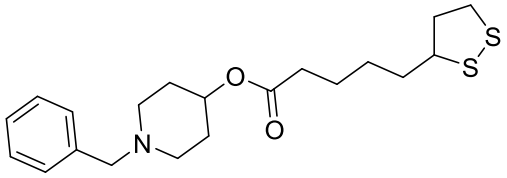

67 [1-Benzylpiperidin-4-yl 5-(1,2-dithiolan-3-yl)pentanoate]

Fig. 24 Donepezil lipoic acid hybrid as MTDL.

The work reported by Zampieri (Zampieri *et al.*, 2009a) is based on a receptor model proposed by Glennon (Glennon *et al.*, 1994) (Fig. 25) which includes an amine binding site flanked by two hydrophobic domains, the primary hydrophobic binding site that binds phenyl ‘‘B’’ and a secondary binding site that binds phenyl ‘‘A’’, placed at optimal reciprocal distances. The authors described the synthesis of a series of new benzo[*d*]oxazol-2(3*H*)-one derivatives variously functionalized on the *N*-benzyl moiety.

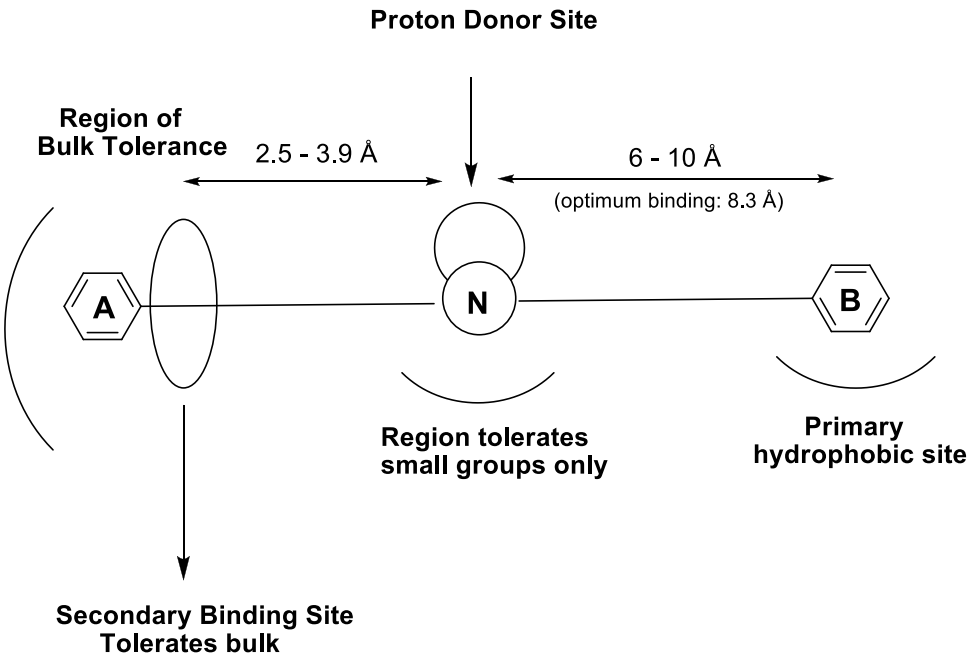

Fig. 25 Pictorial presentation of Glennon's model.

In this study, the most potent compound was the one bearing a chlorine atom at C-4 position of the benzene ring (**68)** (Fig. 26). This compound showed the highest affinity and selectivity toward σ_1 receptors (about 4000-fold). Interestingly, the non-substituted benzene analogue **69** (Fig. 26) was less active than chlorine derivatives but exhibited an interesting affinity for the σ_1 receptor (Ki = 3.6 nM) compared with the reference haloperidol and (±)-pentazocine. In another study, (Zampieri *et al.*, 2009b) benzo[*d*]oxazol-2(3*H*)-one derivatives were prepared and employed for a pharmacophore modelling study. A predictive pharmacophore was generated by means of Catalyst software package (Catalyst, version 4.9; Accelrys Inc.: San Diego, CA) by using the HypoGen method. This pharmacophore consists of five features: two hydrophobic aromatics, one hydrophobic aliphatic, one H-bond acceptor, and one positive ionisable group. The computational tool could reasonably predict the affinity of the test set molecules with a correlation coefficient of 0.896 and showed the best statistical

significance among all the generated models. In addition, the authors presented a second generation of benzylpiperidine-4-carboxamides, **70** and **71** (Fig. 26) able to bind σ_1 receptor with excellent affinity (Ki σ_1 = 48.1 nM and 22.5 nM, for compound **70** and **71**, respectively).

The same group (Laurini *et al.*, 2012) identified a novel series of acetamide derivatives and particularly **72** (Fig. 26), which showed an excellent affinity (Ki = 0.09 nM) toward the σ_1 receptor. The results obtained supported the previously developed pharmacophore model, in fact **72** was able to match all the features of the model. Their recently developed analogues (Zampieri *et al*., 2014) displayed lower affinity than **72** but remained strongly active toward the σ_1 receptor (Ki = 13.6 nM) with higher selectivity than σ_2 **73** (Fig. 26).

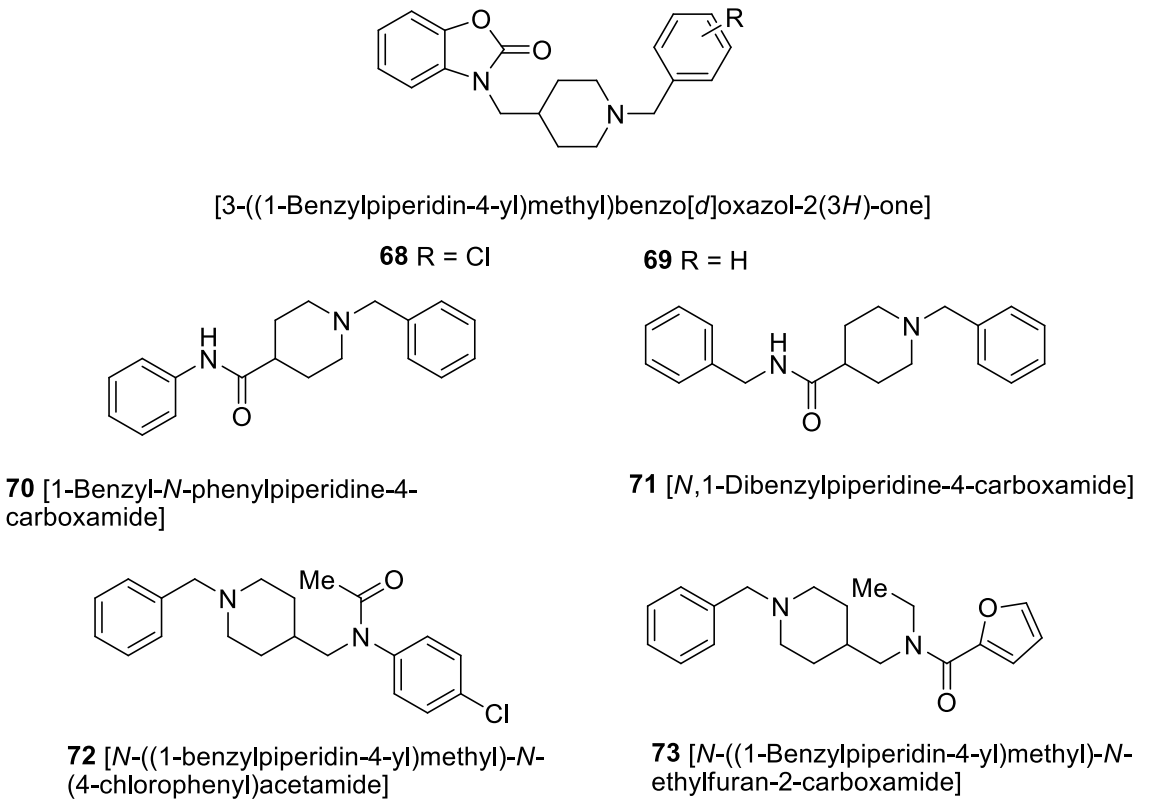

Fig. 26 Compounds developed by two research group directed by Zampieri and Pricl.

March *et al.* designed analogues of haloperidol: *N*-(1-benzylpiperidin-4-yl)phenylacetamide **74** (Fig. 27) (Huang *et al.*, 1998) and *N*-(1-benzylpiperidin-4-yl)arylacetamide **75** (Fig. 27) (Huang *et al.*, 2001a). For the first series, different substituents were introduced at various positions on the phenyl ring of the phenylacetamide moiety and, when tested for their binding affinities for σ_1 and σ_2 receptors, they showed higher affinities for σ_1 receptors. It was also noted that the introduction of hydrophilic substituents (NO_2, OH, OMe, and NH_2) caused a reduction of the affinity for the σ_1 receptor. The most potent and selective compounds were **74** (Fig. 27) and its analogues bearing a fluorine substituent at position 2, which possess critical distances according to Glennon's model. In the second series, the phenyl group of **74** (Fig. 27) was replaced by different aryl groups. However, these latter did not lead to an improvement of affinity and selectivity for the σ_1 receptor. The best compound **75** (Fig. 27) showed a Ki = 3.93 nM and 100-fold selectivity.

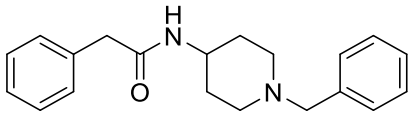

74 [*N*-(1-Benzylpiperidin-4-yl)-2-phenylacetamide]

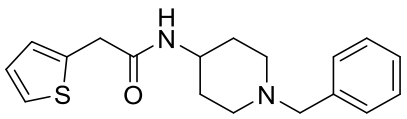

75 [*N*-(1-Benzylpiperidin-4-yl)-2-(thiophen-2-yl) acetamide]

Fig. 27 Compounds developed by March and co-workers.

In an attempt to find new compounds able to bind dopamine D_2 and D_3 receptors, a series of 2-(2,3-dimethoxyphenyl)-4-(aminomethyl)imidazole analogues (Huang *et al.*, 2001b) were developed and evaluated also for their binding affinities to σ_1 and σ_2 receptors. Among them, two compounds containing the *N*-benzylpiperidine moiety **76** and **77** (Fig. 28) showed a potent affinity (Ki = 33.6 nM) and good selectivity for σ_1 versus σ_2, D_2 and D_3 and equal to 4, 50 and 53, respectively. The bromo-substituted

analogue **77** presented 2.5-fold lower affinities against σ_1 than **76**, but comparable affinities were observed for D_3 and 3.5-fold higher affinities for D_2.

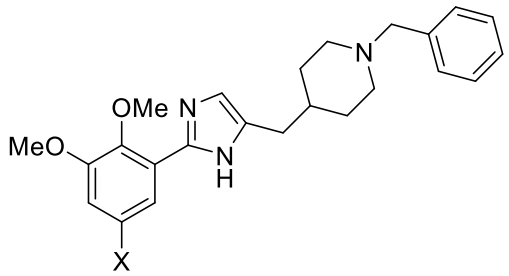

76 X=H

77 X = Br

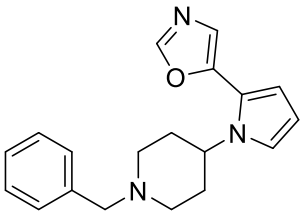

78 [5-(1-(1-Benzylpiperidin-4-yl)-1*H*-pyrrol-2-yl)oxazole]

Fig. 28 Donepezil imidazole hybrids with affinities against dopamine and σ receptors and piperidinylpyrole as dopamine receptors binding.

A series of piperidinylpyrole (Haubmann *et al.*, 1999) was synthesized according to the modified Paal-Knorr reaction and evaluated on dopamine receptor subtypes. Eleven products were prepared and evaluated on D_1, D_2, D_3 and D_4 receptors leading to the following conclusions: the strongest D_4 recognition was exhibited by the oxazolylpyrroles **78** (Fig. 28), which indicated higher affinity (Ki = 63 nM) but reduced selectivity over the D_2 and D_3 subtypes. Compared to clozapine, the compound showed 4-fold lower affinity for the human D_4 receptor and comparable D_3 binding affinity. However, the selectivity for D_4 over D_2 and D_1 was significantly higher.

4. Computational approaches

In the continuous effort to discover potential DMAAD, molecular modeling has played a crucial role for the rational design and the identification of novel chemical entities behaving as ChEIs. The release of a consistent number of 3D structures of ChEs in the Protein Data Bank (PDB), which were also employed in a number of Structure-Based Drug Design (SBDD) approaches (Bajda *et al.*, 2013; Chen *et al.*, 2012a; Remya *et*

al., 2013) has also enabled molecular modelling approaches which, in this field, were mainly used for explaining the activity of enzyme inhibitors based on the X-ray structure of the enzyme in complex with different ligands. In the case of tacrine- and donepezil-like compounds molecular modelling was mainly used, in the most recent reports, for comparing the predicted binding mode of a novel derivative with the crystal structures of the reference ligands (Fig. 2). Accordingly, the most relevant examples have already been discussed allover the text.

Neverthless the ligand-based approach still exerts a very important role in ChEIs drug discovery. In particular, many computational efforts based on Ligand-Based Drug Design (LBDD), mainly 3D-quantitative structure−activity relationship (QSAR) approaches, have been successfully developed and also employed in virtual screening procedures aiming at discovering novel scaffolds. Further, some ligand-based models have been employed to rationally decorate existing scaffolds in order to optimize their AChE inhibition properties. All these aspects have been widely reviewed elsewhere (Bermudez-Lugo *et al.*, 2011; Speck-Planche *et al.*, 2012a, b) and we herein will limit our description to the most fruitful and recent QSAR approaches for providing a picture of the state-of-the-art on LBDD in ChEIs field in the modern computational era. A specific focus will be given to those efforts that effectively led to the identification of novel ChEIs. Accordingly, the reports concerning the rationalization of AChE inhibition of known or newly synthesized compounds using computational techniques such as 3D-QSAR/pharmacophore modeling were not taken into account. MD simulation have represented, as discussed in paragraph 4.2, a key step for the comprehension of AChE trafficking and functioning for orienting the design of potent ChEIs.

4.1 Quantitative structure−activity relationship (QSAR) studies

In last 50 years, the field of QSAR modeling (Hansch *et al.*, 1962) has been one of the most commonly used theoretical approach to model the biological and physical properties of compounds. Statistically-based QSAR approaches are widely developed and applied in helping to guide lead optimization and computer-aided-drug-design (CADD), as crucial initial step in drug discovery (Cherkasov *et al.*, 2014; Cramer, 2012).

The QSAR approach and related chemoinformatic methods have been successfully applied in polypharmacology for studying multitarget compounds and to rationally design ligands endowed with unique polypharmacological profile (Besnard *et al.*, 2012; Ning *et al.*, 2009). For multipotent ligands drug design, the development of multiple QSAR models considering each target of interest have been applied in order to evaluate the potential ability of designed ligands to interact with all the considered targets. The cross-analysis of the results obtained from each model can indicate if a compound is suitable for being a MTDL (Cherkasov *et al.*, 2014).

The rational design of compounds characterized by unique polypharmacological profile, coupled with overall safety, is performed by a sequence of steps. The process begins with the design of a series of chemical analogues of an identified MTDL lead, followed by the *in silico* prediction of their polypharmacological profiles in turn formulated by using the appropriate ligand-based QSAR models. This approach will prioritize for synthesis only the compounds predicted to possess the desired multitarget activities (Besnard *et al.*, 2012; Hajjo *et al.*, 2010; Hajjo *et al.*, 2012; Zhang *et al.*, 2013).

A successful example of this approach was reported where the *in silico* generated analogues of the AChEI donepezil were QSAR-tested for their polypharmacology toward a series G-protein-coupled receptors, and more that 75% of ligand-target predictions were experimentally confirmed (Besnard *et al.*, 2012).

The MAO-A/B and AChE/BuChE inhibitory activities of multitarget donepezil and tacrine derivatives (Bautista-Aguilera *et al.*, 2014a; Bolea *et al.*, 2013; Bolea *et al.*, 2011; Perez *et al.*, 1999; Samadi *et al.*, 2011) were used in recent 3D-QSAR studies and lead-improving work with multipotent compound **63** (**ASS234)** (Fig 22) (Bautista-Aguilera *et al.*, 2014a; Bautista-Aguilera *et al.*, 2014b). Based on the 3D-QSAR studies it was concluded that substitution in *ortho* position of the benzyl moiety of **ASS234** with small groups could enhance the MAO-A, MAO-B, and AChE inhibiting activity while substitution with bulky substituents at *para* position of the benzyl moiety could decrease BuChE inhibiting activity of the **ASS234** derivatives. The designed **ASS234** analogues were synthesized and few ligands were identified as very potent MAO/ChE inhibitors. The novel donepezil-indolyl MAO/ChE inhibitors confirmed the quality of the generated 3D-QSAR model (Bautista-Aguilera *et al.*, 2014c).

A very interesting work combining molecular mechanics to QSAR technique was carried out by Gharaghani and colleagues who flanked MD simulation to docking studies for developing a structure-based QSAR model which was able to predict AChE inhibitory activity of known compounds as well as to find novel AChEIs (Gharaghani *et al.*, 2013). Another relevant protocol combining different computational approaches was described by Valsani and co-workers with the aim to design novel AChEIs (Valasani *et al.*, 2013). By using 2D-QSAR, pharmacophore modeling, ADME descriptors and molecular docking, the authors reported the rational design of AChEIs more potent and selective with respect to donepezil. Similarly, Mishra and collaborators, by using pharmacophore modeling and molecular docking, evaluated *in silico* a comprehensive virtual screening protocol to discover potent AChEIs (Mishra and Basu, 2013). Concerning pure ligand-based methods, a ligand-based approach was recently developed by Abuhamdah and colleagues, allowing them to discover novel derivatives with a good inhibitory activity

against *h*AChE. In particular, they reported the generation of a pharmacophore model by using 85 AChEIs. Subsequently, they implemented a genetic algorithm-based QSAR modeling to select optimal combination of pharmacophore models and 2D physicochemical descriptors able to explain the bioactivity variation among training set compounds. Finally, the resulting model was employed to screen the National Cancer Institute (NCI) chemical database, and the outcome of this approach was the identification of 24 AChEIs with potencies in the low micromolar range, where the best molecule **79** (Fig. 29) showed an IC_{50} value of 1.0 μM (Abuhamdah *et al.*, 2013). By using a classical structure-affinity relationship (SAR) approach, Richmond and collaborators identified a polyhydroxylated sulfated steroid as promising novel scaffold able to inhibit AChE (Richmond *et al.*, 2013).

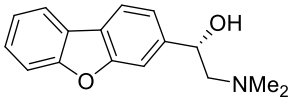

79 [(*S*)-1-(Dibenzo[*b*,*d*]furan-3-yl)-2-(dimethylamino)ethan-1-ol]

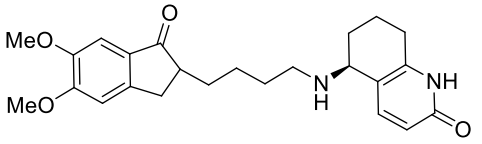

80 [(5*R*)-5-((4-(5,6-Dimethoxy-1-oxo-2,3-dihydro-1*H*-inden-2-yl) butyl)amino)-5,6,7,8-tetrahydroquinolin-2(1*H*)-one]

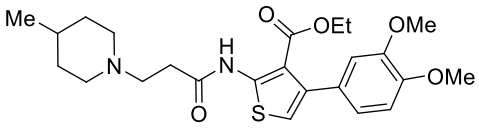

81 [Ethyl 4-(3,4-dimethoxyphenyl)-2-(3-(4-methylpiperidin-1-yl)propanamido)thiophene-3-carboxylate]

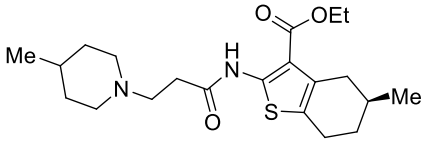

82 [Ethyl (*S*)-5-methyl-2-(3-(4-methylpiperidin-1-yl) propanamido)-4,5,6,7-tetrahydrobenzo[*b*] thiophene-3-carboxylate]

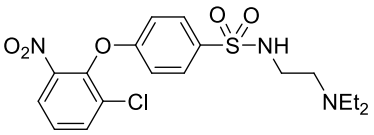

83 [4-(2-Chloro-6-nitrophenoxy)-*N*-(2-(diethylamino)ethyl)benzenesulfonamide]

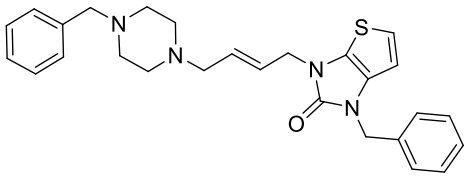

84 [(*E*)-1-Benzyl-3-(4-(4-benzylpiperazin-1-yl) but-2-en-1-yl)-1,3-dihydro-2*H*-thieno[2,3-*d*]imidazol-2-one]

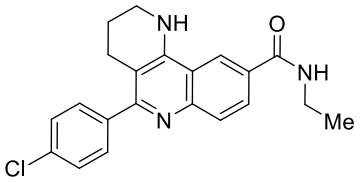

85 [5-(4-Chlorophenyl)-*N*-ethyl-1,2,3,4-tetrahydrobenzo[*h*][1,6]naphthyridine-9-carboxamide]

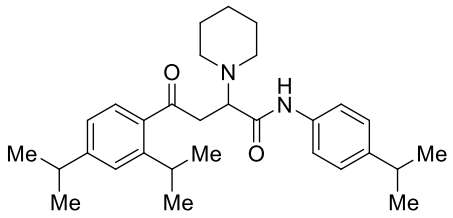

86 [4-(2,4-Diisopropylphenyl)-*N*-(4-isopropylphenyl) -4-oxo-2-(piperidin-1-yl)butanamide]

Fig.29 Structure of the compunds selected by ligand-based approaches.

Interestingly, a rational design performed by Hu and colleagues provided hybrid molecules containing donepezil and huperzine fragments. Following this approach the potent and selective derivative **80** (Fig. 29) showing an IC_{50} value of 9 nM was identified (Hu *et al.*, 2013). Similarly, Li and colleagues, by using a ligand-based approach, were able to rationally design tacrine-flavonoid hybrid compounds interacting simultaneously with CAS, PAS and mid-gorge sites of AChE. Particularly, compound **17** (Fig. 9) was found to be highly potent showing a balanced inhibitory profile against ChEs and $A\beta_{1-42}$ spontaneous aggregation (Li *et al.*, 2013a). Gupta and collaborators reported a successful

ligand-based virtual screening protocol employing the pharmacophore modeling technique. The 3D model was used as a query in a sequential virtual screening protocol to filter three small compound databases which allowed the selection of nine compounds for biological evaluation and two lead compounds **81** and **82** (Fig. 29), possessing low micromolar AChE inhibitory activity, were found (Gupta *et al.*, 2011). By adopting divergent-SAR analysis, Andersson and co-workers analyzed the molecular interactions between AChE and two compound classes consisting of *N*-[2-(diethylamino)ethyl]benzenesulfonamides and *N*-[2-(diethylamino)ethyl]benzenemethanesulfonamide. By combining SAR analysis, synthesis, enzymatic assays, X-ray crystallography, and thermodynamic profiling, the authors identified and crystallized a potent inhibitor **83** (Fig. 29) with AChE (Andersson *et al.*, 2013).

The ligand-based approach demonstrated to be also very helpful in the selection of AChEIs as reported by Chaudhaery and collaborators (Chaudhaery *et al.*, 2010) which, by using pharmacophore-based virtual screening approach, and employing 3D-predictive pharmacophore model and in-house virtual library, identified novel derivatives able to inhibit AChE. In particular, the predictive pharmacophore model (correlation= 0.955) with one H-bond donor and three hydrophobic features was developed using HypoGen, implemented in Discovery Studio suite, on a training set of 24 carbamates as AChEIs. The model was validated on a test set of 40 carbamates (correlation = 0.844) and subsequently used in the virtual screening protocol employing a virtual chemical library. This approach allowed the identification of novel carbamates as potent AChEIs. In addition to "classical" ligand-based pharmacophore, de Oliveira Santos and co-workers generated a protocol combining ligand- and structure-based methods to perform a virtual screening of the Centre d'Etudes et de Recherche sur le Médicament de Normandie

(CERMN) chemical library. The authors used two kinds of virtual screening of the CERMN database in the search for new and original gorge-spanning AChEIs, capable to interact with both the CAS and the PAS: i) a structure-based screening using a docking approach and, ii) a ligand-based screening using a 3D pharmacophore developed taking into account two AChEIs (donepezil and (*S*,*S*)-(-)-*bis*(10)-hupyridone). The application of this two steps screening led the identification of new structurally original compounds inhibiting AChE in the micromolar range. Notably, **84** (Fig. 29) showed an IC_{50} value close to that of donepezil (Sopkova-de Oliveira Santos *et al.*, 2010). An *in silico* screening workflow was recently adopted by Lakshmi and colleagues for the identification and prioritization of potential compounds that could interact not only with the CAS but also with the PAS of AChE. Phase software, implemented in Maestro molecular modeling environment suite, was employed to generate different pharmacophore models starting from different AChE/inhibitors co-crystal structures. Multiple pharmacophore virtual screening was performed using ZINC natural products database. The obtained hits were docked into AChE binding site to narrow down the number of potential hits be to evaluated. The computational approach provided 12 hit compounds (Lakshmi *et al.*, 2013). SAR investigation carried out by Pudlo and collaborators guided the design of a series of quinolone-benzylpiperidine derivatives with potential activity against AChE. Among the series, the most potent compounds showed effective AChE inhibitions with IC_{50} values in the low micromolar range, high selectivity over BuChE and high radical scavenging activities (Pudlo *et al.*, 2014). A 3D-QSAR/CoMFA technique was adopted by Li and colleagues for identifying a series of novel azaoxoisoaporphine derivatives with inhibitory activity against AChE, as experimentally demonstrated (Li *et al.*, 2013b). Four point pharmacophore modeling approach was generated by Bag and co-workers for virtually screening Drug Bank

Database and natural alkaloids dataset in order to find AChEIs. The generation of the pharmacophore was based on a structurally diverse set of reported AChEIs and was validated using a different and unrelated set of known inhibitors. The developed pharmacophore indicated that the presence of one H-bond acceptor motif, one H-bond donor motif, one positively charged group and one aromatic ring is needed for AChE inhibition. The selected hits were further investigated by means of molecular docking and *in vitro* testing. A consistent number of selected compounds showed a reasonable inhibitory activity against AChE, outlining the reliability of pharmacophore modeling and ligand-based methods in searching AChEIs (Bag *et al.*, 2013). Differently, molecular docking procedure helped Di Pietro and co-workers to rationally design and optimize a series of ligands with remarkable activity towards AChE (Di Pietro *et al.*, 2014). In fact, a series of naphthyridines were synthesized according to the suggestion derived from the computational approach indicating strong interaction with peripheral and mid-gorge regions. Among the compounds obtained by chemical synthesis, **85** (Fig. 29) showed an IC_{50} of 65 nM against AChE, and it was demonstrated to inhibit also BuChE in the low micromolar range. Recently, SAR studies supported by molecular docking coupled to MD simulation, were carried out by Vitorović-Todorović and colleagues on a series of 4-aryl-4-oxo-2-aminylbutanamides **86** (Fig. 29). By using the mentioned approach a set of selected molecules showed a significant inhibitory activity against *h*AChE in the low micromolar range (Vitorovic-Todorovic *et al.*, 2014).

In summary, we have highlighted the relevance of ligand-based approaches to discover novel chemical entities for a known drug target, despite the presence of its crystal structures. Computational tools such as QSAR, pharmacophore modeling, rational design have been demonstrated and are still useful tools in AChE drug discovery as well as for other targets (Brogi *et al.*, 2011; Brogi *et al.*, 2009; Brogi *et al.*, 2013; Cappelli *et*

al., 2013; Castelli *et al.*, 2012; Gemma *et al.*, 2014; Giovani *et al.*, 2014; Pasquini *et al.*, 2012). Moreover, the large improvement in hits identification rate and reliability of results clearly appears evident when different computational techniques are combined.

4.2 Molecular dynamics (MD) simulation studies.

In addition to QSAR studies, which are useful tools to identify novel chemical entities interacting with the active site of AChE, other computational procedures such as MD simulation coupled to molecular docking studies or *ab initio* modeling resulted extremely relevant for investigating the behavior of the enzyme as well as the influence of the elements governing the ligand-recognition occurrence (i.e water molecules) (Karplus and McCammon, 2002). Pioneering works applying MD simulation to examine the active site gorge of AChE in ligand-recognition, in the protein functions and for evaluating the role of water molecules in this process have been reported by McCammon and co-workers (Shen *et al.*, 2002; Wlodek *et al.*, 1997). By applying MD simulation, the scientists examined the trafficking of water molecules in the gorge. For an in depth investigation of the water molecules in the enzyme gorge, the authors extracted a water density averaged over an MD simulation of AChE using averaged residue coordinates (ARC). This density was mapped to a single protein coordinate frame for the analysis and the properties of the hydration sites such as occupancy, residence, H-bonds and dipole moment were examined coupled to a study of complementary properties of gorge volume and empty space. The proposed computational approach highlighted how a ligand acts in the gorge under the influence of water molecules. Waters move in and out of the gorge through the main gorge entrance once every 200 ps, on average. Fluctuations in gorge volume also influenced the number of water molecules inside it (resulting in a gorge water population of 16 to 22 water molecules). The paper also described that the size and

frequency of variation of water molecules number may influence ligands trafficking also in terms of ligands' size. A detailed analysis of the hydration sites in the gorge provided additional information. In fact, the waters in the middle, the main gorge entrance, and near S203 and E202 (human numbering) appeared to be more disordered in density and dipole moment orientation, displaying more variable occupancy and cavities, lower residence times with more intersite traffic, and in the case of the main gorge entrance, fewer H-bonds. Contrarily, the water molecules in the choline binding site and in the pocket between D74 and W86 (human numbering) showed opposite properties, being more ordered, having single occupancy, longer residence times, and little intersite traffic. These differences may be attributed to the more confining shape of the D74/W86 pocket and to the presence of the sodium in the choline binding pocket. This difference is relevant since the more mobile class of water shapes ACh binding site and provides a path for the natural substrate to enter the gorge. The more mobile and less structured waters would allow faster ligand diffusion with reduced stability of waters itself. So, displacement of these waters by a ligand may conduct to stronger binding as observed for the large cavity adjacent to S203. The choline binding site is a portion of the ACh binding site that is relatively fixed since water appeared unable to displace sodium from this region, while choline can to do it and this provides high affinity for the binding site. Collectively, these MD studies relative to water molecules movements and their effect on the binding of ligands into AChE, provided crucial information for SBDD (Henchman and McCammon, 2002; Henchman *et al.*, 2002).

The same research group have also computationally investigated the role of catalytic triad (S203, H447 and E334 human numbering) and oxyanion hole of AChE (G121, G122, and A204 human numbering) by combining *ab initio* quantum mechanical/molecular mechanical (QM/MM) approach (Zhang *et al.*, 2002). The findings

clearly suggested that the reaction proceeds through the nucleophilic addition of the oxygen of S203 to the carbon of carbonyl group of ACh. Furthermore, the authors observed that the reaction is facilitated by simultaneous proton transfer from S203 to H447. The calculated potential energy barrier at the MP2(6-31+G*) QM/MM level was found to be 10.5 kcal/mol, in agreement with the experimental reaction rate. By using this computational technique, the authors proposed for the first time a consistent role for the other component of the catalytic triad, E334. In fact, this residue was found to be essential in stabilizing the transition state through electrostatic interactions. Concerning the oxyanion hole, the authors underlined its crucial role in catalysis. Indeed, in the AChE-Ach Michaelis complex, two H-bonds were formed between the carbonyl oxygen of ACh and the peptidic NH groups of G121 and G122 belonging to the oxyanion hole. During the process, the distance between the carbonyl oxygen of ACh and NH group of A204 became smaller, and a third H-bond was formed both in the transition state and in the tetrahedral intermediate (Zhang *et al.*, 2002). Moreover also a combination of multiple docking and MD simulation was applyied for investigating the different factors affecting the binding affinity and specificity of ligands in AChE by using ACh derivatives (Kua *et al*., 2002) or tetramethylammonium (Bui *et al.*, 2003) as substrates. The QM/MM hybrid calculation was also reported for different ligands to simulate the reaction into the active site of the enzyme. Recently, the mentioned computational scheme was used for modeling the structure–reaction rate correlations for the hydrolysis of a set of neutral esters in the active site of AChE (Lushchekina *et al.*, 2010). Interestingly, a Born–Oppenheimer *ab initio* QM/MM MD simulations with umbrella sampling was used by Zhang and colleagues to simulate the covalent inhibition mechanism between *Tc*AChE and the toxin soman determining its free energy profile for the first time. The results provided by authors indicated that phosphonylation of the

catalytic serine by soman employed an addition–elimination mechanism, which was found to be highly associative and stepwise. First, in the initial addition step, which is also rate-limiting, H440 (*Tc*AChE numbering; H447 in human sequence) acts as a general base to facilitate the nucleophilic attack of the catalityc serine on the soman's phosphorus atom to form a trigonal bipyrimidal pentacovalent intermediate. Secondly, in the elimination step, Y121 (*Tc*AChE numbering; Y124 in human sequence) of the catalytic gorge stabilizes the leaving fluorine atom prior to its dissociation from the active site. The reported simulations revealed detailed molecular mechanistic insights into the damaging function of the nerve agent soman (Sirin and Zhang, 2014). In addition to the mechanism above reported, Bennion and colleagues also described conformational changes in the enzyme when soman binds AChE. In particular, the complex was found to be stabilized by the interaction with the residues located in the oxyanion hole as well as those located in the Ω loop (C69-C96 in human sequence) increased non-polar contacts with nearby aromatic residues normally responsible for moderating substrate access to the active site. These observation obtained by MD simulation concerning the structural modification of AChE include aromatic and hydrophobic interactions with the soman adduct, limiting access to the soman adduct from the main gorge even though the gorge entrance is larger. The altered motions and resulting structures provided alternative pathways into and out of the AChE active site. MD trajectories analysis of the *apo* and soman adducted showed that the correlation of gorge entrance and back door motions are disrupted when AChE is adducted. This supports the hypothesis that substrate and product can use two different pathways as entry and exit sites in the *apo* form of the protein. These alternative pathways could represent important implications for the rational design of medical countermeasures as well as for understanding the effects of covalent modifications on the

network of connected motions that are responsible for the dynamics of the enzyme (Bennion *et al*., 2015).

Computational studies combining MD simulation and multiple ligand docking resulted very useful also to understand the roles of the anionic subsite residues (W86, E202, Y337 in human sequence) in the binding of ACh to AChE. The selected work highlighted the crucial role of electrostatic interactions in stabilizing the docking of ACh established by E202, while the aromatic residues covered only a marginal role concerning the electrostatic interaction in ligand binding. Moreover, *in silico* mutagenesis studies on this residues resulted in a significant reduction in binding of ACh in the catalytically productive orientation. E202A and W86A showed the largest reduction in docking score among the mutants (Kua *et al*., 2003).

MD simulation was also employed to better understand the crucial region involved in ligand binding. In particular, the Ω loop was extensively investigated coupling experimental and *in silico* studies (Shi *et al*., 2003). Specifically, the flexibility of three residues (L76, E81, and E84) in the Ω loop and one residue (Y124) across the gorge from the Ω loop were studied in the absence and presence of two inhibitors of different size, fasciculin and huperzine. The authors observed that the Ω loop residues were significantly more mobile than the Y124. Based on the experimental findings the examined mentioned residues showed torsional motion and segmental fluctuations and therefore could contribute to transient gorge enlargements. So, these rapid fluctuations, occurring in a time frame that was found shorter with respect to diffusional translation of substrate, could be expected to enhance substrate accessibility and product exit. Moreover the analysis of the effects of two ligands, one of which interacts directly with the exterior portion of the Ω loop (fasciculin) and one without this kind of contacts (huperzine), revealed internal loop flexibility and that the backbone movements are not all strongly

coupled. The obtained results suggested the opportunity that transient gorge enlargements result from random or near random (non-concerted) fluctuations that periodically widen the gorge (Bui *et al*., 2004; Shi *et al*., 2003). The loop fluctuation investigated by MD simulation by Wiesner and colleagues was found to be influenced by different protonation states of two glutamate residues located at the bottom of the active site gorge (E202 and E450 in *Mus musculus* and *human* AChE sequence), making the opening of the back door much more frequent (14% of trajectory time) and where the opening of side door was observed quite frequently (78%) in the studied condition according to the high AChE catalytic efficiency (Wiesner *et al*., 2010). A similar opened back door conformation was found by other researchers related to the movement of W84 (*Tc*AChE numbering; W86 in human sequence) (Sanson *et al.*, 2011). Concerning the investigation of AChE-ligand interactions by means of computational studies, Bai and co-workers recently reported a methodology to assess the kinetic parameters governing the binding affinity for huperzine into AChE. The authors developed a computational framework able to construct a complete ligand-target binding free energy landscape. The methodology was employed to simulate the binding event of huperzine to AChE and could be useful also for studying other protein-ligand complexes (Bai *et al.*, 2013). Differently from huperzine and other AChEIs that go through the greatest barrier placed at the bottleneck of the gorge, the MD simulation (steered molecular dynamics (SMD)) studies conducted by Niu and colleagues on the complex *Tc*AChE/donepezil revealed a major resistance preventing donepezil from leaving the gorge ascribable to the PAS where donepezil strongly interacts with several aromatic residues (Y70, Y121, and W279 in *Tc*AChE; Y72, Y124, and W286 in human sequence) through its benzene ring and forms a strong direct hydrogen bond and a water bridge with S286 (S293 in human sequence). In

summary the article highlighted the different mechanism governing the activity of diverse AChEIs (Niu *et al*., 2005).

More recently, Butini and colleagues carried out bioinformatics studies aimed at better understanding the role of specific hot spots, responsible for protein fluctuations and functions. Combining exhaustive conformational search analysis and molecular docking studies, the research group was able to detect the active-site residues that played a role in modulating the cooperative network between the key substructures and their implication in rational drug design. In particular, the computational studies highlighted protein-protein interaction domains in *h*ChEs, defining several putative protein hot spots in the active-site gorges of *h*ChEs that can be targeted to develop extremely potent ligands. Using all the X-ray structures of AChEs available in the PDB, conformational shifts in key residues located in different regions of the gorge upon complexation with an inhibitor were calculated. This approach led to the identification of concerted movements of specific AChE residues (i.e., CAS: Y337; mid gorge: D74 and Y341; PAS: W286) upon binding of an inhibitor, and these conformational changes were related to inhibitor potency and binding mode. In particular, a relevant relationship between potency and inhibitor-induced conformational shifts in W286 of the PAS was detected. Taken together these findings allowed the authors to develop extremely potent and highly flexible reversible inhibitors characterized by *K*i values in the high to low picomolar range (Butini *et al.*, 2008a).

MD simulation was applied by Xu and co-workers on *Tc*AChE with the aimed of understanding the role of the aromatic residues in the active site gorge of AChE. The authors analyzed the conformational flexibility of the side chains of the 14 conserved aromatic residues in the active-site gorge of *Tc*AChE based on the 47 crystal structures available for the native enzyme and for the enzyme bound to ligands. The article reported

a different degree of flexibility of the mentioned 14 aromatic aminoacid side chains. The authors reported that the side-chain conformations of F330 and W279 (Y337 and W286 in human sequence respectively) were both very flexible, while the side-chain conformations of F120, W233, W432, Y70, Y121, F288, F290 and F331 appeared to be fixed (F123, W236, W439, Y72, Y124, F295, F297, and F338 in human sequence). Moreover, residues located on, or adjacent to, the Ω-loop (W84, Y130, Y442, and Y334, (W86, Y133, Y449, and Y341 in human numbering) displayed different flexibilities in the MD simulations and in the crystal structures. An important result of this work was that the majority of the side chain conformations observed in the 47 *Tc*AChE crystal structures were faithfully reproduced by the MD simulation on the native enzyme (Xu *et al.*, 2008). More recently, similar findings on the flexibility of the active site gorge aromatic residues have been reported (GhattyVenkataKrishna *et al.*, 2013).

In the frame of tacrine-based MTDLs very recently Brogi and colleagues (Brogi *et al.*, 2014) carried out computational studies by coupling molecular docking studies and MD simulation to investigate the mechanism governing the ability of compound **3** (Fig. 4 of paragraph 2.1 where the profile of compound **3** is briefly discussed) to inhibit spontaneus Aβ fibrils formation as well as to disrupt Aβ preformed fibrils. Based on the computational results the authors observed that compound **3** strongly interacts with Aβ by its bis-tacrine system with H13 (hydrophobic contacts) and P19 by a π-π stacking, while the peptide portion of the molecule forms H-bond with K16, a cation-π stacking with K28 by the benzyl ester function and a π-π stacking with F20 by the benzyl carbamate. The MD simulation also highlighted the role of the protonated terminal tacrine, forming a H-bond with D23 and I32. During the simulation compound **3** maintained a similar position on the Aβ peptide. These findings support a high affinity of **3** for $A\beta_{1-42}$ explaining its mechanism of action. In fact, **3** could prevent the misfolding of the C-terminal region to

β-sheet, since no change of secondary structure was observed **3** for $A\beta_{1–42}$ during the 100 ns of simulation and consequently the helix appeared constantly conserved (the simulation without inhibitor revealed that earlier misfolding events can be already detected after 20 ns of simulation). On the other hand, the mentioned compound is also able to disrupt the Aβ fibrils establishing a relevant number of polar contacts with key residues of the fibril complex such as the hydrophobic region comprised between L17-E22 as well as the residues D23 and K28. In particular, the hydrophobic central region L17-E22 is crucial for fibrils assembly while the salt bridge formed between D23 and K28 is necessary for the fibrils stability. Based on the MD results the authors observed conserved interactions of **3** with these regions. Indeed, a tacrine system interacts with the hydrophobic region L17-E22 and the peptide moiety and established a series of polar contact with K28 and/or D23, hampering the formation of the mentioned salt bridge. Accordingly, already after 40 ns the disruption of fibrils started. Remarkably, the computational approaches above presented allow to unequivocally establish the mechanism of action of compound **3** (Brogi *et al.*, 2014).

In conclusion, in this review we have reported a comprehensive overview concerning the latest advance in multifunctional ligand design to potentially treat AD, discussing all the aspect of the development of the most promising compounds including rational design, synthetic strategies, biological and pharmaceutical evaluation as well as the most relevant computational approaches that led to the understanding of AChE functions and to the discovery of novel and potent AChE ligands.

Conflicts of interest

The authors declare no conflicts of interest.

Acknowledgements

LI, BR MB and TG thank the Regional Council of Franche-Comté (Besançon, France) for financial support European COST Actions CM1103, and CM1207 are kindly acknowledged. KN, SF and DA acknowledge project supported by the Ministry of Education, Science and Technological Development of the Republic of Serbia, Project number 172033. JMC and MU thanks MINECO (Spain) for support (SAF2012-33304).

References

Abuhamdah, S., Habash, M., Taha, M.O., 2013. Elaborate ligand-based modeling coupled with QSAR analysis and in silico screening reveal new potent acetylcholinesterase inhibitors. *J Comput Aided Mol Des* 27**,** 1075-1092.

Adayev, T., Wegiel, J., Hwang, Y.W., 2011. Harmine is an ATP-competitive inhibitor for dual-specificity tyrosine phosphorylation-regulated kinase 1A (Dyrk1A). *Arch Biochem Biophys* 507**,** 212-218.

Alvarez, A., Opazo, C., Alarcon, R., Garrido, J., Inestrosa, N.C., 1997. Acetylcholinesterase promotes the aggregation of amyloid-beta-peptide fragments by forming a complex with the growing fibrils. *J Mol Biol* 272**,** 348-361.

Anand, P., Singh, B., Singh, N., 2012. A review on coumarins as acetylcholinesterase inhibitors for Alzheimer's disease. *Bioorg. Med. Chem.* 20**,** 1175-1180.

Andersson, C.D., Forsgren, N., Akfur, C., Allgardsson, A., Berg, L., Engdahl, C., Qian, W., Ekstrom, F., Linusson, A., 2013. Divergent structure-activity relationships of structurally similar acetylcholinesterase inhibitors. *J Med Chem* 56**,** 7615-7624.

Arce, M.P., Rodriguez-Franco, M.I., Gonzalez-Munoz, G.C., Perez, C., Lopez, B., Villarroya, M., Lopez, M.G., Garcia, A.G., Conde, S., 2009. Neuroprotective and cholinergic properties of multifunctional glutamic acid derivatives for the treatment of Alzheimer's disease. *J Med Chem* 52**,** 7249-7257.

Asadipour, A., Alipour, M., Jafari, M., Khoobi, M., Emami, S., Nadri, H., Sakhteman, A., Moradi, A., Sheibani, V., Homayouni Moghadam, F., Shafiee, A., Foroumadi, A., 2013. Novel coumarin-3-carboxamides bearing N-benzylpiperidine moiety as potent acetylcholinesterase inhibitors. *Eur J Med Chem* 70**,** 623-630.

Avramovich-Tirosh, Y., Amit, T., Bar-Am, O., Zheng, H., Fridkin, M., Youdim, M.B., 2007. Therapeutic targets and potential of the novel brain- permeable multifunctional iron chelator-monoamine oxidase inhibitor drug, M-30, for the treatment of Alzheimer's disease. *J Neurochem* 100**,** 490-502.

Bag, S., Tulsan, R., Sood, A., Datta, S., Torok, M., 2013. Pharmacophore Modeling, virtual and in vitro screening for acetylcholinesterase inhibitors and their effects on amyloid-beta self- assembly. *Curr Comput Aided Drug Des* 9**,** 2-14.

Bai, F., Xu, Y., Chen, J., Liu, Q., Gu, J., Wang, X., Ma, J., Li, H., Onuchic, J.N., Jiang, H., 2013. Free energy landscape for the binding process of Huperzine A to acetylcholinesterase. *Proc Natl Acad Sci U S A* 110**,** 4273-4278.

Bajda, M., Guzior, N., Ignasik, M., Malawska, B., 2011. Multi-target-directed ligands in Alzheimer's disease treatment. *Curr Med Chem* 18**,** 4949-4975.

Bajda, M., Wieckowska, A., Hebda, M., Guzior, N., Sotriffer, C.A., Malawska, B., 2013. Structure-based search for new inhibitors of cholinesterases. *Int J Mol Sci* 14**,** 5608-5632.

Bartolini, M., Bertucci, C., Cavrini, V., Andrisano, V., 2003. beta-Amyloid aggregation induced by human acetylcholinesterase: inhibition studies. *Biochem Pharmacol* 65**,** 407-416.

Bautista-Aguilera, O.M., Esteban, G., Bolea, I., Nikolic, K., Agbaba, D., Moraleda, I., Iriepa, I., Samadi, A., Soriano, E., Unzeta, M., Marco-Contelles, J., 2014a. Design, synthesis, pharmacological evaluation, QSAR analysis, molecular modeling and ADMET of novel donepezil-indolyl hybrids as multipotent cholinesterase/monoamine oxidase inhibitors for the potential treatment of Alzheimer's disease. *Eur J Med Chem* 75**,** 82-95.

Bautista-Aguilera, O.M., Esteban, G., Chioua, M., Nikolic, K., Agbaba, D., Moraleda, I., Iriepa, I., Soriano, E., Samadi, A., Unzeta, M., Marco-Contelles, J., 2014b. Multipotent cholinesterase/monoamine oxidase inhibitors for the treatment of Alzheimer's disease: design, synthesis, biochemical evaluation, ADMET, molecular modeling, and QSAR analysis of novel donepezil-pyridyl hybrids. *Drug Des Devel Ther* 8**,** 1893-1910.

Bautista-Aguilera, O.M., Samadi, A., Chioua, M., Nikolic, K., Filipic, S., Agbaba, D., Soriano, E., de Andres, L., Rodriguez-Franco, M.I., Alcaro, S., Ramsay, R.R., Ortuso, F., Yanez, M., Marco-Contelles, J., 2014c. N-Methyl-N-((1-methyl-5-(3-(1-(2-methylbenzyl)piperidin-4-yl)propoxy)-1H-indol-2- yl)methyl)prop-2-yn-1-amine, a New Cholinesterase and Monoamine Oxidase Dual Inhibitor. *J Med Chem*.

Benchekroun, M., Bartolini, M., Egea, J., Romero, A., Soriano, E., Pudlo, M., Luzet, V., Andrisano, V., Jimeno, M.L., Lopez, M.G., Wehle, S., Gharbi, T., Refouvelet, B., de Andres, L., Herrera-Arozamena, C., Monti, B., Bolognesi, M.L., Rodriguez-Franco, M.I., Decker, M., Marco-Contelles, J., Ismaili, L., 2015a. Novel tacrine-grafted Ugi adducts as multipotent anti-Alzheimer drugs: a synthetic renewal in tacrine-ferulic acid hybrids. *ChemMedChem* 10**,** 523-539.

Benchekroun, M., Ismaili, L., Pudlo, M., Luzet, V., Gharbi, T., Refouvelet, B., Marco-Contelles, J., 2015b. Donepezil-ferulic acid hybrids as anti-Alzheimer drugs. *Future Med Chem* 7**,** 15-21.

Benilova, I., Karran, E., De Strooper, B., 2012. The toxic Abeta oligomer and Alzheimer's disease: an emperor in need of clothes. *Nature neuroscience* 15**,** 349-357.

Bennion, B.J., Essiz, S.G., Lau, E.Y., Fattebert, J.L., Emigh, A., Lightstone, F.C., 2015. A wrench in the works of human acetylcholinesterase: soman induced conformational changes revealed by molecular dynamics simulations. *PLoS One* 10**,** e0121092.

Benzie, I.F., Strain, J.J., 1999. Ferric reducing/antioxidant power assay: direct measure of total antioxidant activity of biological fluids and modified version for simultaneous measurement of total antioxidant power and ascorbic acid concentration. *Methods Enzymol* 299**,** 15-27.

Bergeron, R., de Montigny, C., Debonnel, G., 1996. Potentiation of neuronal NMDA response induced by dehydroepiandrosterone and its suppression by progesterone: effects mediated via sigma receptors. *J Neurosci* 16**,** 1193-1202.

Bermudez-Lugo, J.A., Rosales-Hernandez, M.C., Deeb, O., Trujillo-Ferrara, J., Correa-Basurto, J., 2011. In silico methods to assist drug developers in acetylcholinesterase inhibitor design. *Curr Med Chem* 18**,** 1122-1136.

Besnard, J., Ruda, G.F., Setola, V., Abecassis, K., Rodriguiz, R.M., Huang, X.P., Norval, S., Sassano, M.F., Shin, A.I., Webster, L.A., Simeons, F.R., Stojanovski, L., Prat, A., Seidah, N.G., Constam, D.B., Bickerton, G.R., Read, K.D., Wetsel, W.C., Gilbert, I.H., Roth, B.L., Hopkins, A.L., 2012. Automated design of ligands to polypharmacological profiles. *Nature* 492**,** 215-220.

Bolea, I., Gella, A., Monjas, L., Perez, C., Rodriguez-Franco, M.I., Marco-Contelles, J., Samadi, A., Unzeta, M., 2013. Multipotent, permeable drug ASS234 inhibits Abeta aggregation, possesses antioxidant properties and protects from Abeta-induced apoptosis in vitro. *Curr Alzheimer Res* 10**,** 797-808.

Bolea, I., Juarez-Jimenez, J., de Los Rios, C., Chioua, M., Pouplana, R., Luque, F.J., Unzeta, M., Marco-Contelles, J., Samadi, A., 2011. Synthesis, biological evaluation, and molecular modeling of donepezil and N-[(5-(benzyloxy)-1-methyl-1H-indol-2-yl)methyl]-N-methylprop-2-yn-1-amine hybrids as new multipotent cholinesterase/monoamine oxidase inhibitors for the treatment of Alzheimer's disease. *J Med Chem* 54**,** 8251-8270.

Bolognesi, M.L., Cavalli, A., Valgimigli, L., Bartolini, M., Rosini, M., Andrisano, V., Recanatini, M., Melchiorre, C., 2007. Multi-target-directed drug design strategy: from a dual binding site acetylcholinesterase inhibitor to a trifunctional compound against Alzheimer's disease. *J. Med. Chem.* 50**,** 6446-6449.

Brogi, S., Butini, S., Maramai, S., Colombo, R., Verga, L., Lanni, C., De Lorenzi, E., Lamponi, S., Andreassi, M., Bartolini, M., Andrisano, V., Novellino, E., Campiani, G., Brindisi, M., Gemma, S., 2014. Disease-modifying anti-Alzheimer's drugs: inhibitors of human cholinesterases interfering with beta-amyloid aggregation. *CNS Neurosci Ther* 20**,** 624-632.

Brogi, S., Corelli, F., Di Marzo, V., Ligresti, A., Mugnaini, C., Pasquini, S., Tafi, A., 2011. Three-dimensional quantitative structure-selectivity relationships analysis guided rational design of a highly selective ligand for the cannabinoid receptor 2. *Eur J Med Chem* 46**,** 547-555.

Brogi, S., Kladi, M., Vagias, C., Papazafiri, P., Roussis, V., Tafi, A., 2009. Pharmacophore modeling for qualitative prediction of antiestrogenic activity. *J Chem Inf Model* 49**,** 2489-2497.

Brogi, S., Papazafiri, P., Roussis, V., Tafi, A., 2013. 3D-QSAR using pharmacophore-based alignment and virtual screening for discovery of novel MCF-7 cell line inhibitors. *Eur J Med Chem* 67**,** 344-351.

Bui, J.M., Henchman, R.H., McCammon, J.A., 2003. The dynamics of ligand barrier crossing inside the acetylcholinesterase gorge. *Biophys J* 85**,** 2267-2272.

Bui, J.M., Tai, K., McCammon, J.A., 2004. Acetylcholinesterase: enhanced fluctuations and alternative routes to the active site in the complex with fasciculin-2. *J Am Chem Soc* 126**,** 7198-7205.

Butini, S., Brindisi, M., Brogi, S., Maramai, S., Guarino, E., Panico, A., Saxena, A., Chauhan, V., Colombo, R., Verga, L., De Lorenzi, E., Bartolini, M., Andrisano, V., Novellino, E., Campiani, G., Gemma, S., 2013a. Multifunctional cholinesterase and amyloid Beta fibrillization modulators. Synthesis and biological investigation. *ACS Med Chem Lett* 4**,** 1178-1182.

Butini, S., Brogi, S., Novellino, E., Campiani, G., Ghosh, A.K., Brindisi, M., Gemma, S., 2013b. The structural evolution of beta-secretase inhibitors: a focus on the development of small-molecule inhibitors. *Current Topics in Medicinal Chemistry* 13**,** 1787-1807.

Butini, S., Campiani, G., Borriello, M., Gemma, S., Panico, A., Persico, M., Catalanotti, B., Ros, S., Brindisi, M., Agnusdei, M., Fiorini, I., Nacci, V., Novellino, E.,

Belinskaya, T., Saxena, A., Fattorusso, C., 2008a. Exploiting protein fluctuations at the active-site gorge of human cholinesterases: further optimization of the design strategy to develop extremely potent inhibitors. *J Med Chem* 51**,** 3154-3170.

Butini, S., Gabellieri, E., Brindisi, M., Giovani, S., Maramai, S., Kshirsagar, G., Guarino, E., Brogi, S., La Pietra, V., Giustiniano, M., Marinelli, L., Novellino, E., Campiani, G., Cappelli, A., Gemma, S., 2013c. A stereoselective approach to peptidomimetic BACE1 inhibitors. *Eur J Med Chem* 70C**,** 233-247.

Butini, S., Guarino, E., Campiani, G., Brindisi, M., Coccone, S.S., Fiorini, I., Novellino, E., Belinskaya, T., Saxena, A., Gemma, S., 2008b. Tacrine based human cholinesterase inhibitors: synthesis of peptidic-tethered derivatives and their effect on potency and selectivity. *Bioorg Med Chem Lett* 18**,** 5213-5216.

Campiani, G., Fattorusso, C., Butini, S., Gaeta, A., Agnusdei, M., Gemma, S., Persico, M., Catalanotti, B., Savini, L., Nacci, V., Novellino, E., Holloway, H.W., Greig, N.H., Belinskaya, T., Fedorko, J.M., Saxena, A., 2005. Development of molecular probes for the identification of extra interaction sites in the mid-gorge and peripheral sites of butyrylcholinesterase (BuChE). Rational design of novel, selective, and highly potent BuChE inhibitors. *J Med Chem* 48**,** 1919-1929.

Camps, P., Cusack, B., Mallender, W.D., El Achab, R.E., Morral, J., Munoz-Torrero, D., Rosenberry, T.L., 2000. Huprine X is a novel high-affinity inhibitor of acetylcholinesterase that is of interest for treatment of Alzheimer's disease. *Mol Pharmacol* 57**,** 409-417.

Cappelli, A., Manini, M., Valenti, S., Castriconi, F., Giuliani, G., Anzini, M., Brogi, S., Butini, S., Gemma, S., Campiani, G., Giorgi, G., Mennuni, L., Lanza, M., Giordani, A., Caselli, G., Letari, O., Makovec, F., 2013. Synthesis and structure-activity relationship studies in serotonin 5-HT(1A) receptor agonists based on fused pyrrolidone scaffolds. *Eur J Med Chem* 63**,** 85-94.

Carlier, P.R., Chow, E.S., Han, Y., Liu, J., El Yazal, J., Pang, Y.P., 1999a. Heterodimeric tacrine-based acetylcholinesterase inhibitors: investigating ligand-peripheral site interactions. *J Med Chem* 42**,** 4225-4231.

Carlier, P.R., Han, Y.F., Chow, E.S., Li, C.P., Wang, H., Lieu, T.X., Wong, H.S., Pang, Y.P., 1999b. Evaluation of short-tether bis-THA AChE inhibitors. A further test of the dual binding site hypothesis. *Bioorg Med Chem* 7**,** 351-357.

Carreiras, M.C., Mendes, E., Perry, M.J., Francisco, A.P., Marco-Contelles, J., 2013. The multifactorial nature of Alzheimer's disease for developing potential therapeutics. *Curr Top Med Chem* 13**,** 1745-1770.

Castelli, M.P., Casu, A., Casti, P., Lobina, C., Carai, M.A., Colombo, G., Solinas, M., Giunta, D., Mugnaini, C., Pasquini, S., Tafi, A., Brogi, S., Gessa, G.L., Corelli, F., 2012. Characterization of COR627 and COR628, two novel positive allosteric modulators of the GABA(B) receptor. *J Pharmacol Exp Ther* 340**,** 529-538.

Catto, M., Pisani, L., Leonetti, F., Nicolotti, O., Pesce, P., Stefanachi, A., Cellamare, S., Carotti, A., 2013. Design, synthesis and biological evaluation of coumarin alkylamines as potent and selective dual binding site inhibitors of acetylcholinesterase. *Bioorg Med Chem* 21**,** 146-152.

Chao, X., He, X., Yang, Y., Zhou, X., Jin, M., Liu, S., Cheng, Z., Liu, P., Wang, Y., Yu, J., Tan, Y., Huang, Y., Qin, J., Rapposelli, S., Pi, R., 2012. Design, synthesis and pharmacological evaluation of novel tacrine-caffeic acid hybrids as multi-targeted compounds against Alzheimer's disease. *Bioorg Med Chem Lett* 22**,** 6498-6502.

Chaudhaery, S.S., Roy, K.K., Shakya, N., Saxena, G., Sammi, S.R., Nazir, A., Nath, C., Saxena, A.K., 2010. Novel carbamates as orally active acetylcholinesterase

inhibitors found to improve scopolamine-induced cognition impairment: pharmacophore-based virtual screening, synthesis, and pharmacology. *J Med Chem* 53**,** 6490-6505.

Chen, H.S., Pellegrini, J.W., Aggarwal, S.K., Lei, S.Z., Warach, S., Jensen, F.E., Lipton, S.A., 1992. Open-channel block of N-methyl-D-aspartate (NMDA) responses by memantine: therapeutic advantage against NMDA receptor-mediated neurotoxicity. *J Neurosci* 12**,** 4427-4436.

Chen, Y., Fang, L., Peng, S., Liao, H., Lehmann, J., Zhang, Y., 2012a. Discovery of a novel acetylcholinesterase inhibitor by structure-based virtual screening techniques. *Bioorg Med Chem Lett* 22**,** 3181-3187.

Chen, Y., Sun, J., Fang, L., Liu, M., Peng, S., Liao, H., Lehmann, J., Zhang, Y., 2012b. Tacrine-ferulic acid-nitric oxide (NO) donor trihybrids as potent, multifunctional acetyl- and butyrylcholinesterase inhibitors. *J Med Chem* 55**,** 4309-4321.

Chen, Y., Sun, J., Peng, S., Liao, H., Zhang, Y., Lehmann, J., 2013. Tacrine-flurbiprofen hybrids as multifunctional drug candidates for the treatment of Alzheimer's disease. *Arch Pharm (Weinheim)* 346**,** 865-871.

Cherkasov, A., Muratov, E.N., Fourches, D., Varnek, A., Baskin, II, Cronin, M., Dearden, J., Gramatica, P., Martin, Y.C., Todeschini, R., Consonni, V., Kuz'min, V.E., Cramer, R., Benigni, R., Yang, C., Rathman, J., Terfloth, L., Gasteiger, J., Richard, A., Tropsha, A., 2014. QSAR modeling: where have you been? Where are you going to? *J Med Chem* 57**,** 4977-5010.

Cheung, J., Rudolph, M.J., Burshteyn, F., Cassidy, M.S., Gary, E.N., Love, J., Franklin, M.C., Height, J.J., 2012. Structures of human acetylcholinesterase in complex with pharmacologically important ligands. *J Med Chem* 55**,** 10282-10286.

Clark, J.K., Cowley, P., Muir, A.W., Palin, R., Pow, E., Prosser, A.B., Taylor, R., Zhang, M.Q., 2002. Quaternary salts of E2020 analogues as acetylcholinesterase inhibitors for the reversal of neuromuscular block. *Bioorg Med Chem Lett* 12**,** 2565-2568.

Contreras, J.M., Parrot, I., Sippl, W., Rival, Y.M., Wermuth, C.G., 2001. Design, synthesis, and structure-activity relationships of a series of 3-[2-(1-benzylpiperidin-4-yl)ethylamino]pyridazine derivatives as acetylcholinesterase inhibitors. *J Med Chem* 44**,** 2707-2718.

Contreras, J.M., Rival, Y.M., Chayer, S., Bourguignon, J.J., Wermuth, C.G., 1999. Aminopyridazines as acetylcholinesterase inhibitors. *J Med Chem* 42**,** 730-741.

Cordes, T., Vogelsang, J., Tinnefeld, P., 2009. On the mechanism of Trolox as antiblinking and antibleaching reagent. *J Am Chem Soc* 131**,** 5018-5019.

Cramer, R.D., 2012. The inevitable QSAR renaissance. *J Comput Aided Mol Des* 26**,** 35-38.

Cuajungco, M.P., Faget, K.Y., 2003. Zinc takes the center stage: its paradoxical role in Alzheimer's disease. *Brain Res Brain Res Rev* 41**,** 44-56.

Cummings, J.L., 2004. Treatment of Alzheimer's disease: current and future therapeutic approaches. *Rev Neurol Dis* 1**,** 60-69.

Danysz, W., Parsons, C.G., 2012. Alzheimer's disease, beta-amyloid, glutamate, NMDA receptors and memantine--searching for the connections. *Br J Pharmacol* 167**,** 324-352.

Davalos, A., Gomez-Cordoves, C., Bartolome, B., 2004. Extending applicability of the oxygen radical absorbance capacity (ORAC-fluorescein) assay. *J Agric Food Chem* 52**,** 48-54.

DeCoster, M.A., Klette, K.L., Knight, E.S., Tortella, F.C., 1995. Sigma receptor-mediated neuroprotection against glutamate toxicity in primary rat neuronal cultures. *Brain Res* 671**,** 45-53.

del Pino, J., Ramos, E., Aguilera, O.M., Marco-Contelles, J., Romero, A., 2014. Wnt signaling pathway, a potential target for Alzheimer's disease treatment, is activated by a novel multitarget compound ASS234. *CNS Neurosci Ther* 20**,** 568-570.

Desideri, N., Bolasco, A., Fioravanti, R., Monaco, L.P., Orallo, F., Yanez, M., Ortuso, F., Alcaro, S., 2011. Homoisoflavonoids: natural scaffolds with potent and selective monoamine oxidase-B inhibition properties. *J Med Chem* 54**,** 2155-2164.

Dewar, M.J.S., Zoebisch, E.G., Healy, E.F., Stewart, J.J.P., 1985. Development and use of quantum mechanical molecular models. 76. AM1: a new general purpose quantum mechanical molecular model. *J. Am. Chem. Soc.* 107**,** 3902-3909.

Di, L., Kerns, E.H., Fan, K., McConnell, O.J., Carter, G.T., 2003. High throughput artificial membrane permeability assay for blood-brain barrier. *Eur J Med Chem* 38**,** 223-232.

Di Pietro, O., Viayna, E., Vicente-Garcia, E., Bartolini, M., Ramon, R., Juarez-Jimenez, J., Clos, M.V., Perez, B., Andrisano, V., Luque, F.J., Lavilla, R., Munoz-Torrero, D., 2014. 1,2,3,4-Tetrahydrobenzo[h][1,6]naphthyridines as a new family of potent peripheral-to-midgorge-site inhibitors of acetylcholinesterase: synthesis, pharmacological evaluation and mechanistic studies. *Eur J Med Chem* 73**,** 141-152.

Eckroat, T.J., Green, K.D., Reed, R.A., Bornstein, J.J., Garneau-Tsodikova, S., 2013. Investigation of the role of linker moieties in bifunctional tacrine hybrids. *Bioorg Med Chem* 21**,** 3614-3623.

Esquivias-Perez, M., Maalej, E., Romero, A., Chabchoub, F., Samadi, A., Marco-Contelles, J., Oset-Gasque, M.J., 2013. Nontoxic and neuroprotective beta-naphthotacrines for Alzheimer's disease. *Chem Res Toxicol* 26**,** 986-992.

Esteban, G., Allan, J., Samadi, A., Mattevi, A., Unzeta, M., Marco-Contelles, J., Binda, C., Ramsay, R.R., 2014. Kinetic and structural analysis of the irreversible inhibition of human monoamine oxidases by ASS234, a multi-target compound designed for use in Alzheimer's disease. *Biochim Biophys Acta* 1844**,** 1104-1110.

Fang, L., Appenroth, D., Decker, M., Kiehntopf, M., Lupp, A., Peng, S., Fleck, C., Zhang, Y., Lehmann, J., 2008a. NO-donating tacrine hybrid compounds improve scopolamine-induced cognition impairment and show less hepatotoxicity. *J Med Chem* 51**,** 7666-7669.

Fang, L., Appenroth, D., Decker, M., Kiehntopf, M., Roegler, C., Deufel, T., Fleck, C., Peng, S., Zhang, Y., Lehmann, J., 2008b. Synthesis and biological evaluation of NO-donor-tacrine hybrids as hepatoprotective anti-Alzheimer drug candidates. *J Med Chem* 51**,** 713-716.

Fang, L., Kraus, B., Lehmann, J., Heilmann, J., Zhang, Y., Decker, M., 2008c. Design and synthesis of tacrine-ferulic acid hybrids as multi-potent anti-Alzheimer drug candidates. *Bioorg Med Chem Lett* 18**,** 2905-2909.

Fernandez-Bachiller, M.I., Perez, C., Monjas, L., Rademann, J., Rodriguez-Franco, M.I., 2012. New tacrine-4-oxo-4H-chromene hybrids as multifunctional agents for the treatment of Alzheimer's disease, with cholinergic, antioxidant, and beta-amyloid-reducing properties. *J Med Chem* 55**,** 1303-1317.

Ferrari, D., Yang, L.H., Miles, E.W., Dunn, M.F., 2001. Beta D305A mutant of tryptophan synthase shows strongly perturbed allosteric regulation and substrate specificity. *Biochemistry-US* 40**,** 7421-7432.

Finberg, J.P., 2014. Update on the pharmacology of selective inhibitors of MAO-A and MAO-B: focus on modulation of CNS monoamine neurotransmitter release. *Pharmacol Ther* 143**,** 133-152.

Frost, D., Meechoovet, B., Wang, T., Gately, S., Giorgetti, M., Shcherbakova, I., Dunckley, T., 2011. beta-carboline compounds, including harmine, inhibit DYRK1A and tau phosphorylation at multiple Alzheimer's disease-related sites. *PLoS One* 6**,** e19264.

Galdeano, C., Viayna, E., Sola, I., Formosa, X., Camps, P., Badia, A., Clos, M.V., Relat, J., Ratia, M., Bartolini, M., Mancini, F., Andrisano, V., Salmona, M., Minguillon, C., Gonzalez-Munoz, G.C., Rodriguez-Franco, M.I., Bidon-Chanal, A., Luque, F.J., Munoz-Torrero, D., 2012. Huprine-tacrine heterodimers as anti-amyloidogenic compounds of potential interest against Alzheimer's and prion diseases. *J Med Chem* 55**,** 661-669.

Gemma, S., Brogi, S., Patil, P.R., Giovani, S., Lamponi, S., Cappelli, A., Novellino, E., Brown, A., Higgins, M.K., Mustafa, K., Szestak, T., Craig, A.G., Campiani, G., Butini, S., Brindisi, M., 2014. From (+)-epigallocatechin gallate to a simplified synthetic analogue as a cytoadherence inhibitor for P. falciparum. *RSC Adv* 4**,** 4769-4781.

Gharaghani, S., Khayamian, T., Ebrahimi, M., 2013. Molecular dynamics simulation study and molecular docking descriptors in structure-based QSAR on acetylcholinesterase (AChE) inhibitors. *SAR QSAR Environ Res* 24**,** 773-794.

GhattyVenkataKrishna, P., Chavali, N., Uberbacher, E. (2013) Flexibility of active-site gorge aromatic residues and non-gorge aromatic residues in acetylcholinesterase. In: *Chemical Papers*. p. 677.

Giovani, S., Penzo, M., Brogi, S., Brindisi, M., Gemma, S., Novellino, E., Savini, L., Blackman, M.J., Campiani, G., Butini, S., 2014. Rational design of the first difluorostatone-based PfSUB1 inhibitors. *Bioorg Med Chem Lett* 24**,** 3582-3586.

Glennon, R.A., Ablordeppey, S.Y., Ismaiel, A.M., el-Ashmawy, M.B., Fischer, J.B., Howie, K.B., 1994. Structural features important for sigma 1 receptor binding. *J Med Chem* 37**,** 1214-1219.

Grant, B.F., Harford, T.C., Dawson, D.A., Chou, P.S., Pickering, R.P., 1995. The Alcohol Use Disorder and Associated Disabilities Interview schedule (AUDADIS): reliability of alcohol and drug modules in a general population sample. *Drug Alcohol Depend* 39**,** 37-44.

Greig, N.H., Utsuki, T., Ingram, D.K., Wang, Y., Pepeu, G., Scali, C., Yu, Q.S., Mamczarz, J., Holloway, H.W., Giordano, T., Chen, D., Furukawa, K., Sambamurti, K., Brossi, A., Lahiri, D.K., 2005. Selective butyrylcholinesterase inhibition elevates brain acetylcholine, augments learning and lowers Alzheimer beta-amyloid peptide in rodent. *Proc Natl Acad Sci U S A* 102**,** 17213-17218.

Gupta, S., Fallarero, A., Jarvinen, P., Karlsson, D., Johnson, M.S., Vuorela, P.M., Mohan, C.G., 2011. Discovery of dual binding site acetylcholinesterase inhibitors identified by pharmacophore modeling and sequential virtual screening techniques. *Bioorg Med Chem Lett* 21**,** 1105-1112.

Hajjo, R., Grulke, C.M., Golbraikh, A., Setola, V., Huang, X.P., Roth, B.L., Tropsha, A., 2010. Development, validation, and use of quantitative structure-activity relationship models of 5-hydroxytryptamine (2B) receptor ligands to identify novel receptor binders and putative valvulopathic compounds among common drugs. *J Med Chem* 53**,** 7573-7586.

Hajjo, R., Setola, V., Roth, B.L., Tropsha, A., 2012. Chemocentric informatics approach to drug discovery: identification and experimental validation of selective estrogen

receptor modulators as ligands of 5-hydroxytryptamine-6 receptors and as potential cognition enhancers. *J Med Chem* 55**,** 5704-5719.

Hamley, I.W., 2012. The amyloid beta peptide: a chemist's perspective. Role in Alzheimer's and fibrillization. *Chem Rev* 112**,** 5147-5192.

Hamulakova, S., Janovec, L., Hrabinova, M., Spilovska, K., Korabecny, J., Kristian, P., Kuca, K., Imrich, J., 2014. Synthesis and biological evaluation of novel tacrine derivatives and tacrine-coumarin hybrids as cholinesterase inhibitors. *J Med Chem* 57**,** 7073-7084.

Hansch, C., Maloney, P.P., Fujita, T., Muir, R.M., 1962. Correlation of Biological Activity of Phenoxyacetic Acids with Hammett Substituent Constants and Partition Coefficients. *Nature* 194**,** 178-180.

Harel, M., Schalk, I., Ehret-Sabatier, L., Bouet, F., Goeldner, M., Hirth, C., Axelsen, P.H., Silman, I., Sussman, J.L., 1993. Quaternary ligand binding to aromatic residues in the active-site gorge of acetylcholinesterase. *Proc Natl Acad Sci U S A* 90**,** 9031-9035.

Haubmann, C., Hubner, H., Gmeiner, P., 1999. Piperidinylpyrroles: design, synthesis and binding properties of novel and selective dopamine D4 receptor ligands. *Bioorg Med Chem Lett* 9**,** 3143-3146.

Hellewell, S.B., Bruce, A., Feinstein, G., Orringer, J., Williams, W., Bowen, W.D., 1994. Rat liver and kidney contain high densities of sigma 1 and sigma 2 receptors: characterization by ligand binding and photoaffinity labeling. *Eur J Pharmacol* 268**,** 9-18.

Henchman, R.H., McCammon, J.A., 2002. Structural and dynamic properties of water around acetylcholinesterase. *Protein Sci* 11**,** 2080-2090.

Henchman, R.H., Tai, K., Shen, T., McCammon, J.A., 2002. Properties of water molecules in the active site gorge of acetylcholinesterase from computer simulation. *Biophys J* 82**,** 2671-2682.

Hom, R.K., Gailunas, A.F., Mamo, S., Fang, L.Y., Tung, J.S., Walker, D.E., Davis, D., Thorsett, E.D., Jewett, N.E., Moon, J.B., John, V., 2004. Design and synthesis of hydroxyethylene-based peptidomimetic inhibitors of human beta-secretase. *J Med Chem* 47**,** 158-164.

Hong, L., Koelsch, G., Lin, X., Wu, S., Terzyan, S., Ghosh, A.K., Zhang, X.C., Tang, J., 2000. Structure of the protease domain of memapsin 2 (beta-secretase) complexed with inhibitor. *Science (New York, N Y)* 290**,** 150-153.

Hu, Y., Zhang, J., Chandrashankra, O., Ip, F.C., Ip, N.Y., 2013. Design, synthesis and evaluation of novel heterodimers of donepezil and huperzine fragments as acetylcholinesterase inhibitors. *Bioorg Med Chem* 21**,** 676-683.

Huang, W., Tang, L., Shi, Y., Huang, S., Xu, L., Sheng, R., Wu, P., Li, J., Zhou, N., Hu, Y., 2011a. Searching for the Multi-Target-Directed Ligands against Alzheimer's disease: discovery of quinoxaline-based hybrid compounds with AChE, H(3)R and BACE 1 inhibitory activities. *Bioorg Med Chem* 19**,** 7158-7167.

Huang, Y., Hammond, P.S., Whirrett, B.R., Kuhner, R.J., Wu, L., Childers, S.R., Mach, R.H., 1998. Synthesis and quantitative structure-activity relationships of N-(1-benzylpiperidin-4-yl)phenylacetamides and related analogues as potent and selective sigma1 receptor ligands. *J Med Chem* 41**,** 2361-2370.

Huang, Y., Hammond, P.S., Wu, L., Mach, R.H., 2001a. Synthesis and structure-activity relationships of N-(1-benzylpiperidin-4-yl)arylacetamide analogues as potent sigma1 receptor ligands. *J Med Chem* 44**,** 4404-4415.

Huang, Y., Luedtke, R.R., Freeman, R.A., Wu, L., Mach, R.H., 2001b. Synthesis of 2-(2,3-dimethoxyphenyl)-4-(aminomethyl)imidazole analogues and their binding affinities for dopamine D(2) and D(3) receptors. *Bioorg Med Chem* 9**,** 3113-3122.

Huang, Y., Zheng, L., Halliday, G., Dobson-Stone, C., Wang, Y., Tang, H.D., Cao, L., Deng, Y.L., Wang, G., Zhang, Y.M., Wang, J.H., Hallupp, M., Kwok, J., Chen, S.D., 2011b. Genetic polymorphisms in sigma-1 receptor and apolipoprotein E interact to influence the severity of Alzheimer's disease. *Curr Alzheimer Res* 8**,** 765-770.

Hui, A.-l., Chen, Y., Zhu, S.-j., Gan, C.-s., Pan, J., Zhou, A., 2014. Design and synthesis of tacrine-phenothiazine hybrids as multitarget drugs for Alzheimer's disease. *Med Chem Res* 23**,** 3546-3557.

Kamei, H., Noda, Y., Kameyama, T., Nabeshima, T., 1997. Role of (+)-SKF-10,047-sensitive sub-population of sigma 1 receptors in amelioration of conditioned fear stress in rats: association with mesolimbic dopaminergic systems. *Eur J Pharmacol* 319**,** 165-172.

Karplus, M., McCammon, J.A., 2002. Molecular dynamics simulations of biomolecules. *Nat Struct Biol* 9**,** 646-652.

Kawakami, Y., Inoue, A., Kawai, T., Wakita, M., Sugimoto, H., Hopfinger, A.J., 1996. The rationale for E2020 as a potent acetylcholinesterase inhibitor. *Bioorg Med Chem* 4**,** 1429-1446.

Keri, R.S., Quintanova, C., Marques, S.M., Esteves, A.R., Cardoso, S.M., Santos, M.A., 2013. Design, synthesis and neuroprotective evaluation of novel tacrine-benzothiazole hybrids as multi-targeted compounds against Alzheimer's disease. *Bioorg Med Chem* 21**,** 4559-4569.

Kerwin, J.F., Jr., Lancaster, J.R., Jr., Feldman, P.L., 1995. Nitric oxide: a new paradigm for second messengers. *J Med Chem* 38**,** 4343-4362.

Kochi, A., Eckroat, T.J., Green, K.D., Mayhoub, A.S., Lim, M.H., Garneau-Tsodikova, S., 2013. A novel hybrid of 6-chlorotacrine and metal-amyloid-[small beta] modulator for inhibition of acetylcholinesterase and metal-induced amyloid-[small beta] aggregation. *Chem Sci* 4**,** 4137-4145.

Kua, J., Zhang, Y., Eslami, A.C., Butler, J.R., McCammon, J.A., 2003. Studying the roles of W86, E202, and Y337 in binding of acetylcholine to acetylcholinesterase using a combined molecular dynamics and multiple docking approach. *Protein Sci* 12**,** 2675-2684.

Kua, J., Zhang, Y., McCammon, J.A., 2002. Studying enzyme binding specificity in acetylcholinesterase using a combined molecular dynamics and multiple docking approach. *J Am Chem Soc* 124**,** 8260-8267.

Lagadic-Gossmann, D., Rissel, M., Le Bot, M.A., Guillouzo, A., 1998. Toxic effects of tacrine on primary hepatocytes and liver epithelial cells in culture. *Cell Biol Toxicol* 14**,** 361-373.

Lakshmi, V., Kannan, V.S., Boopathy, R., 2013. Identification of potential bivalent inhibitors from natural compounds for acetylcholinesterase through in silico screening using multiple pharmacophores. *J Mol Graph Model* 40**,** 72-79.

Lan, J.S., Xie, S.S., Li, S.Y., Pan, L.F., Wang, X.B., Kong, L.Y., 2014. Design, synthesis and evaluation of novel tacrine-(beta-carboline) hybrids as multifunctional agents for the treatment of Alzheimer's disease. *Bioorg Med Chem* 22**,** 6089-6104.

Lauren, J., Gimbel, D.A., Nygaard, H.B., Gilbert, J.W., Strittmatter, S.M., 2009. Cellular prion protein mediates impairment of synaptic plasticity by amyloid-beta oligomers. *Nature* 457**,** 1128-1132.

Laurini, E., Marson, D., Dal Col, V., Fermeglia, M., Mamolo, M.G., Zampieri, D., Vio, L., Pricl, S., 2012. Another brick in the wall. Validation of the sigma1 receptor 3D model by computer-assisted design, synthesis, and activity of new sigma1 ligands. *Mol Pharm* 9**,** 3107-3126.

Lecoutey, C., Rochais, C., Genest, D., Butt-Gueulle, S., Ballandonne, C., Corvaisier, S., Dulin, F., Lepailleur, A., Sopkova-de Oliveira Santos, J., Dallemagne, P., 2012. Synthesis of dual AChE/5-HT4 receptor multi-target directed ligands. *Med. Chem. Commun.* 3**,** 627-634.

Leon, R., Garcia, A.G., Marco-Contelles, J., 2013. Recent advances in the multitarget-directed ligands approach for the treatment of Alzheimer's disease. *Med Res Rev* 33**,** 139-189.

Li, S.Y., Jiang, N., Xie, S.S., Wang, K.D., Wang, X.B., Kong, L.Y., 2014. Design, synthesis and evaluation of novel tacrine-rhein hybrids as multifunctional agents for the treatment of Alzheimer's disease. *Org Biomol Chem* 12**,** 801-814.

Li, S.Y., Wang, X.B., Xie, S.S., Jiang, N., Wang, K.D., Yao, H.Q., Sun, H.B., Kong, L.Y., 2013a. Multifunctional tacrine-flavonoid hybrids with cholinergic, beta-amyloid-reducing, and metal chelating properties for the treatment of Alzheimer's disease. *Eur J Med Chem* 69**,** 632-646.

Li, Y.P., Weng, X., Ning, F.X., Ou, J.B., Hou, J.Q., Luo, H.B., Li, D., Huang, Z.S., Huang, S.L., Gu, L.Q., 2013b. 3D-QSAR studies of azaoxoisoaporphine, oxoaporphine, and oxoisoaporphine derivatives as anti-AChE and anti-AD agents by the CoMFA method. *J Mol Graph Model* 41**,** 61-67.

Lu, C., Zhou, Q., Yan, J., Du, Z., Huang, L., Li, X., 2013. A novel series of tacrine-selegiline hybrids with cholinesterase and monoamine oxidase inhibition activities for the treatment of Alzheimer's disease. *Eur J Med Chem* 62**,** 745-753.

Luo, W., Li, Y.P., He, Y., Huang, S.L., Li, D., Gu, L.Q., Huang, Z.S., 2011. Synthesis and evaluation of heterobivalent tacrine derivatives as potential multi-functional anti-Alzheimer agents. *Eur J Med Chem* 46**,** 2609-2616.

Luo, X., Yan, R., 2010. Inhibition of BACE1 for therapeutic use in Alzheimer's disease. *Int J Clin Exp Pathol* 3**,** 618-628.

Luo, Z., Sheng, J., Sun, Y., Lu, C., Yan, J., Liu, A., Luo, H.B., Huang, L., Li, X., 2013. Synthesis and evaluation of multi-target-directed ligands against Alzheimer's disease based on the fusion of donepezil and ebselen. *J Med Chem* 56**,** 9089-9099.

Lushchekina, S.V., Nemukhin, A.V., Morozov, D.I., Varfolomeev, S.D., 2010. Correlation between the substrate structure and the rate of acetylcholinesterase hydrolysis modeled with the combined quantum mechanical/molecular mechanical studies. *Chem Biol Interact* 187**,** 59-63.

Maalej, E., Chabchoub, F., Oset-Gasque, M.J., Esquivias-Perez, M., Gonzalez, M.P., Monjas, L., Perez, C., de los Rios, C., Rodriguez-Franco, M.I., Iriepa, I., Moraleda, I., Chioua, M., Romero, A., Marco-Contelles, J., Samadi, A., 2012. Synthesis, biological assessment, and molecular modeling of racemic 7-aryl-9,10,11,12-tetrahydro-7H-benzo[7,8]chromeno[2,3-b]quinolin-8-amines as potential drugs for the treatment of Alzheimer's disease. *Eur J Med Chem* 54**,** 750-763.

Maalej, E., Chabchoub, F., Samadi, A., de los Rios, C., Perona, A., Morreale, A., Marco-Contelles, J., 2011. Synthesis, biological assessment and molecular modeling of 14-aryl-10,11,12,14-tetrahydro-9H-benzo[5,6]chromeno[2,3-b]quinolin-13-amines. *Bioorg Med Chem Lett* 21**,** 2384-2388.

Mao, F., Chen, J., Zhou, Q., Luo, Z., Huang, L., Li, X., 2013. Novel tacrine-ebselen hybrids with improved cholinesterase inhibitory, hydrogen peroxide and peroxynitrite scavenging activity. *Bioorg Med Chem Lett* 23**,** 6737-6742.

Martin, W.R., Eades, C.G., Thompson, J.A., Huppler, R.E., Gilbert, P.E., 1976. The effects of morphine- and nalorphine- like drugs in the nondependent and morphine-dependent chronic spinal dog. *J Pharmacol Exp Ther* 197**,** 517-532.

Matsutomo, T., Stark, T.D., Hofmann, T., 2013. In vitro activity-guided identification of antioxidants in aged garlic extract. *J Agric Food Chem* 61**,** 3059-3067.

Maurice, T., Privat, A., 1997. SA4503, a novel cognitive enhancer with sigma1 receptor agonist properties, facilitates NMDA receptor-dependent learning in mice. *Eur J Pharmacol* 328**,** 9-18.

Maurice, T., Su, T.P., 2009. The pharmacology of sigma-1 receptors. *Pharmacol Ther* 124**,** 195-206.

Mishina, M., Ishiwata, K., Ishii, K., Kitamura, S., Kimura, Y., Kawamura, K., Oda, K., Sasaki, T., Sakayori, O., Hamamoto, M., Kobayashi, S., Katayama, Y., 2005. Function of sigma1 receptors in Parkinson's disease. *Acta Neurol Scand* 112**,** 103-107.

Mishra, N., Basu, A., 2013. Exploring different virtual screening strategies for acetylcholinesterase inhibitors. *Biomed Res Int* 2013**,** 236850.

Mohamed, T., Yeung, J.C., Vasefi, M.S., Beazely, M.A., Rao, P.P., 2012. Development and evaluation of multifunctional agents for potential treatment of Alzheimer's disease: application to a pyrimidine-2,4-diamine template. *Bioorg Med Chem Lett* 22**,** 4707-4712.

Mount, C., Downton, C., 2006. Alzheimer disease: progress or profit? *Nat Med* 12**,** 780-784.

Naito, Y., Yoshikawa, T., Tanigawa, T., Sakurai, K., Yamasaki, K., Uchida, M., Kondo, M., 1995. Hydroxyl radical scavenging by rebamipide and related compounds: electron paramagnetic resonance study. *Free Radic Biol Med* 18**,** 117-123.

Nakazawa, M., Matsuno, K., Mita, S., 1998. Activation of sigma1 receptor subtype leads to neuroprotection in the rat primary neuronal cultures. *Neurochem Int* 32**,** 337-343.

Nasica-Labouze, J., Nguyen, P.H., Sterpone, F., Berthoumieu, O., Buchete, N.V., Cote, S., De Simone, A., Doig, A.J., Faller, P., Garcia, A., Laio, A., Li, M.S., Melchionna, S., Mousseau, N., Mu, Y., Paravastu, A., Pasquali, S., Rosenman, D.J., Strodel, B., Tarus, B., Viles, J.H., Zhang, T., Wang, C., Derreumaux, P., 2015. Amyloid beta Protein and Alzheimer's Disease: When Computer Simulations Complement Experimental Studies. *Chem Rev* 115**,** 3518-3563.

Nepovimova, E., Uliassi, E., Korabecny, J., Pena-Altamira, L.E., Samez, S., Pesaresi, A., Garcia, G.E., Bartolini, M., Andrisano, V., Bergamini, C., Fato, R., Lamba, D., Roberti, M., Kuca, K., Monti, B., Bolognesi, M.L., 2014. Multitarget drug design strategy: quinone-tacrine hybrids designed to block amyloid-beta aggregation and to exert anticholinesterase and antioxidant effects. *J Med Chem* 57**,** 8576-8589.

Ning, X., Rangwala, H., Karypis, G., 2009. Multi-assay-based structure-activity relationship models: improving structure-activity relationship models by incorporating activity information from related targets. *J Chem Inf Model* 49**,** 2444-2456.

Niu, C., Xu, Y., Luo, X., Duan, W., Silman, I., Sussman, J.L., Zhu, W., Chen, K., Shen, J., Jiang, H., 2005. Dynamic mechanism of E2020 binding to acetylcholinesterase: a steered molecular dynamics simulation. *J Phys Chem B* 109**,** 23730-23738.

O'Leary, J.C., 3rd, Li, Q., Marinec, P., Blair, L.J., Congdon, E.E., Johnson, A.G., Jinwal, U.K., Koren, J., 3rd, Jones, J.R., Kraft, C., Peters, M., Abisambra, J.F., Duff, K.E., Weeber, E.J., Gestwicki, J.E., Dickey, C.A., 2010. Phenothiazine-mediated rescue of cognition in tau transgenic mice requires neuroprotection and reduced soluble tau burden. *Mol Neurodegener* 5**,** 45.

Ozturan Ozer, E., Tan, O.U., Ozadali, K., Kucukkilinc, T., Balkan, A., Ucar, G., 2013. Synthesis, molecular modeling and evaluation of novel N'-2-(4-benzylpiperidin-/piperazin-1-yl)acylhydrazone derivatives as dual inhibitors for cholinesterases and Abeta aggregation. *Bioorg Med Chem Lett* 23**,** 440-443.

Pasquini, S., Mugnaini, C., Ligresti, A., Tafi, A., Brogi, S., Falciani, C., Pedani, V., Pesco, N., Guida, F., Luongo, L., Varani, K., Borea, P.A., Maione, S., Di Marzo, V., Corelli, F., 2012. Design, synthesis, and pharmacological characterization of indol-3-ylacetamides, indol-3-yloxoacetamides, and indol-3-ylcarboxamides: potent and selective CB2 cannabinoid receptor inverse agonists. *J Med Chem* 55**,** 5391-5402.

Patocka, J., Jun, D., Kuca, K., 2008. Possible role of hydroxylated metabolites of tacrine in drug toxicity and therapy of Alzheimer's disease. *Curr Drug Metab* 9**,** 332-335.

Peng, D.Y., Sun, Q., Zhu, X.L., Lin, H.Y., Chen, Q., Yu, N.X., Yang, W.C., Yang, G.F., 2012 Acetylcholinesterase inhibitors with multi-functions on butylcholinesterase, A*β* aggregation, and β-secretase. *Bioorg. Med. Chem*. 20, 6739–675.

Perez, V., Marco, J.L., Fernandez-Alvarez, E., Unzeta, M., 1999. Relevance of benzyloxy group in 2-indolyl methylamines in the selective MAO-B inhibition. *Br J Pharmacol* 127**,** 869-876.

Pi, R., Mao, X., Chao, X., Cheng, Z., Liu, M., Duan, X., Ye, M., Chen, X., Mei, Z., Liu, P., Li, W., Han, Y., 2012. Tacrine-6-ferulic acid, a novel multifunctional dimer, inhibits amyloid-beta-mediated Alzheimer's disease-associated pathogenesis in vitro and in vivo. *PLoS One* 7**,** e31921.

Podoly, E., Shalev, D.E., Shenhar-Tsarfaty, S., Bennett, E.R., Ben Assayag, E., Wilgus, H., Livnah, O., Soreq, H., 2009. The butyrylcholinesterase K variant confers structurally derived risks for Alzheimer pathology. *J Biol Chem* 284**,** 17170-17179.

Prezzavento, O., Arena, E., Parenti, C., Pasquinucci, L., Arico, G., Scoto, G.M., Grancara, S., Toninello, A., Ronsisvalle, S., 2013. Design and synthesis of new bifunctional sigma-1 selective ligands with antioxidant activity. *J Med Chem* 56**,** 2447-2455.

Pudlo, M., Luzet, V., Ismaili, L., Tomassoli, I., Iutzeler, A., Refouvelet, B., 2014. Quinolone-benzylpiperidine derivatives as novel acetylcholinesterase inhibitor and antioxidant hybrids for Alzheimer disease. *Bioorg Med Chem* 22**,** 2496-2507.

Qian, S., He, L., Mak, M., Han, Y., Ho, C.Y., Zuo, Z., 2014. Synthesis, biological activity, and biopharmaceutical characterization of tacrine dimers as acetylcholinesterase inhibitors. *Int J Pharm* 477**,** 442-453.

Qizilbash, N., Birks, J., Lopez Arrieta, J., Lewington, S., Szeto, S., 2007. WITHDRAWN: Tacrine for Alzheimer's disease. *Cochrane Database Syst Rev***,** CD000202.

Razavi, S.F., Khoobi, M., Nadri, H., Sakhteman, A., Moradi, A., Emami, S., Foroumadi, A., Shafiee, A., 2013. Synthesis and evaluation of 4-substituted coumarins as novel acetylcholinesterase inhibitors. *Eur J Med Chem* 64**,** 252-259.

Reid, G.A., Chilukuri, N., Darvesh, S., 2013. Butyrylcholinesterase and the cholinergic system. *Neuroscience* 234**,** 53-68.

Remya, C., Dileep, K.V., Tintu, I., Variyar, E.J., Sadasivan, C., 2013. In vitro inhibitory profile of NDGA against AChE and its in silico structural modifications based on ADME profile. *J Mol Model* 19**,** 1179-1194.

Richmond, V., Murray, A.P., Maier, M.S., 2013. Synthesis and acetylcholinesterase inhibitory activity of polyhydroxylated sulfated steroids: structure/activity studies. *Steroids* 78**,** 1141-1147.

Rodrigues Simoes, M.C., Dias Viegas, F.P., Moreira, M.S., de Freitas Silva, M., Riquiel, M.M., da Rosa, P.M., Castelli, M.R., dos Santos, M.H., Soares, M.G., Viegas, C., Jr., 2014. Donepezil: an important prototype to the design of new drug candidates for Alzheimer's disease. *Mini Rev Med Chem* 14**,** 2-19.

Rodriguez-Franco, M.I., Fernandez-Bachiller, M.I., Perez, C., Castro, A., Martinez, A., 2005. Design and synthesis of N-benzylpiperidine-purine derivatives as new dual inhibitors of acetyl- and butyrylcholinesterase. *Bioorg Med Chem* 13**,** 6795-6802.

Romero, A., Cacabelos, R., Oset-Gasque, M.J., Samadi, A., Marco-Contelles, J., 2013. Novel tacrine-related drugs as potential candidates for the treatment of Alzheimer's disease. *Bioorg Med Chem Lett* 23**,** 1916-1922.

Rook, Y., Schmidtke, K.U., Gaube, F., Schepmann, D., Wunsch, B., Heilmann, J., Lehmann, J., Winckler, T., 2010. Bivalent beta-carbolines as potential multitarget anti-Alzheimer agents. *J Med Chem* 53**,** 3611-3617.

Rosini, M., Simoni, E., Minarini, A., Melchiorre, C., 2014. Multi-target design strategies in the context of Alzheimer's disease: acetylcholinesterase inhibition and NMDA receptor antagonism as the driving forces. *Neurochem Res* 39**,** 1914-1923.

Sadowski, M., Wisniewski, T., 2007. Disease modifying approaches for Alzheimer's pathology. *Curr Pharm Des* 13**,** 1943-1954.

Samadi, A., Chioua, M., Bolea, I., de Los Rios, C., Iriepa, I., Moraleda, I., Bastida, A., Esteban, G., Unzeta, M., Galvez, E., Marco-Contelles, J., 2011. Synthesis, biological assessment and molecular modeling of new multipotent MAO and cholinesterase inhibitors as potential drugs for the treatment of Alzheimer's disease. *Eur J Med Chem* 46**,** 4665-4668.

Samadi, A., de la Fuente Revenga, M., Perez, C., Iriepa, I., Moraleda, I., Rodriguez-Franco, M.I., Marco-Contelles, J., 2013. Synthesis, pharmacological assessment, and molecular modeling of 6-chloro-pyridonepezils: new dual AChE inhibitors as potential drugs for the treatment of Alzheimer's disease. *Eur J Med Chem* 67**,** 64-74.

Samadi, A., de los Rios, C., Bolea, I., Chioua, M., Iriepa, I., Moraleda, I., Bartolini, M., Andrisano, V., Galvez, E., Valderas, C., Unzeta, M., Marco-Contelles, J., 2012. Multipotent MAO and cholinesterase inhibitors for the treatment of Alzheimer's disease: synthesis, pharmacological analysis and molecular modeling of heterocyclic substituted alkyl and cycloalkyl propargyl amine. *Eur J Med Chem* 52**,** 251-262.

Samadi, A., Marco-Contelles, J., Soriano, E., Alvarez-Perez, M., Chioua, M., Romero, A., Gonzalez-Lafuente, L., Gandia, L., Roda, J.M., Lopez, M.G., Villarroya, M., Garcia, A.G., Rios Cde, L., 2010. Multipotent drugs with cholinergic and neuroprotective properties for the treatment of Alzheimer and neuronal vascular diseases. I. Synthesis, biological assessment, and molecular modeling of simple and readily available 2-aminopyridine-, and 2-chloropyridine-3,5-dicarbonitriles. *Bioorg Med Chem* 18**,** 5861-5872.

Sanson, B., Colletier, J.P., Xu, Y., Lang, P.T., Jiang, H., Silman, I., Sussman, J.L., Weik, M., 2011. Backdoor opening mechanism in acetylcholinesterase based on X-ray crystallography and molecular dynamics simulations. *Protein Sci* 20**,** 1114-1118.

Savini, L., Gaeta, A., Fattorusso, C., Catalanotti, B., Campiani, G., Chiasserini, L., Pellerano, C., Novellino, E., McKissic, D., Saxena, A., 2003. Specific targeting of acetylcholinesterase and butyrylcholinesterase recognition sites. Rational design of novel, selective, and highly potent cholinesterase inhibitors. *J Med Chem* 46**,** 1-4.

Schott, Y., Decker, M., Rommelspacher, H., Lehmann, J., 2006. 6-Hydroxy- and 6-methoxy-beta-carbolines as acetyl- and butyrylcholinesterase inhibitors. *Bioorg Med Chem Lett* 16**,** 5840-5843.

Senda, T., Matsuno, K., Kobayashi, T., Nakazawa, M., Nakata, K., Mita, S., 1998. Ameliorative effect of SA4503, a novel cognitive enhancer, on the basal forebrain lesion-induced impairment of the spatial learning performance in rats. *Pharmacol Biochem Behav* 59**,** 129-134.

Senda, T., Matsuno, K., Okamoto, K., Kobayashi, T., Nakata, K., Mita, S., 1996. Ameliorating effect of SA4503, a novel sigma 1 receptor agonist, on memory impairments induced by cholinergic dysfunction in rats. *Eur J Pharmacol* 315**,** 1-10.

Shao, D., Zou, C., Luo, C., Tang, X., Li, Y., 2004. Synthesis and evaluation of tacrine-E2020 hybrids as acetylcholinesterase inhibitors for the treatment of Alzheimer's disease. *Bioorg Med Chem Lett* 14**,** 4639-4642.

Shen, T., Tai, K., Henchman, R.H., McCammon, J.A., 2002. Molecular dynamics of acetylcholinesterase. *Acc Chem Res* 35**,** 332-340.

Sheng, R., Lin, X., Li, J., Jiang, Y., Shang, Z., Hu, Y., 2005. Design, synthesis, and evaluation of 2-phenoxy-indan-1-one derivatives as acetylcholinesterase inhibitors. *Bioorg Med Chem Lett* 15**,** 3834-3837.

Shi, J., Tai, K., McCammon, J.A., Taylor, P., Johnson, D.A., 2003. Nanosecond dynamics of the mouse acetylcholinesterase cys69-cys96 omega loop. *J Biol Chem* 278**,** 30905-30911.

Silva, D., Chioua, M., Samadi, A., Agostinho, P., Garcao, P., Lajarin-Cuesta, R., de Los Rios, C., Iriepa, I., Moraleda, I., Gonzalez-Lafuente, L., Mendes, E., Perez, C., Rodriguez-Franco, M.I., Marco-Contelles, J., Carmo Carreiras, M., 2013. Synthesis, pharmacological assessment, and molecular modeling of acetylcholinesterase/butyrylcholinesterase inhibitors: effect against amyloid-beta-induced neurotoxicity. *ACS Chem Neurosci* 4**,** 547-565.

Sirin, G.S., Zhang, Y., 2014. How is acetylcholinesterase phosphonylated by soman? An ab initio QM/MM molecular dynamics study. *J Phys Chem A* 118**,** 9132-9139.

Smith, D.G., Cappai, R., Barnham, K.J., 2007. The redox chemistry of the Alzheimer's disease amyloid beta peptide. *Biochim Biophys Acta* 1768**,** 1976-1990.

Song, M.S., Matveychuk, D., MacKenzie, E.M., Duchcherer, M., Mousseau, D.D., Baker, G.B., 2013. An update on amine oxidase inhibitors: multifaceted drugs. *Prog Neuropsychopharmacol Biol Psychiatry* 44**,** 118-124.

Songsiang, U., Thongthoom, T., Boonyarat, C., Yenjai, C., 2011. Claurailas A-D, cytotoxic carbazole alkaloids from the roots of Clausena harmandiana. *J Nat Prod* 74**,** 208-212.

Sopkova-de Oliveira Santos, J., Lesnard, A., Agondanou, J.H., Dupont, N., Godard, A.M., Stiebing, S., Rochais, C., Fabis, F., Dallemagne, P., Bureau, R., Rault, S., 2010. Virtual screening discovery of new acetylcholinesterase inhibitors issued from CERMN chemical library. *J Chem Inf Model* 50**,** 422-428.

Speck-Planche, A., Luan, F., Cordeiro, M.N., 2012a. Discovery of anti-Alzheimer agents: current ligand-based approaches toward the design of acetylcholinesterase inhibitors. *Mini Rev Med Chem* 12**,** 583-591.

Speck-Planche, A., Luan, F., Cordeiro, M.N., 2012b. Role of ligand-based drug design methodologies toward the discovery of new anti- Alzheimer agents: futures perspectives in Fragment-Based Ligand Design. *Curr Med Chem* 19**,** 1635-1645.

Spilovska, K., Korabecny, J., Kral, J., Horova, A., Musilek, K., Soukup, O., Drtinova, L., Gazova, Z., Siposova, K., Kuca, K., 2013. 7-Methoxytacrine-adamantylamine heterodimers as cholinesterase inhibitors in Alzheimer's disease treatment--synthesis, biological evaluation and molecular modeling studies. *Molecules* 18**,** 2397-2418.

Standridge, J.B., 2004. Pharmacotherapeutic approaches to the prevention of Alzheimer's disease. *Am J Geriatr Pharmacother* 2**,** 119-132.

Stasiak, A., Mussur, M., Unzeta, M., Samadi, A., Marco-Contelles, J.L., Fogel, W.A., 2014. Effects of novel monoamine oxidases and cholinesterases targeting compounds on brain neurotransmitters and behavior in rat model of vascular dementia. *Curr Pharm Des* 20**,** 161-171.

Storr, T., Thompson, K.H., Orvig, C., 2006. Design of targeting ligands in medicinal inorganic chemistry. *Chem Soc Rev* 35**,** 534-544.

Sugimoto, H., 2008. The new approach in development of anti-Alzheimer's disease drugs via the cholinergic hypothesis. *Chem Biol Interact* 175**,** 204-208.

Sugimoto, H., Iimura, Y., Yamanishi, Y., Yamatsu, K., 1992. Synthesis and anti-acetylcholinesterase activity of 1-benzyl-4-[(5,6-dimethoxy-1-indanon-2-yl)methyl]piperidine hydrochloride (E2020) and related compounds. *Bioorg. Med. Chem. Lett.* 2**,** 871-876.

Sugimoto, H., Ogura, H., Arai, Y., Limura, Y., Yamanishi, Y., 2002. Research and development of donepezil hydrochloride, a new type of acetylcholinesterase inhibitor. *Jpn J Pharmacol* 89**,** 7-20.

Sugimoto, H., Tsuchiya, Y., Sugumi, H., Higurashi, K., Karibe, N., Iimura, Y., Sasaki, A., Kawakami, Y., Nakamura, T., Araki, S., et al., 1990. Novel piperidine derivatives. Synthesis and anti-acetylcholinesterase activity of 1-benzyl-4-[2-(N-benzoylamino)ethyl]piperidine derivatives. *J Med Chem* 33**,** 1880-1887.

Sun, Q., Peng, D.Y., Yang, S.G., Zhu, X.L., Yang, W.C., Yang, G.F., 2014a. Syntheses of coumarin-tacrine hybrids as dual-site acetylcholinesterase inhibitors and their activity against butylcholinesterase, Abeta aggregation, and beta-secretase. *Bioorg Med Chem* 22**,** 4784-4791.

Sun, X., Zhang, P., Pi, R., Zhou, Y., Deng, X., Xie, Z., Liao, Q., 2014b. Determination of tacrine-6-ferulic acid in rat plasma by LC-MS/MS and its application to pharmacokinetics study. *Biomed Chromatogr* 28**,** 1352-1359.

Sun, Y., Chen, J., Chen, X., Huang, L., Li, X., 2013. Inhibition of cholinesterase and monoamine oxidase-B activity by Tacrine-Homoisoflavonoid hybrids. *Bioorg Med Chem* 21**,** 7406-7417.

Tang, H., Ning, F.X., Wei, Y.B., Huang, S.L., Huang, Z.S., Chan, A.S., Gu, L.Q., 2007. Derivatives of oxoisoaporphine alkaloids: a novel class of selective acetylcholinesterase inhibitors. *Bioorg Med Chem Lett* 17**,** 3765-3768.

Tang, H., Zhao, L.Z., Zhao, H.T., Huang, S.L., Zhong, S.M., Qin, J.K., Chen, Z.F., Huang, Z.S., Liang, H., 2011. Hybrids of oxoisoaporphine-tacrine congeners: novel acetylcholinesterase and acetylcholinesterase-induced beta-amyloid aggregation inhibitors. *Eur J Med Chem* 46**,** 4970-4979.

Taniguchi, S., Suzuki, N., Masuda, M., Hisanaga, S., Iwatsubo, T., Goedert, M., Hasegawa, M., 2005. Inhibition of heparin-induced tau filament formation by phenothiazines, polyphenols, and porphyrins. *J Biol Chem* 280**,** 7614-7623.

Tchedre, K.T., Yorio, T., 2008. sigma-1 receptors protect RGC-5 cells from apoptosis by regulating intracellular calcium, Bax levels, and caspase-3 activation. *Invest Ophthalmol Vis Sci* 49**,** 2577-2588.

Thathiah, A., De Strooper, B., 2011. The role of G protein-coupled receptors in the pathology of Alzheimer's disease. *Nat Rev Neurosci* 12**,** 73-87.

Thiratmatrakul, S., Yenjai, C., Waiwut, P., Vajragupta, O., Reubroycharoen, P., Tohda, M., Boonyarat, C., 2014. Synthesis, biological evaluation and molecular modeling study of novel tacrine-carbazole hybrids as potential multifunctional agents for the treatment of Alzheimer's disease. *Eur J Med Chem* 75**,** 21-30.

Thomas, D.D., Ridnour, L.A., Isenberg, J.S., Flores-Santana, W., Switzer, C.H., Donzelli, S., Hussain, P., Vecoli, C., Paolocci, N., Ambs, S., Colton, C.A., Harris, C.C., Roberts, D.D., Wink, D.A., 2008. The chemical biology of nitric oxide: implications in cellular signaling. *Free Radic Biol Med* 45**,** 18-31.

Valasani, K.R., Chaney, M.O., Day, V.W., Shidu Yan, S., 2013. Acetylcholinesterase inhibitors: structure based design, synthesis, pharmacophore modeling, and virtual screening. *J Chem Inf Model* 53**,** 2033-2046.

Venugopal, C., Demos, C.M., Rao, K.S., Pappolla, M.A., Sambamurti, K., 2008. Beta-secretase: structure, function, and evolution. *CNS Neurol Disord Drug Targets* 7**,** 278-294.

Viayna, E., Sola, I., Bartolini, M., De Simone, A., Tapia-Rojas, C., Serrano, F.G., Sabate, R., Juarez-Jimenez, J., Perez, B., Luque, F.J., Andrisano, V., Clos, M.V., Inestrosa, N.C., Munoz-Torrero, D., 2014. Synthesis and multitarget biological profiling of a novel family of rhein derivatives as disease-modifying anti-Alzheimer agents. *J Med Chem* 57**,** 2549-2567.

Vitorovic-Todorovic, M.D., Koukoulitsa, C., Juranic, I.O., Mandic, L.M., Drakulic, B.J., 2014. Structural modifications of 4-aryl-4-oxo-2-aminylbutanamides and their acetyl- and butyrylcholinesterase inhibitory activity. Investigation of AChE-ligand interactions by docking calculations and molecular dynamics simulations. *Eur J Med Chem* 81**,** 158-175.

Walsh, D.M., Selkoe, D.J., 2007. A beta oligomers - a decade of discovery. *J Neurochem* 101**,** 1172-1184.

Wang, L., Esteban, G., Ojima, M., Bautista-Aguilera, O.M., Inokuchi, T., Moraleda, I., Iriepa, I., Samadi, A., Youdim, M.B., Romero, A., Soriano, E., Herrero, R., Fernandez Fernandez, A.P., Ricardo Martinez, M., Marco-Contelles, J., Unzeta, M., 2014. Donepezil + propargylamine + 8-hydroxyquinoline hybrids as new multifunctional metal-chelators, ChE and MAO inhibitors for the potential treatment of Alzheimer's disease. *Eur J Med Chem* 80**,** 543-561.

Wang, Y., Wang, F., Yu, J.P., Jiang, F.C., Guan, X.L., Wang, C.M., Li, L., Cao, H., Li, M.X., Chen, J.G., 2012. Novel multipotent phenylthiazole-tacrine hybrids for the inhibition of cholinesterase activity, beta-amyloid aggregation and Ca(2)(+) overload. *Bioorg Med Chem* 20**,** 6513-6522.

Watkins, P.B., Zimmerman, H.J., Knapp, M.J., Gracon, S.I., Lewis, K.W., 1994. Hepatotoxic effects of tacrine administration in patients with Alzheimer's disease. *JAMA* 271**,** 992-998.

Wermuth, C.G., Exinger, A., 1972. [Morpholinoethylamino-3 methyl-4 phenyl-6 pyridazine dihydrochloride (Agar 1240)]. *Agressologie* 13**,** 285-289.

Wieckowska, A., Bajda, M., Guzior, N., Malawska, B., 2010. Novel alkyl- and arylcarbamate derivatives with N-benzylpiperidine and N-benzylpiperazine moieties as cholinesterases inhibitors. *Eur J Med Chem* 45**,** 5602-5611.

Wiesner, J., Kriz, Z., Kuca, K., Jun, D., Koca, J., 2010. Influence of the acetylcholinesterase active site protonation on omega loop and active site dynamics. *J Biomol Struct Dyn* 28**,** 393-403.

Wilson, S.R., Zucker, P.A., Huang, R.R.C., Spector, A., 1989. Development of synthetic compounds with glutathione peroxidase activity. *J. Am. Chem. Soc.* 111**,** 5936-5939.

Wlodek, S.T., Clark, T.W., Scott, L.R., McCammon, J.A., 1997. Molecular Dynamics of Acetylcholinesterase Dimer Complexed with Tacrine. .*J Am Chem Soc* 119**,** 9513-9522.

Wu, M.Y., Esteban, G., Brogi, S., Shionoya, M., Wang, L., Campiani, G., Unzeta, M., Inokuchi, T., Butini, S., Marco-Contelles, J., 2015. Donepezil-like multifunctional agents: Design, synthesis, molecular modeling and biological evaluation. *Eur J Med Chem*.

Xie, L., Zheng, W., Xin, N., Xie, J.W., Wang, T., Wang, Z.Y., 2012. Ebselen inhibits iron-induced tau phosphorylation by attenuating DMT1 up-regulation and cellular iron uptake. *Neurochem Int* 61**,** 334-340.

Xie, S.S., Lan, J.S., Wang, X.B., Jiang, N., Dong, G., Li, Z.R., Wang, K.D., Guo, P.P., Kong, L.Y., 2015. Multifunctional tacrine-trolox hybrids for the treatment of Alzheimer's disease with cholinergic, antioxidant, neuroprotective and hepatoprotective properties. *Eur J Med Chem* 93**,** 42-50.

Xie, S.S., Wang, X.B., Li, J.Y., Yang, L., Kong, L.Y., 2013. Design, synthesis and evaluation of novel tacrine-coumarin hybrids as multifunctional cholinesterase inhibitors against Alzheimer's disease. *Eur J Med Chem* 64**,** 540-553.

Xu, Y., Colletier, J.P., Weik, M., Jiang, H., Moult, J., Silman, I., Sussman, J.L., 2008. Flexibility of aromatic residues in the active-site gorge of acetylcholinesterase: X-ray versus molecular dynamics. *Biophys J* 95**,** 2500-2511.

Zampieri, D., Grazia Mamolo, M., Laurini, E., Zanette, C., Florio, C., Collina, S., Rossi, D., Azzolina, O., Vio, L., 2009a. Substituted benzo[d]oxazol-2(3H)-one derivatives with preference for the sigma1 binding site. *Eur J Med Chem* 44**,** 124-130.

Zampieri, D., Laurini, E., Vio, L., Golob, S., Fermeglia, M., Pricl, S., Mamolo, M.G., 2014. Synthesis and receptor binding studies of some new arylcarboxamide derivatives as sigma-1 ligands. *Bioorg Med Chem Lett* 24**,** 1021-1025.

Zampieri, D., Mamolo, M.G., Laurini, E., Florio, C., Zanette, C., Fermeglia, M., Posocco, P., Paneni, M.S., Pricl, S., Vio, L., 2009b. Synthesis, biological evaluation, and three-dimensional in silico pharmacophore model for sigma(1) receptor ligands based on a series of substituted benzo[d]oxazol-2(3H)-one derivatives. *J Med Chem* 52**,** 5380-5393.

Zhang, L., Fourches, D., Sedykh, A., Zhu, H., Golbraikh, A., Ekins, S., Clark, J., Connelly, M.C., Sigal, M., Hodges, D., Guiguemde, A., Guy, R.K., Tropsha, A., 2013. Discovery of novel antimalarial compounds enabled by QSAR-based virtual screening. *J Chem Inf Model* 53**,** 475-492.

Zhang, W.T., Ruan, J.L., Wu, P.F., Jiang, F.C., Zhang, L.N., Fang, W., Chen, X.L., Wang, Y., Cao, B.S., Chen, G.Y., Zhu, Y.J., Gu, J., Chen, J.G., 2009. Design, synthesis, and cytoprotective effect of 2-aminothiazole analogues as potent poly(ADP-ribose) polymerase-1 inhibitors. *J Med Chem* 52**,** 718-725.

Zhang, Y., Kua, J., McCammon, J.A., 2002. Role of the catalytic triad and oxyanion hole in acetylcholinesterase catalysis: an ab initio QM/MM study. *J Am Chem Soc* 124**,** 10572-10577.

Zheng, H., Youdim, M.B., Fridkin, M., 2009. Site-activated multifunctional chelator with acetylcholinesterase and neuroprotective-neurorestorative moieties for Alzheimer's therapy. *J Med Chem* 52**,** 4095-4098.

Zhu, X., Raina, A.K., Perry, G., Smith, M.A., 2004. Alzheimer's disease: the two-hit hypothesis. *Lancet Neurol* 3**,** 219-226.

Zhu, Y., Xiao, K., Ma, L., Xiong, B., Fu, Y., Yu, H., Wang, W., Wang, X., Hu, D., Peng, H., Li, J., Gong, Q., Chai, Q., Tang, X., Zhang, H., Shen, J., 2009. Design, synthesis and biological evaluation of novel dual inhibitors of acetylcholinesterase and beta-secretase. *Bioorg Med Chem* 17**,** 1600-1613.

Zou, Y., Xu, L., Chen, W., Zhu, Y., Chen, T., Fu, Y., Li, L., Ma, L., Xiong, B., Wang, X., Li, J., He, J., Zhang, H., Xu, Y., Shen, J., 2013. Discovery of pyrazole as C-terminus of selective BACE1 inhibitors. *Eur J Med Chem* 68**,** 270-283.